University of Alberta

Reinforcement Learning and Simulation-Based Search in Computer Go

by

David Silver

A thesis submitted to the Faculty of Graduate Studies and Research
in partial fulfillment of the requirements for the degree of

Doctor of Philosophy

Department of Computing Science

Examining Committee

Richard Sutton, Department of Computing Science, University of Alberta

Martin Müller, Department of Computing Science, University of Alberta

Csaba Szepesvari, Department of Computing Science, University of Alberta

Jonathan Schaeffer, Department of Computing Science, University of Alberta

Petr Musilek, Electrical and Computer Engineering, University of Alberta

Andrew Ng, Computer Science, Stanford University

Abstract

Learning and planning are two fundamental problems in artificial intelligence. The learning problem can be tackled by reinforcement learning methods, such as temporal-difference learning, which update a value function from real experience, and use function approximation to generalise across states. The planning problem can be tackled by simulation-based search methods, such as Monte-Carlo tree search, which update a value function from simulated experience, but treat each state individually. We introduce a new method, *temporal-difference search*, that combines elements of both reinforcement learning and simulation-based search methods. In this new method the value function is updated from simulated experience, but it uses function approximation to efficiently generalise across states. We also introduce the *Dyna-2* architecture, which combines temporal-difference learning with temporal-difference search. Whereas temporal-difference learning acquires general domain knowledge from its past experience, temporal-difference search acquires local knowledge that is specialised to the agent's current state, by simulating future experience. Dyna-2 combines both forms of knowledge together.

We apply our algorithms to the game of 9×9 Go. Using temporal-difference learning, with a million binary features matching simple patterns of stones, and using no prior knowledge except the grid structure of the board, we learnt a fast and effective evaluation function. Using temporal-difference search with the same representation produced a dramatic improvement: without any explicit search tree, and with equivalent domain knowledge, it achieved better performance than a vanilla Monte-Carlo tree search. When combined together using the Dyna-2 architecture, our program outperformed all handcrafted, traditional search, and traditional machine learning programs on the 9×9 Computer Go Server.

We also use our framework to extend the Monte-Carlo tree search algorithm. By forming a rapid generalisation over subtrees of the search space, and incorporating heuristic pattern knowledge that was learnt or handcrafted offline, we were able to significantly improve the performance of the Go program *MoGo*. Using these enhancements, *MoGo* became the first 9×9 Go program to achieve human master level.

Acknowledgements

The following document uses the first person plural to indicate the collaborative nature of much of this work. In particular, Rich Sutton has been a constant source of inspiration and wisdom. Martin Müller has provided invaluable advice on many topics, and his formidable Go expertise has time and again proven to be priceless. I'd also like to thank Gerry Tesauro for his keen insights and many constructive suggestions.

The results presented in this thesis were generated using the computer Go programs *RLGO* and *Mogo*. I developed the *RLGO* program on top of the SmartGo library, which was written by Markus Enzenberger and Martin Müller. I would like to acknowledge contributions to *RLGO* from numerous individuals, including Anna Koop and Leah Hackman. In addition I'd like to thank the members of the Computer Go mailing list for their feedback and ideas.

The *Mogo* progam was originally developed by Sylvain Gelly and Yizao Wang at the University of South Paris, with research contributions from Remi Munos and Olivier Teytaud. The heuristic MC–RAVE algorithm described in Chapter 8 was developed in collaboration with Sylvain Gelly, who should receive most of the credit for developing it into a practical and effective technique. Subsequent work on *Mogo*, including massive parallelisation and a number of other improvements, has been led by Olivier Teytaud and his team at the University of South Paris, but includes contributions from Computer Go researchers around the globe.

I'd like to thank Jessica Meserve for her enormous depths of patience, love and support that have gone well beyond reasonable expectations. Finally, I'd like to thank Elodie Silver for bringing joy and balance to my life. Writing this thesis has never been a burden, when I know I can return home to your smile.

Table of Contents

List of Figures

List of Tables

Chapter 1

Introduction

This thesis investigates the game of Go as a case study for artificial intelligence (AI) in large, challenging domains.

1.1 Computer Go

In many ways, computer Go is the best case for AI. The rules of the game are simple, known, and deterministic. The state is fully observable; the state space and action space are both discrete and finite. Games are of finite length, and always terminate with a binary win or loss outcome.[1] The state changes slowly and incrementally, with a single stone added at every move.[2] And yet until recently, and despite significant effort, computer Go has resisted significant progress, and is viewed by many as a grand challenge for AI (McCarthy, 1997; Harmon, 2003; Mechner, 1998).

Certainly, the game of Go is big. 19×19 Go has more than 10^{170} states and up to 361 legal moves. Its enormous search space is orders of magnitude too big for the search algorithms that have proven so successful in chess and checkers. Although the rules are simple, the emergent complexity of the game is profound. The long-term effect of a move may only be revealed after 50 or 100 additional moves. Professional Go players accumulate Go knowledge over a lifetime; mankind has accumulated Go knowledge over several millennia. For the last 30 years, attempts to precisely encode this knowledge in machine usable form have led to a positional understanding that is at best comparable to weak amateur-level humans. But are these properties really exceptional to Go? In real-world planning and decision-making problems, most actions have delayed, long-term consequences, leading to surprising complexity and enormous search spaces that are intractable to traditional search algorithms. Furthermore, also just like Go, in many of these problems expert knowledge is either unavailable, unreliable, or unencodable.

So before we consider any broader challenges in artificial intelligence, and attempt to tackle continuous action, continuous state, partially observable, and infinite horizon problems, perhaps we should consider computer Go.

[1]Draws are only possible with an integer *komi* (see Chapter 4).
[2]Except for captures, which occur relatively rarely.

1.2 Reinforcement Learning

Reinforcement learning is the study of approximately optimal decision-making in natural and artificial systems. In the field of artificial intelligence, it has been used to defeat human champions at games of skill (Tesauro, 1994); in robotics, to fly stunt manoeuvres in robot-controlled helicopters (Abbeel et al., 2007). In neuroscience it is used to model the human brain (Schultz et al., 1997); in psychology to predict animal behaviour (Sutton and Barto, 1990). In economics, it is used to understand the decisions of human investors (Choi et al., 2007), and to build automated trading systems (Nevmyvaka et al., 2006). In engineering, it has been used to allocate bandwidth to mobile phones (Singh and Bertsekas, 1997) and to manage complex power systems (Ernst et al., 2005).

A reinforcement learning task requires decisions to be made over many time steps. At each step an agent selects actions (e.g. motor commands); receives observations from the world (e.g. robotic sensors); and receives a reward indicating its success or failure (e.g. a negative reward for crashing). Given only its actions, observations and rewards, how can an agent improve its performance?

Reinforcement learning (RL) can be subdivided into two fundamental problems: *learning* and *planning*. The goal of learning is for an agent to improve its policy from its interactions with the world. The goal of planning is for an agent to improve its policy without further interaction with the world. The agent can deliberate, reason, ponder, think or search, so as to find the best behaviour in the available computation time.

Despite the apparent differences between these two problems, they are intimately related. During learning, the agent interacts with the real world, by executing actions and observing their consequences. During planning the agent can interact with a *model* of the world: by simulating actions and observing their consequences. In both cases the agent updates its policy from its experience. Our thesis is that an agent can both learn and plan effectively using reinforcement learning algorithms.

1.3 Simple Ideas for Big Worlds

Artificial intelligence research often focuses on toy domains: small microworlds which can be easily understood and implemented, and are used to test, compare, and develop new ideas and algorithms. However, the simplicity of toy domains can also be misleading: many sophisticated ideas that work well in small worlds do not, in practice, scale up to larger and more realistic domains. In contrast, big worlds can act as a form of Occam's razor, so that the simplest and clearest ideas tend to achieve the greatest success. This can be true not only in terms of memory and computation, but also in terms of the practical challenges of implementing, debugging and testing a large program in a challenging domain.

In this thesis we combine five simple ideas for achieving high performance in big worlds. Four of the five ideas are well-established in the reinforcement learning community; the fifth idea of *temporality* is developed in this thesis. All five ideas are brought together in the *temporal-difference* *search* algorithm (see Chapter 6).

1.3.1 Value Function

The *value function* estimates the expected outcome from any given state, after any given action. The value function can be a crucial component of efficient decision-making, as it summarises the long-term effects of the agent's decisions into a single number. The best action can then be selected by simply maximising the value function.

1.3.2 State Abstraction

In large worlds, it is not possible to store a distinct value for every individual state. *State abstraction* compresses the state into a smaller number of features, which are then used in place of the complete state. Using state abstraction, the value function can be approximated by a parameterised function of the features, using many fewer parameters than there are states. Furthermore, state abstraction enables the agent to *generalise* between related states, so that a single outcome can update the value of many states.

1.3.3 Temporality

In very large worlds, state abstraction cannot usually provide an accurate approximation to the value function. For example, there are 10^{170} states in 19×19 Go. Even if the agent can store 10^{10} parameters, it is compressing the values of 10^{160} states into every parameter. The idea of *temporality* is to focus the agent's representation on the *current* region of the state space – the subproblem it is facing right now – rather than attempting to approximate the entire state space.

1.3.4 Bootstrapping

Large problems typically entail making decisions with long-term consequences. Hundreds or thousands of time-steps may elapse before the final outcome is known. These outcomes depend on all of the agent's decisions, and on the world's uncertain responses to those decisions, throughout all of these time-steps. *Bootstrapping* provides a mechanism for reducing the variance of the agent's evaluation. Rather than waiting until the final outcome is reached, the idea of bootstrapping is to make an evaluation based on subsequent evaluations. For example, the *temporal-difference learning* algorithm estimates the current value from the estimated value at the next time-step.

1.3.5 Sample-Based Planning

The agent's experience with its world is limited, and may not be sufficient to achieve good performance in the world. The idea of *sample-based planning* is to simulate hypothetical experience, using a *model* of the world. The agent can use this simulated experience, in place of or in addition to its real experience, to learn to achieve better performance.

1.4 Game-Tree Search

The challenge of search is to find, by a process of computation, an approximately optimal action from some root state. The importance of search is clearly demonstrated in two-player games, where *game-tree search* algorithms such as alpha-beta search and Monte-Carlo tree search have achieved remarkable success.

1.4.1 Alpha-Beta Search

In classic games such as chess (Campbell et al., 2002), checkers (Schaeffer et al., 1992) and Othello (Buro, 1999), traditional search algorithms have exceeded human levels of performance. In each of these games, master-level play has also been achieved by a reinforcement learning approach (Veness et al., 2009; Schaeffer et al., 2001; Buro, 1999):

- Positions are represented by many binary features corresponding to useful concepts: for example features identifying the presence of a particular piece, or a particular configuration of pieces.
- Positions are evaluated by summing the values of all features that are matched by the current position.
- The value of each feature is learnt offline, from many training games of self-play.
- The learnt evaluation function is used in a high-performance alpha-beta search.

Despite these impressive successes, there are many domains in which traditional search methods have had limited success. In very large domains, it is often difficult to construct an evaluation function with any degree of accuracy. We cannot reasonably expect to accurately approximate the value of all distinct states in the game of Go; all attempts to do so have achieved a position evaluation that, at best, corresponds to weak amateur-level humans (Müller, 2002).

We introduce a new approach to position evaluation in large domains. Rather than trying to approximate the entire state space, our idea is to specialise the evaluation function to the current region of the state space. Instead of approximating the value of every possible position, we only approximate the positions that occur in the subgame starting from *now*. In this way, the evaluation function can represent much more detailed knowledge than would otherwise be possible, and can adapt to the nuances and exceptional circumstances of the current position. In chess, it could know that the black rook should defend the unprotected queenside and not be developed to the open file; in checkers that a particular configuration of checkers is vulnerable to the opponent's dynamic king; or in Othello that two adjacent White discs at the top of the board give a crucial advantage in the embattled central columns.

We implement this new idea by a simple modification to the above framework:

- The value of each feature is learnt *online*, from many training games of self-play *from the current position*.

In prior work on learning to evaluate positions, the evaluation function was trained offline, typically over weeks or even months of computation (Tesauro, 1994; Enzenberger, 2003). In our approach, this training is performed in real-time, in just a few seconds of computation. At the start of each game the evaluation function is initialised to the best global weights. But after every move, the evaluation function is retrained online, from games of self-play that start from the current position. In this way, the evaluation function evolves dynamically throughout the course of the game, specialising more and more to the particular tactics and strategies that are relevant to *this* game and *this* position. We demonstrate that this approach can provide a dramatic improvement to the quality of position evaluation; in 9×9 Go it increased the performance of our alpha-beta search program by 800 Elo points in competitive play (see Chapter 7).

1.4.2 Monte-Carlo Tree Search

Monte-Carlo tree search (Coulom, 2006) is a new paradigm for search, which has revolutionised computer Go (Coulom, 2007; Gelly and Silver, 2008), and is rapidly replacing traditional search algorithms as the method of choice in challenging domains such as General Game Playing (Finnsson and Björnsson, 2008), multi-player card games (Schäfer, 2008; Sturtevant, 2008), and real-time strategy games (Balla and Fern, 2009).

The key idea is to simulate many thousands of games from the current position, using self-play. New positions are added into a search tree, and each node of the tree contains a value that predicts whether the game will be won from that position. These predictions are learnt by Monte-Carlo simulation: the value of a node is simply the average outcome of all simulated games that visit the position. The search tree is used to guide simulations along promising paths, by selecting the child node with the highest potential value (Kocsis and Szepesvari, 2006). This encourages exploration of rarely visited positions, and results in a highly selective search that very quickly identifies good move sequences.

The evaluation function of Monte-Carlo tree search is grounded in experience: it depends only on the observed outcomes of simulations, and does not require any human knowledge. Additional simulations continue to improve the evaluation function; given infinite memory and computation, it will converge on the true minimax value (Kocsis and Szepesvari, 2006). Furthermore, also unlike full-width search algorithms such as alpha-beta search, Monte-Carlo tree search develops in a highly selective, best-first manner, expanding the most promising regions of the search space much more deeply.

However, despite its revolutionary impact, Monte-Carlo tree search suffers from a number of serious deficiencies:

- The first time a position is encountered, its value is completely unknown.

- Each position is evaluated independently, with no generalisation between similar positions.
- Many simulations are required before Monte-Carlo can establish a high confidence estimate of the value.
- The overall performance depends critically on the rollout policy used to complete simulations.

This thesis extends the core concept of Monte-Carlo search into a broader framework for simulation-based search, which specifically addresses these weaknesses:

- New positions are assigned initial values using a learnt, global evaluation function (Chapters 7, 8).
- Positions are evaluated by a linear combination of features (Chapters 6 and 7), or by generalising between the value of the same move in similar situations (Chapter 8).
- Positions are evaluated by applying temporal-difference learning, rather than Monte-Carlo, to the simulations (Chapters 6 and 7).
- The rollout policy is learnt and optimised automatically by simulation balancing (Chapter 9).

1.5 Overview

In the first part of the thesis, we survey the relevant research literature:

- In Chapter 2 we review the key concepts of reinforcement learning.
- In Chapter 3 we review sample-based planning and simulation-based search methods.
- In Chapter 4 we review the recent history of computer Go, focusing in particular on reinforcement learning approaches and the Monte-Carlo revolution.

In the second part of the thesis, we introduce our general framework for learning and search.

- In Chapter 5 we investigate how a position evaluation function can be learnt for the game of Go, with no prior knowledge except for the basic grid structure of the board. We introduce the idea of *local shape features*, which abstract the state into a large vector of binary features, and we use temporal-difference learning to train the weights of these features. Using this approach, we were able to learn a fast and effective position evaluation function.
- In Chapter 6 we develop temporal-difference learning into a high-performance search algorithm. The *temporal-difference search* algorithm is a new approach to simulation-based search that uses state abstraction and bootstrapping to search more efficiently in large domains. We demonstrate that temporal-difference search substantially outperforms temporal-difference learning in 9×9 Go. In addition, we show that temporal-difference search, without

any explicit search tree, outperforms an unenhanced Monte-Carlo tree search with equivalent domain knowledge, for up to 10,000 simulations per move.

- In Chapter 7 we combine temporal-difference learning and temporal-difference search, using long and short-term memories, in the *Dyna-2* architecture. We implement Dyna-2, using local shape features in both the long and short-term memories, in our Go program *RLGO*. Using Dyna-2 in 9×9 Go, *RLGO* achieved a higher rating on the Computer Go Server than any handcrafted, traditional search , or traditional machine learning program. We also introduce a *hybrid search* that combines Dyna-2 with alpha-beta. Using hybrid search, *RLGO* achieved a rating comparable to or exceeding many Monte-Carlo tree search programs, although still significantly weaker than the strongest programs.

In the third part of the thesis, we apply our general framework to Monte-Carlo tree search.

- In Chapter 8 we introduce two extensions to Monte-Carlo tree search. The *RAVE* algorithm rapidly generalises between related parts of the search-tree. The *heuristic Monte-Carlo tree search* algorithm incorporates prior knowledge into the nodes of the search-tree. The new algorithms were implemented in the Monte-Carlo program *MoGo*. Using these extensions, *MoGo* became the first program to achieve *dan*-strength at 9×9 Go, and the first program to beat a professional human player at 9×9 Go. In addition, *MoGo* won the gold medal at the 2007 19×19 computer Go olympiad.

- In Chapter 9 we introduce the paradigm of *Monte-Carlo simulation balancing*, and develop the first efficient algorithms for optimising the performance of Monte-Carlo search by adjusting the parameters of a rollout policy. On small 5×5 and 6×6 boards, given equivalent representations and equivalent training data, we demonstrate that rollout policies learnt by our new paradigm exceed the performance of both supervised learning and reinforcement learning paradigms, by a margin of more than 200 Elo.

Finally, we conclude with a general discussion and appendices.

- In Chapter 10 we discuss several of the ideas we tried that were not successful in computer Go. We also suggest some possible directions for future work, and discuss how the ideas in this thesis could be used in other applications.

- In Appendix A we introduce the *logistic temporal-difference learning* algorithm. This algorithm is specifically tailored to problems, such as games or puzzles, in which there is a binary outcome for success or failure. By treating the value function as a *success probability*, we extend the probabilistic framework of logistic regression to temporal-difference learning.

Part I

Literature Review

Chapter 2

Reinforcement Learning

2.1 Learning and Planning

A wide variety of tasks in artificial intelligence and control can be formalised as sequential decision-making processes. We refer to the decision-making entity as the *agent*, and everything outside of the agent as its *environment*. At each time-step t the agent receives observations $s_t \in \mathcal{S}$ from its environment, and executes an action $a_t \in \mathcal{A}$ according to its behaviour policy. The environment then provides a feedback signal in the form of a reward $r_{t+1} \in \mathbb{R}$. This time series of actions, observations and rewards defines the agent's *experience*. The goal of *reinforcement learning* is to improve the agent's future reward given its past experience.

2.2 Markov Decision Processes

If the next observation and reward depend only on the current observation and action,

$$Pr(s_{t+1}, r_{t+1} | s_1, a_1, r_1, ..., s_t, a_t, r_t) = Pr(s_{t+1}, r_{t+1} | s_t, a_t), \tag{2.1}$$

then the task is a *Markov decision-making process* (MDP) (Puterman, 1994). The current observation s_t summarises all previous experience and is described as the *Markov state*. If a task is *fully observable* then the agent receives a Markov state s_t at every time-step; otherwise the task is described as *partially observable*. This thesis is concerned primarily with fully observable tasks; unless otherwise specified all states s are assumed to be Markov. It is also primarily concerned with MDPs in which both the state space $\mathcal{S}$ and the action space $\mathcal{A}$ are finite.

The dynamics of an MDP, from any state s and for any action a, are determined by *transition probabilities*, $\mathcal{P}^a_{ss'}$, specifying the distribution over the next state s'. A *reward function*, $\mathcal{R}^a_{ss'}$, specifies the expected reward for a given state transition,

$$\mathcal{P}^a_{ss'} = Pr(s_{t+1} = s' | s_t = s, a_t = a) \tag{2.2}$$

$$\mathcal{R}^a_{ss'} = \mathbb{E}[r_{t+1} | s_t = s, s_{t+1} = s', a_t = a]. \tag{2.3}$$

Model-based reinforcement learning methods, such as dynamic programming, assume that the dynamics of the MDP are known. *Model-free* reinforcement learning methods, such as Monte-Carlo evaluation or temporal-difference learning, learn directly from experience and do not assume any knowledge of the environment's dynamics.

In episodic (finite horizon) tasks there is a distinguished terminal state. The *return* $R_t = \sum_{k=t}^{T} r_k$ is the total reward accumulated in that episode from time t until reaching the terminal state at time T. For example, the reward function for a game could be $r_t = 0$ at every move $t < T$, and $r_T = z$ at the end of the game, where z is the final score or outcome; the return would then simply be the score for that game.[1]

The agent's action-selection behaviour can be described by a *policy*, $\pi(s, a)$, that maps a state s to a probability distribution over actions, $\pi(s, a) = Pr(a_t = a | s_t = s)$.

2.3 Value-Based Reinforcement Learning

Many successful examples of reinforcement learning use a *value function* to summarise the long-term consequences of a particular decision-making policy (Abbeel et al., 2007; Tesauro, 1994; Schaeffer et al., 2001; Singh and Bertsekas, 1997; Ernst et al., 2005).

The value function $V^\pi(s)$ is the expected return from state s when following policy π. The action value function $Q^\pi(s, a)$ is the expected return after selecting action a in state s and then following policy π,

$$V^\pi(s) = \mathbb{E}_\pi[R_t | s_t = s] \tag{2.4}$$

$$Q^\pi(s, a) = \mathbb{E}_\pi[R_t | s_t = s, a_t = a]. \tag{2.5}$$

where $\mathbb{E}_\pi$ indicates the expectation over episodes of experience generated with policy π.

The *optimal value function* $V^*(s)$ is the unique value function that maximises the value of every state, $V^*(s) = \max\limits_\pi V^\pi(s) \forall s \in \mathcal{S}$ and $Q^*(s, a) = \max\limits_\pi Q^\pi(s, a) \forall s \in \mathcal{S}, a \in \mathcal{A}$. An *optimal policy* $\pi^*(s, a)$ is a policy that maximises the action value function from every state in the MDP, $\pi^*(s, a) = \operatorname*{argmax}\limits_\pi Q^\pi(s, a)$.

Value-based reinforcement learning algorithms use an iterative cycle of *policy evaluation* and *policy improvement*. During policy evaluation, a value function $V(s) \approx V^\pi(s)$ or $Q(s, a) \approx Q^\pi(s, a)$ is estimated for the agent's current policy. This value function can then be used to improve the policy, for example by selecting actions greedily with respect to the new value function. The improved policy is then evaluated, and so on, in a cyclic process that lies at the heart of value-based reinforcement learning (Sutton and Barto, 1998).

[1] In continuing (infinite horizon) tasks, it is common to discount the future rewards. For clarity of presentation, we restrict our attention to episodic tasks with no discounting.

The value function is updated by an appropriate *backup* operator. In model-based reinforcement learning algorithms such as value iteration, the value function is updated by a *full backup*, which uses the model to perform a full-width lookahead over all possible actions and all possible state transitions. In model-free reinforcement learning algorithms such as Monte-Carlo evaluation and temporal-difference learning, the value function is updated by a *sample backup*. At each time-step a single action is sampled from the agent's policy, and a single state transition and reward are sampled from the environment. The value function is then updated from this sampled experience.

2.3.1 Dynamic Programming

An important property of the optimal value function is that it maximises the expected value following from any action. This recursive property is known as the *Bellman equation* (Bellman, 1957),

$$V^*(s) = \max_{a \in \mathcal{A}} \sum_{s' \in \mathcal{S}} \mathcal{P}^a_{ss'} \left[\mathcal{R}^a_{ss'} + V^*(s') \right] \forall s \in \mathcal{S} \tag{2.6}$$

Dynamic programming can be used to iteratively update the value function, so as to satisfy the Bellman equation. The *value iteration* algorithm updates the value function using a full backup based directly on the Bellman equation, which we call an *expectimax backup*,

$$V(s) \leftarrow \max_{a \in \mathcal{A}} \sum_{s' \in \mathcal{S}} \mathcal{P}^a_{ss'} \left[\mathcal{R}^a_{ss'} + V(s') \right] \tag{2.7}$$

If all states are updated by expectimax backups infinitely many times, value iteration converges on the optimal value function (Bertsekas, 2007).

2.3.2 Monte-Carlo Evaluation

Monte-Carlo evaluation provides a particularly simple, model-free method for policy evaluation (Sutton and Barto, 1998). The value function for each state s is estimated by the average return from all episodes that visited state s,

$$V(s) = \frac{1}{N(s)} \sum_{i=1}^{N(s)} R^i(s), \tag{2.8}$$

where $R^i(s)$ is the return following the i^{th} visit to s, and $N(s)$ counts the total number of visits to state s. Monte-Carlo evaluation can equivalently be implemented by a sample backup, called a *Monte-Carlo backup*, that is applied incrementally at each time-step t,

$$N(s_t) \leftarrow N(s_t) + 1 \tag{2.9}$$

$$V(s_t) \leftarrow V(s_t) + \frac{1}{N(s_t)}(R_t - V(s_t)), \tag{2.10}$$

where $N(s)$ and $V(s)$ are initialised to zero.

At each time-step, Monte-Carlo evaluation updates the value of the current state towards the return. However, this return depends on the action and state transitions that were sampled in every subsequent state, which may be a very noisy signal. In general, Monte-Carlo provides an unbiased, but high variance estimate of the true value function $V^\pi(s)$.

2.3.3 Temporal Difference Learning

Bootstrapping is a general method for reducing the variance of an estimate, by updating a guess from a guess. *Temporal-difference learning* is a model-free method for policy evaluation that bootstraps the value function from subsequent estimates of the value function.

In the TD(0) algorithm, the value function is bootstrapped from the very next time-step. Rather than waiting until the complete return has been observed, the value function of the next state is used to approximate the expected return. The *TD-error* $\delta_t = r_{t+1} + V(s_{t+1}) - V(s_t)$ is measured between the value at state s_t, and the value at the subsequent state s_{t+1}, plus any reward r_{t+1} accumulated along the way. For example, if the agent thinks that Black is winning in position s_t, but that White is winning in the next position s_{t+1}, then this inconsistency generates a TD-error. The TD(0) algorithm adjusts the value function so as to correct the TD-error and make it more consistent with the subsequent value,

$$\delta_t = r_{t+1} + V(s_{t+1}) - V(s_t) \tag{2.11}$$

$$\Delta V(s_t) = \alpha \delta_t \tag{2.12}$$

where α is a step-size parameter controlling the learning rate.

2.3.4 TD(λ)

The idea of the TD(λ) algorithm is to bootstrap the value of a state from the subsequent values many steps into the future. The parameter λ determines the temporal span over which bootstrapping occurs. At one extreme, TD(0) bootstraps the value of a state only from its immediate successor. At the other extreme, TD(1) updates the value of a state from the final return; it is equivalent to Monte-Carlo evaluation.

To implement TD(λ) incrementally, an eligibility trace $e(s)$ is maintained for each state. The eligibility trace represents the total credit that should be assigned to a state for any subsequent errors in evaluation. It combines a *recency heuristic* with a *frequency heuristic*: states which are visited most frequently and most recently are given the greatest eligibility (Sutton, 1984). The eligibility trace is incremented each time the state is visited, and decayed by a constant parameter λ at every time-step (Equation 2.13). Every time a difference is seen between the predicted value and the subsequent value, a *TD-error* δ_t is generated. The value function for all states is updated in proportion to both the TD-error and the eligibility of the state,

$$e_t(s) = \begin{cases} \lambda e_{t-1}(s) & \text{if } s \neq s_t \\ \lambda e_{t-1}(s) + 1 & \text{if } s = s_t \end{cases} \tag{2.13}$$

$$\delta_t = r_{t+1} + V_t(s_{t+1}) - V_t(s_t) \tag{2.14}$$

$$\Delta V_t(s) = \alpha \delta_t e_t(s). \tag{2.15}$$

This form of eligibility update is known as an *accumulating* eligibility trace. An alternative update, known as a *replacing* eligibility trace, can be more efficient in some environments (Singh and Sutton, 2004),

$$e_t(s) = \begin{cases} \lambda e_{t-1}(s) & \text{if } s \neq s_t \\ 1 & \text{if } s = s_t \end{cases} \tag{2.16}$$

$$\delta_t = r_{t+1} + V_t(s_{t+1}) - V_t(s_t) \tag{2.17}$$

$$\Delta V_t(s) = \alpha \delta_t e_t(s). \tag{2.18}$$

If all states are visited infinitely many times, and with appropriate choice of step-size, temporal-difference learning converges on the true value function V^π for all values of λ, for both accumulating traces (Dayan, 1994) and replacing traces (Singh and Sutton, 2004).

2.3.5 Control

Policy evaluation methods, such as Monte-Carlo evaluation or temporal-difference learning, can be combined with policy improvement to learn the optimal policy in an MDP. Rather than evaluating the value function $V(s)$, the action value function $Q(s, a)$ is evaluated instead. After each step of evaluation, the policy is improved, by using the latest action values to select the best actions.

The Sarsa algorithm (Rummery and Niranjan, 1994) combines temporal difference learning with ϵ*-greedy* policy improvement. The action value function is evaluated by the TD(λ) algorithm. An ϵ-greedy policy is used to combine exploration (selecting a random action with probability ϵ) with exploitation (selecting $\underset{a}{\text{argmax}}\ Q(s, a)$ with probability $1 - \epsilon$). The action value function is updated online from each tuple $(s_t, a_t, r_{t+1}, s_{t+1}, a_{t+1})$ of experience, using the TD(λ) update rule for action values. If all states are visited infinitely many times, and ϵ decays to zero in the limit, the Sarsa(0) algorithm converges on the optimal policy (Singh et al., 2000).

Similarly, *Monte-Carlo control* (Sutton and Barto, 1998) combines Monte-Carlo evaluation with ϵ-greedy policy improvement. The action value function is updated after each episode. Each action value $Q(s_t, a_t)$ is updated to the mean outcome of all episodes in which action a_t was selected in state s_t. Monte-Carlo control is equivalent to the Sarsa algorithm with $\lambda = 1$ and updates applied offline after each episode (Sutton and Barto, 1998). Under the same conditions as Sarsa, Monte-Carlo control also converges on the optimal policy (Tsitsiklis, 2002).

2.3.6 Value Function Approximation

In large environments, it is not possible or practical to learn a value for each individual state. In this case, it is necessary to represent the state more compactly, by using some set of *features* $\phi(s)$ of the state s. The value function can then be approximated by a function of the features and parameters θ. For example, a set of binary features $\phi(s) \in \{0,1\}^n$ can be used to abstract the state space, where each binary feature $\phi_i(s)$ identifies a particular property of the state. A common and successful methodology (Sutton, 1996) is to use a linear combination of features and parameters to approximate the value function, $V(s) = \phi(s) \cdot \theta$.

We refer to the case when no value function approximation is used, in other words when each state has a distinct value, as *table lookup*. Linear function approximation includes table lookup as one possible representation. In this special case, we define a *table lookup feature*, $I^{s'}$, to match each individual state $s' \in \mathcal{S}$,

$$I^{s'}(s) = \begin{cases} 1 & \text{if } s = s' \\ 0 & \text{otherwise.} \end{cases} \tag{2.19}$$

The feature vector consists of one table lookup feature for each state, $\phi_i(s) = I^{s_i}(s)$. A state s is then represented by a unit vector of size $|\mathcal{S}|$ with a one in the sth component and zeros elsewhere. The value of state s is represented by the sth parameter, $V(s) = \theta_s$.

2.3.7 Linear Monte-Carlo Evaluation

When the value function is approximated by a parameterised function of features, errors could be attributed to any or all of those features. *Gradient descent* provides a principled approach to this problem of credit assignment: the parameters are updated in the direction that minimises the mean-squared error.

Monte-Carlo evaluation can be generalised to use value function approximation. The parameters are adjusted so as to reduce the mean-squared error between the estimated value and the actual return. When linear function approximation is used, Monte-Carlo evaluation has a particularly simple form. The parameters are updated by stochastic gradient descent (Widrow and Stearns, 1985), with a step-size of α,

$$\begin{aligned} \Delta\theta &= -\frac{\alpha}{2}\nabla_\theta(R_t - V(s_t))^2 && (2.20) \\ &= \alpha(R_t - V(s_t))\nabla_\theta V(s_t) && (2.21) \\ &= \alpha(R_t - V(s_t))\phi(s_t) && (2.22) \end{aligned}$$

If table lookup features are used, and the step-size varies according to the schedule $\alpha_t = \frac{1}{N(s_t)}$, then linear Monte-Carlo evaluation is equivalent to incremental Monte-Carlo evaluation (see Section 2.3.2),

$$\Delta V(s) = (\Delta\theta) \cdot \phi(s) \tag{2.23}$$
$$= \alpha_t(R_t - V(s_t))\phi(s_t) \cdot \phi(s) \tag{2.24}$$
$$= \frac{1}{N(s_t)}(R_t - V(s_t))I(s_t) \cdot I(s) \tag{2.25}$$
$$= \frac{1}{N(s)}(R_t - V(s)) \tag{2.26}$$

2.3.8 Linear Temporal-Difference Learning

The gradient descent method of the previous section can be extended to temporal difference learning. The key idea is to replace the target, R_t, in Equation 2.21, with the estimated value at the next time-step, $r_{t+1} + V(s_{t+1})$ (Sutton, 1984). It is important to note that this introduces bias, and it is no longer a true gradient descent algorithm. Nevertheless, the analogy with gradient descent methods provides a useful intuition for understanding the algorithm.

Temporal-difference learning with linear function approximation is a particularly simple case (Sutton and Barto, 1998). The parameters are updated in proportion to the TD-error and the feature value,

$$\Delta\theta = (r_{t+1} + V(s_{t+1}) - V(s_t))\nabla_\theta V(s_t) \tag{2.27}$$
$$= \alpha\delta_t\phi(s_t). \tag{2.28}$$

The linear TD(λ) algorithm is defined similarly (Sutton, 1988). Using accumulating traces, the weights are updated in proportion to the TD-error and the eligibility trace,

$$e_t = \lambda e_{t-1} + \phi(s) \tag{2.29}$$
$$\Delta\theta = \alpha\delta_t e_t. \tag{2.30}$$

If the agent's experience is generated from its own policy, a case known as *on-policy* learning, linear temporal-difference learning converges to a value function that has a mean-squared error within $(1 - \gamma\lambda)/(1 - \gamma)$ of the best possible approximation (Tsitsiklis and Roy, 1997), where γ is a discount factor in continuing environments, or a horizon dependent constant in episodic environments.

The linear Sarsa algorithm combines linear temporal-difference learning with the Sarsa algorithm, by updating an action value function and using an epsilon-greedy policy to select actions. The complete linear Sarsa(λ) algorithm is shown in Algorithm 1. Although there are no guarantees of convergence, on-policy linear Sarsa chatters without divergence (Gordon, 1996).

Algorithm 1 Sarsa(λ)

```
procedure SARSA($\lambda$)
    $\theta \leftarrow 0$                                        ▷ Clear weights
    loop
        $s \leftarrow s_0$                                 ▷ Start new episode in initial state
        $e \leftarrow 0$                                   ▷ Clear eligibility trace
        $a \leftarrow \epsilon$-greedy action from state $s$
        while $s$ is not terminal do
            Execute $a$, observe reward $r$ and next state $s'$
            $a' \leftarrow \epsilon$-greedy action from state $s'$
            $\delta \leftarrow r + Q(s', a') - Q(s, a)$            ▷ Calculate TD-error
            $\theta \leftarrow \theta + \alpha \delta e$                 ▷ Update weights
            $e \leftarrow \lambda e + \phi(s, a)$                ▷ Update eligibility trace
            $s \leftarrow s', a \leftarrow a'$
        end while
    end loop
end procedure
```

2.4 Policy Gradient Reinforcement Learning

Instead of updating a value function, the idea of policy gradient reinforcement learning is to directly update the parameters of the agent's policy by gradient ascent, so as to maximise the agent's average reward per time-step. Policy gradient methods are typically higher variance and therefore less efficient than value-based approaches, but they have three significant advantages. First, they are able to directly learn *mixed strategies* that are a stochastic balance of different actions. Second, they have better convergence properties than value-based methods: they are guaranteed to converge on a policy that is at least locally optimal. Finally, they are able to learn a parameterised policy even in problems with continuous action spaces.

The REINFORCE algorithm (Williams, 1992) updates the parameters of the agent's policy by stochastic gradient ascent. Given a differentiable policy $\pi_p(s, a)$ that is parameterised by a vector of adjustable weights p, the REINFORCE algorithm updates those weights at every time-step t,

$$\Delta p = \beta(R_t - b(s_t)) \log \nabla_p \pi_p(s_t, a_t) \tag{2.31}$$

where β is a step-size parameter and b is a *reinforcement baseline* that does not depend on the current action a_t.

Policy gradient algorithms (Sutton et al., 2000) extend this approach to use the action value function in place of the actual return,

$$\Delta p = \beta(Q^\pi(s_t, a_t) - b(s_t)) \log \nabla_p \pi_p(s_t, a_t) \tag{2.32}$$

Actor-critic algorithms combine the advantages of policy gradient methods with the efficiency of value-based reinforcement learning. They consist of two components: an *actor* that updates the agent's policy, and a *critic* that updates the action value function. When value function approximation is used, care must be taken to ensure that the critic's parameters θ are *compatible* with the actor's parameters p. The compatibility requirement is that $\nabla_\theta Q_\theta(s,a) = \nabla_p \log \pi_p(s,a)$.

2.5 Exploration and Exploitation

The ϵ-greedy policy used in the Sarsa algorithm provides one simple approach to balancing exploration with exploitation. However, more sophisticated strategies are also possible. We mention two of the most common approaches here.

First, exploration can be skewed towards more highly valued states, for example by using a *softmax policy*,

$$\pi(s,a) = \frac{e^{Q(s,a)/\tau}}{\sum_b e^{Q(s,b)/\tau}} \tag{2.33}$$

where τ is a parameter controlling the temperature (level of stochasticity) in the policy.

A second approach is to apply the principle of *optimism in the face of uncertainty*, for example by adding a bonus to the value function that is largest in the most uncertain states. The UCB1 algorithm (Auer et al., 2002) follows this principle, by maximising an upper confidence bound on the value function,

$$Q^\oplus(s,a) = Q(s,a) + \sqrt{\frac{2\log N(s)}{N(s,a)}} \tag{2.34}$$

$$\pi(s,a) = \operatorname*{argmax}_b Q^\oplus(s,b) \tag{2.35}$$

where $N(s)$ counts the number of visits to state s, and $N(s,a)$ counts the number of times that action a has been selected from state s.

Chapter 3

Search and Planning

3.1 Introduction

Planning and *search* have been widely applied, in a variety of different forms, across much of artificial intelligence. We adopt the definition of planning typically used in reinforcement learning (Sutton and Barto, 1998), and the definition of search that is often used in two-player games (Schaeffer, 2000).

Planning is the process of computation by which the agent updates its action selection policy $\pi(s, a)$. The agent is given some amount of thinking time in which to plan. During this time it has no interaction with the environment, but can perform many steps of internal computation. The result of planning is a new policy, which can then be used to select actions in any state s in the problem.

Search refers to the process of computation that is used to select an action from a particular root state s_0. A search algorithm can be used for planning, by executing a search from the agent's current state s_t, an approach that is sometimes referred to as *real-time search* (Korf, 1990). Rather than providing a complete policy over all states, this provides a partial policy for the current state s_t and its successors. By focusing on the current state, real-time search methods can be considerably more efficient than general planning methods.

3.2 Planning

Most planning methods use a model of the environment. This model can either be solved directly, by applying model-based reinforcement learning methods, or indirectly, by sampling the model and applying model-free reinforcement learning methods.

3.2.1 Model-Based Planning

As we saw in the previous chapter, fully observable environments can be represented by an MDP M with state transition probabilities $\mathcal{P}^a_{ss'}$ and a reward function $\mathcal{R}^a_{ss'}$. In general, the agent does not know the true dynamics of the environment, but it may know or learn an approximate *model* of its environment, represented by state transition probabilities $\hat{\mathcal{P}}^a_{ss'}$ and a reward function $\hat{\mathcal{R}}^a_{ss'}$.

The idea of model-based planning is to apply model-based reinforcement learning methods, such as dynamic programming, to the MDP $\hat{M}$ described by the model $\hat{\mathcal{P}}^a_{ss'}, \hat{\mathcal{R}}^a_{ss'}$. The success of this approach depends largely on the accuracy of the model. If the model is accurate, then a good policy for $\hat{M}$ will also perform well in the agent's actual environment M. If the model is inaccurate, the policy acquired from planning can perform arbitrarily poorly in M.

3.2.2 Sample-Based Planning

In reinforcement learning, the agent samples experience from the real world: it executes an action at each time-step, observes its consequences, and updates its policy. In sample-based planning the agent samples experience from a model of the world: it *simulates* an action at each computational step, observes its consequences, and updates its policy. This symmetry between learning and planning has an important consequence: algorithms for reinforcement learning can also become algorithms for planning, simply by substituting simulated experience in place of real experience.

Sample-based planning requires a *generative model* that can sample state transitions and rewards from $\hat{\mathcal{P}}^a_{ss'}$ and $\hat{\mathcal{R}}^a_{ss'}$ respectively. However, it is not necessary to know these probability distributions; the next state and reward could, for example, be generated by a black box simulator. In complex problems, such as large MDPs or two-player games, it can be much easier to provide a generative model (e.g. a program simulating the environment or the opponent's behaviour) than to describe the complete probability distribution.

Given a generative model, the agent can sample experience and receive a hypothetical reward. The agent's task is to learn how to maximise its total expected reward, from this hypothetical experience. Thus, each model specifies a new reinforcement learning problem, which itself can be solved by model-free reinforcement learning algorithms.

3.2.3 Dyna

The Dyna architecture (Sutton, 1990) combines reinforcement learning with sample-based planning. The agent learns a model of the world from real experience, and updates its action-value function from both real and sampled experience. Before each real action is selected, the agent executes some number of iterations of sample-based planning.

The *Dyna-Q* algorithm utilises a memory-based model of the world. It remembers all state transitions and rewards from all visited states and selected actions. During each iteration of planning, a previously visited start state and action is selected, and a state transition and reward are sampled from the memorised experience. Temporal-difference learning is used to update the action-value function after each sampled transition (planning), and also after each real transition (learning).

Algorithm	Traversal	Backup
A*	Best-first	Max
Alpha-Beta	Depth-first	Minimax
Expectimax	Depth-first	Expectimax
Sparse sampling	Depth-first	Sample max
Simulation-based tree search	Sequentially best-first	Sample max
Monte-Carlo tree search	Sequentially best-first	Monte-Carlo

Table 3.1: A taxonomy of search algorithms.

3.3 Search

Most search algorithms construct a *search tree* from a root state s_0, where each node of the tree corresponds to a descendent state of s_0. The nodes of the search tree are *traversed* in a particular order. Leaf nodes may be *expanded* by the search algorithm, to add their successors into the search tree. Interior nodes are evaluated by a *backup* of the values in the search tree. Table 3.1 summarises the traversal and backup strategies of several well-known search algorithms.

3.3.1 Full-Width Search

A *full-width search* considers all possible actions and all successor states from each internal node of the search tree. A *fixed-depth* search expands nodes of the search tree exhaustively up to some fixed depth. A *variable-depth* search uses a selective expansion criterion to decide which leaf nodes should be developed. The tree may be traversed in a depth-first, breadth-first, or best-first order, where the latter utilises a *heuristic function* to guide the search towards the most promising states (Russell and Norvig, 1995).

Full-width search can be applied to MDPs, so as to find the sequence of actions that leads to the maximum expected return from the current state. Full-width search can also be applied in deterministic environments, to find the sequence of actions with minimum cost. It can also be applied in two-player games, to find the optimal minimax move sequence under alternating play. In each case, heuristic search algorithms operate in a very similar manner. Leaf nodes are evaluated by the heuristic function, and interior nodes are evaluated by a full backup that updates each parent value from all of its children: an expectimax backup in MDPs, a max backup in deterministic environments, or a minimax backup in two-player games.

This very general framework can be used to categorise a number of well-known search algorithms: for example A* (Hart et al., 1968) is a best-first search with max backups; *expectimax search* (Davies et al., 1998) is a depth-first search with expectimax backups; and alpha-beta (Knuth and Moore, 1975) is a depth-first search with minimax backups.

A value function (see Chapter 2) can be used as a heuristic function. In this approach, leaf nodes are evaluated by estimating the expected return or outcome from that node (Davies et al., 1998).

3.3.2 Sample-Based Search

In *sample-based search*, instead of considering all possible successors, the next state and reward is sampled from a generative model. These samples are typically used to construct a tree, and the value of each interior node is updated by an appropriate backup operation. Random sampling in this manner breaks the curse of dimensionality (Rust, 1997). In environments with large branching factors or stochastic dynamics, sample-based search can be much more effective than full-width search.

Sparse lookahead (Kearns et al., 2002) is a depth-first approach to sample-based search. A state s is expanded by executing each action a, and sampling C successor states from the model, to generate a total of $|\mathcal{A}|C$ children. Each child is expanded recursively in depth-first order, and then evaluated by a *sample max backup*,

$$V(s) \leftarrow \max_{a \in \mathcal{A}} \frac{1}{C} \sum_{i=1}^{C} V(child(s, a, i)) \tag{3.1}$$

where $child(s, a, i)$ denotes the i^{th} child of state s for action a. Leaf nodes at maximum depth D are evaluated by a fixed value function. Finally, the action with maximum evaluation at the root node s_0 is selected. Given sufficient depth D and breadth C, this approach will generate a near-optimal policy for any MDP.

Sparse lookahead can be extended to use a more informed exploration policy. Rather than uniformly sampling each action C times, the UCB1 algorithm (see Chapter 2) can be used to select the next action to sample (Chang et al., 2005). This ensures that the best actions are tried most often, but that actions with high uncertainty are also explored.

3.3.3 Simulation-Based Search

The basic idea of *simulation-based search* is to sequentially sample episodes of experience, without backtracking, that start from the root state s_0. At each step t of simulation, an action a_t is selected according to a *simulation policy*, and a new state s_{t+1} and reward r_{t+1} is generated by the model. After every simulation, the values of states or actions are updated from the simulated experience.

Simulation-based search algorithms can be used to selectively construct a search tree. Each simulation starts from the root of the search tree, and the best action is selected at each step according to the current values in the search tree. We refer to this approach as *simulation-based tree search*. After each simulation, every visited state is added to the search tree, and the values of these states are backed up through the search tree, for example by a sample max backup (Péret and Garcia, 2004). Unlike sparse lookahead, which expands nodes in a depth-first order, simulation-based tree search is *sequentially best-first*: it selects the best child at each step of a sequential simulation. This allows the search to continually refocus its attention, each simulation, on the highest value regions of the state space. As the simulations progress, the values in the search tree become more accurate and the simulation policy becomes better informed, in a cycle of policy improvement (see Chapter 2).

3.3.4 Monte-Carlo Simulation

Monte-Carlo simulation is a very simple simulation-based search algorithm for evaluating candidate actions from a root position s_0. The search proceeds by simulating complete episodes from s_0 until termination, using a fixed simulation policy. The action-values $Q(s_0, a)$ are estimated by the mean outcome of all simulations with candidate action a.[1]

In its most basic form, Monte-Carlo simulation is only used to evaluate actions, but not to improve the simulation policy. However, the basic algorithm can be extended by progressively favouring the most successful actions, or by progressively pruning away the least successful actions (Billings et al., 1999; Bouzy and Helmstetter, 2003)

In some problems, such as backgammon (Tesauro and Galperin, 1996), Scrabble (Sheppard, 2002), Amazons (Lorentz, 2008) and Lines of Action (Winands and Y. Björnsson, 2009), it is possible to construct an accurate approximation to the value function. In these cases it can be beneficial to stop simulation before the end of the episode, and bootstrap from the estimated value at the time of stopping. This approach, known as *truncated Monte-Carlo simulation*, provides faster simulations with lower variance evaluations. In more challenging problems, such as Go (Bouzy and Helmstetter, 2003), it is hard to construct an accurate global approximation to the value function. In this case truncating simulations increases the evaluation bias more than it reduces the evaluation variance, and it is better to simulate until termination.

3.3.5 Monte-Carlo Tree Search

Monte-Carlo tree search (MCTS) is a simulation-based tree search algorithm that uses Monte-Carlo simulation to evaluate the nodes of a search tree $\mathcal{T}$ (Coulom, 2006). There is one node, $n(s)$, corresponding to each state s in the search tree. Each node contains a total count for the state, $N(s)$, and a value $Q(s, a)$ and count $N(s, a)$ for each action $a \in \mathcal{A}$.

Simulations start from the root state s_0, and are divided into two stages. When state s_t is represented in the search tree, $s_t \in \mathcal{T}$, a *tree policy* is used to select actions. Otherwise, a *default policy* is used to roll out simulations to completion. The simplest version of the algorithm, which we call *greedy MCTS*, uses a greedy tree policy during the first stage, which selects the action with the highest value, $\underset{a}{\operatorname{argmax}}\, Q(s_t, a)$; and a uniform random default policy during the second stage.

After each simulation $s_0, a_0, s_1, a_1, ..., s_T$ with return R, each node in the search tree, $\{n(s_t) | s_t \in \mathcal{T}\}$, is updated. The counts are incremented, and the value is updated to the mean return (see Section 2.3.2),

[1]In deterministic single-agent domains, the max outcome is sometimes used instead, e.g. nested Monte-Carlo search (Cazenave, 2009).

$$N(s_t) \leftarrow N(s_t) + 1 \tag{3.2}$$

$$N(s_t, a_t) \leftarrow N(s_t, a_t) + 1 \tag{3.3}$$

$$Q(s_t, a_t) \leftarrow Q(s_t, a_t) + \frac{R - Q(s_t, a_t)}{N(s_t, a_t)}, \tag{3.4}$$

In addition, each visited node is added to the search tree. Alternatively, to reduce memory requirements, just one new node can be added to the search tree, for the first state that is not represented in the tree. Figure 3.1 illustrates several steps of the MCTS algorithm.

3.3.6 UCT

The UCT algorithm (Kocsis and Szepesvari, 2006) is a Monte-Carlo tree search that treats each state of the search tree as a multi-armed bandit.[2] The tree policy selects actions by using the UCB1 algorithm (see Chapter 2). The action value is augmented by an exploration bonus that is highest for rarely visited state-action pairs, and the tree policy selects the action a^* maximising the augmented value,

$$Q^{\oplus}(s, a) = Q(s, a) + c\sqrt{\frac{2 \log N(s)}{N(s, a)}} \tag{3.5}$$

$$a^* = \operatorname*{argmax}_a Q^{\oplus}(s, a) \tag{3.6}$$

where c is a scalar *exploration constant*. Pseudocode for the UCT algorithm is given in Algorithm 2.

UCT is proven to converge in MDPs with finite horizon T, rewards in the interval $[0, 1]$, and an exploration constant $c = T$. As the number of simulations N grows to infinity, the root values converge in probability to the optimal values, $\forall a \in \mathcal{A}, \operatorname*{plim}_{n \to \infty} Q(s_0, a) = Q^*(s_0, a)$. Furthermore, the bias of the root values, $\mathbb{E}[Q(s_0, a) - Q^*(s_0, a)]$, is $O(\log(n)/n)$, and the probability of selecting a suboptimal action, $Pr(\operatorname*{argmax}_{a \in \mathcal{A}} Q(s_0, a) \neq \operatorname*{argmax}_{a \in \mathcal{A}} Q^*(s_0, a))$, converges to zero at a polynomial rate.

The performance of UCT can often be significantly improved by incorporating domain knowledge into the default policy (Gelly et al., 2006). The UCT algorithm, using a carefully chosen default policy, has outperformed previous approaches to search in a variety of challenging games, including Go (Gelly et al., 2006), General Game Playing (Finnsson and Björnsson, 2008), Amazons (Lorentz, 2008), Lines of Action (Winands and Y. Björnsson, 2009), multi-player card games (Schäfer, 2008; Sturtevant, 2008), and real-time strategy games (Balla and Fern, 2009). Much additional research in Monte-Carlo tree search has been developed in the context of computer Go, and is discussed in more detail in the next chapter.

[2]In fact, the search tree is not a true multi-armed bandit, as there is no real cost to exploration during planning. In addition the simulation policy continues to change as the search tree is updated, which means that the payoff is non-stationary.

Algorithm 2 UCT

```
procedure UctSearch($s_0$)
    while time remaining do
        $\{s_0, ..., s_T\}, R = $ Simulate($s_0$)
        Backup($\{s_0, ..., s_T\}, R$)
    end while
    return $\underset{a \in \mathcal{A}}{\operatorname{argmax}} Q(s_0, a)$
end procedure

procedure Simulate($s_0$)
    $t = 0$
    $R = 0$
    repeat
        if $s_t \in \mathcal{T}$ then
            $a = $ UCB1($s_t$)
        else
            NewNode($s_t$)
            $a_t = $ DefaultPolicy($s_t$)
        end if
        $s_{t+1} = $ SampleTransition($s_t, a_t$)
        $r_{t+1} = $ SampleReward($s_t, a_t, s_{t+1}$)
        $R = R + r_{t+1}$
        $t \mathrel{+}= 1$
    until $Terminal(s_t)$
    return $\{s_0, ..., s_t\}, R$
end procedure

procedure UCB1($s$)
    $a^* = \underset{a}{\operatorname{argmax}}\ Q(s, a) + c\sqrt{\frac{2 \log N(s)}{N(s,a)}}$
    return $a^*$
end procedure

procedure Backup($\{s_0, ..., s_T\}, R$)
    for $t = 0$ to $T - 1$ do
        $N(s_t) \mathrel{+}= 1$
        $N(s_t, a_t) \mathrel{+}= 1$
        $Q(s_t, a_t) \mathrel{+}= \frac{R - Q(s_t, a_t)}{N(s_t, a_t)}$
    end for
end procedure

procedure NewNode(s)
    $N(s) = 0$
    for all $a \in \mathcal{A}$ do
        $N(s, a) = 0$
        $Q(s, a) = \infty$
    end for
    $\mathcal{T}.Insert(s)$
end procedure
```

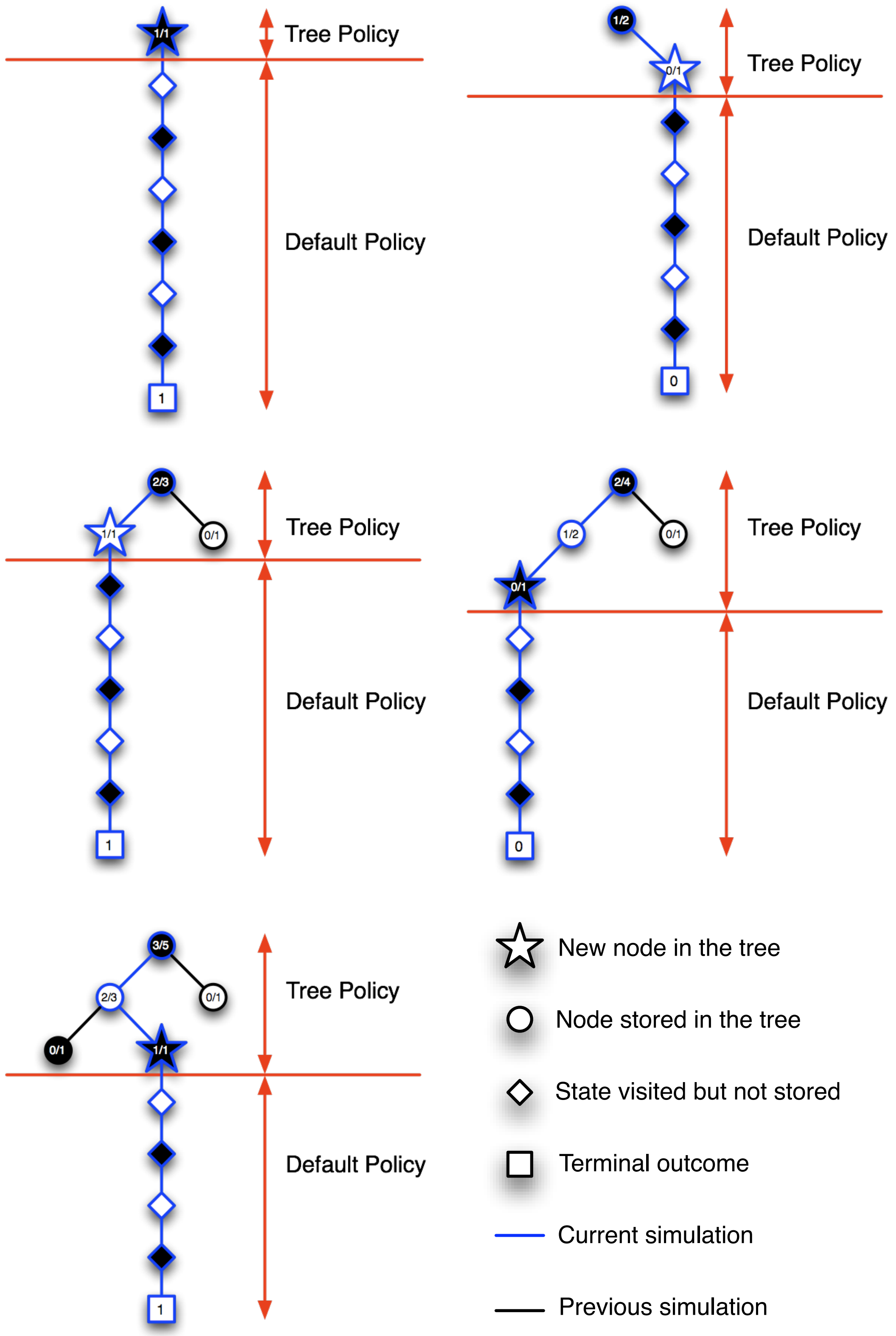

Figure 3.1: Five simulations of Monte-Carlo tree search.

Chapter 4

Computer Go

4.1 The Challenge of Go

For many years, computer chess was considered to be "the *drosophila* of AI",[1] and a "grand challenge task" (McCarthy, 1997). It provided a sandbox for new ideas, a straightforward performance comparison between algorithms, and measurable progress against human capabilities. With the dominance of alpha-beta search programs over human players now conclusive in chess (McClain, 2006), many researchers have sought out a new challenge. Computer Go has emerged as the "new *drosophila* of AI" (McCarthy, 1997), a "task *par excellence*" (Harmon, 2003), and "a grand challenge task for our generation" (Mechner, 1998).

In the last few years, a new paradigm for AI has been developed in computer Go. This approach, based on Monte-Carlo simulation, has provided dramatic progress and led to the first master-level programs (Gelly and Silver, 2007; Coulom, 2007). Unlike alpha-beta search, these algorithms are still in their infancy, and the arena is still wide open to new ideas. In addition, this new approach to search requires little or no human knowledge in order to produce good results. Although this paradigm has been pioneered in computer Go, it is not specific to Go, and the core concept of simulation-based search is widely applicable. Ultimately, the study of computer Go may illuminate a path towards high performance AI in a wide variety of challenging domains.

4.2 The Rules of Go

The game of Go is usually played on a 19×19 grid, with 13×13 and 9×9 as popular alternatives. Black and White play alternately, placing a single stone on an intersection of the grid. Stones cannot be moved once played, but may be captured. Sets of adjacent, connected stones of one colour are known as *blocks*. The empty intersections adjacent to a block are called its *liberties*. If a block is reduced to zero liberties by the opponent, it is captured and removed from the board (Figure 4.1a, A). Stones with just one remaining liberty are said to be in *atari*. Playing a stone with zero liberties is illegal (Figure 4.1a, B), unless it also reduces an opponent block to zero liberties. In this case the

[1] *Drosophila* is the fruit fly, the most extensively studied organism in genetics research.

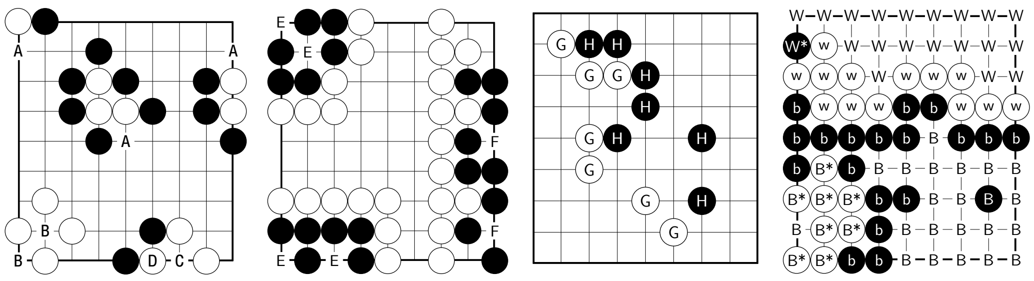
Figure 4.1: a) The White stones are in *atari* and can be captured by playing at the points marked A. It is illegal for Black to play at B, as the stone would have no liberties. Black may, however, play at C to capture the stone at D. White cannot recapture immediately by playing at D; as this would repeat the position - it is a *ko*. b) The points marked E are *eyes* for Black. The black groups on the left can never be captured by White, they are *alive*. The points marked F are *false eyes*: the black stones on the right will eventually be captured by White and are *dead*. c) *Groups* of loosely connected white stones (G) and black stones (H). d) A final position. Dead stones ($B*, W*$) are removed from the board. All surrounded intersections (B, W) and all remaining stones (b, w) are counted for each player. If *komi* is 6.5 then Black wins by 8.5 points in this example.

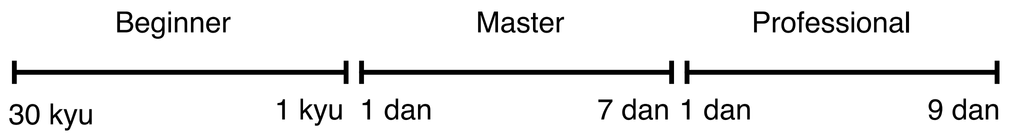

Figure 4.2: Performance ranks in Go, in increasing order of strength from left to right.

opponent block is captured, and the player's stone remains on the board (Figure 4.1a, C). Finally, repeating a previous board position is illegal. A situation in which a repeat could otherwise occur is known as *ko* (Figure 4.1a, D).

A connected set of empty intersections that is wholly enclosed by stones of one colour is known as an *eye*. One natural consequence of the rules is that a block with two eyes can never be captured by the opponent (Figure 4.1b, E). Blocks which cannot be captured are described as *alive*; blocks which will certainly be captured are described as *dead* (Figure 4.1b, F). A loosely connected set of stones is described as a *group* (Figure 4.1c, G, H). Determining the life and death status of a group is a fundamental aspect of Go strategy.

The game ends when both players pass. Dead blocks are removed from the board (Figure 4.1d, $B*, W*$). In Chinese rules, all alive stones, and all intersections that are enclosed by a player, are counted as a point of *territory* for that player (Figure 4.1d, B, W).[2] Black always plays first in Go; White receives compensation, known as *komi*, for playing second. The winner is the player with the greatest territory, after adding *komi* for White.

4.3 Go Ratings

Human Go players are rated on a three-class scale, divided into *kyu* (beginner), *dan* (master), and *professional dan* ranks (see Figure 4.2). *Kyu* ranks are in descending order of strength, whereas *dan* and *professional dan* ranks are in ascending order. At amateur level, the difference in rank corresponds to the number of handicap stones required by the weaker player to ensure an even game.[3]

The Elo rating system is also used to evaluate human Go players. This rating system assumes that each player's performance in a game is an independent random variable, and that the player with higher performance will win the game. The original Elo scale assumed that the player's performance is normally distributed; modern incarnations of the Elo scale assume a logistic distribution. In either case, each player's Elo rating is their mean performance, which is estimated and updated from their results. Unfortunately, several different Elo scales are used to evaluate human Go ratings, based on different assumptions about the performance distribution.

The majority of computer Go programs compete on the Computer Go Server (CGOS). This server runs an ongoing rapid-play tournament of 5 minute games for 9×9 and 20 minute games for 19×19 boards. The Elo rating of each program on the server is continually updated. The Elo scale on CGOS, and all other Elo ratings reported in this thesis, assume a logistic distribution with winning probability $Pr(A \text{ beats } B) = \frac{1}{1+10^{\frac{\mu_B - \mu_A}{400}}}$, where μ_A and μ_B are the Elo ratings for player A and player B respectively. On this scale, a difference of 200 Elo corresponds to a 75% winning rate for the stronger player, and a difference of 500 Elo corresponds to a 95% winning rate. Following convention, the Go program *GnuGo* (level 10) anchors this scale with a rating of 1800 Elo.

4.4 Position Evaluation in Computer Go

A rational Go player selects moves so as to maximise an *evaluation function* $V(s)$. We denote this greedy move selection strategy by a deterministic function $\pi(s)$ that takes a position $s \in \mathcal{S}$ and produces the move $a \in \mathcal{A}$ with the highest evaluation,

$$\pi(s) = \operatorname*{argmax}_a V(s \circ a) \tag{4.1}$$

where $s \circ a$ denotes the position reached after playing move a from position s.

The evaluation function is a summary of Go knowledge, and is used to estimate the goodness of each move. A *heuristic function* is a measure of goodness, such as the material count in chess, that is presumed but not required to have some positive correlation with the outcome of the game. A *value function* (see Chapter 2) specifically estimates the outcome of the game from that position,

[2]The Japanese scoring system is somewhat different, but usually has the same outcome.

[3]The difference between 1 *kyu* and 1 *dan* is normally considered to be 1 stone.

$V(s) \approx V^*(s)$, where $V^*(s)$ denotes the optimal (minimax) value of position s. A *static evaluation function* is stored in memory, whereas a *dynamic evaluation function* is computed by a process of search from the current position s.

4.5 Static Evaluation in Computer Go

Constructing an evaluation function for Go is a challenging task. First, as we have already seen, the state space is enormous. Second, the evaluation function can be highly volatile: changing a single stone can transform a position from lost to won or vice versa. Third, interactions between stones may extend across the whole board, making it difficult to decompose the global evaluation into local features.

A static evaluation function cannot usually store a separate value for each distinct position s. Instead, it is represented by *features* $\phi(s)$ of the position s, and some number of adjustable *parameters* θ. For example, a position can be evaluated by a neural network that uses features of the position as its inputs (Schraudolph et al., 1994; Enzenberger, 1996; Dahl, 1999; Enzenberger, 2003).

4.5.1 Symmetry

The Go board has a high degree of symmetry. It has eight-fold rotational and reflectional symmetry, and it has colour symmetry: if all stone colours are inverted, the colour to play is swapped, and *komi* is reversed, then the position is exactly equivalent. This suggests that the evaluation function should be invariant to rotational, reflectional and colour inversion symmetries. When considering the status of a particular intersection, the Go board also exhibits translational symmetry: a local configuration of stones in one part of the board has similar properties to the same configuration of stones in another part of the board, subject to edge effects.

Schraudolph et al. (1994) exploit these symmetries in a convolutional neural network. The network predicts the final territory status of a particular target intersection. It receives one input from each intersection ($-1, 0$ or $+1$ for White, Empty and Black respectively) in a local region around the target, contains a fixed number of hidden nodes, and outputs the predicted territory for the target intersection. The global position is evaluated by summing the territory predictions for all intersections on the board. Weights are shared between rotationally and reflectionally symmetric patterns of input features,[4] and between all target intersections. In addition, the input features, squashing function and bias weights are all antisymmetric, and on each alternate move the sign of the bias weight is flipped, so that network evaluation is invariant to colour inversion.

A further symmetry of the Go board is that stones within the same block will live or die together as a unit, sometimes described as the *common fate* property (Graepel et al., 2001). One way to make use of this invariance (Enzenberger, 1996; Graepel et al., 2001) is to treat each complete block or

[4]Surprisingly this impeded learning in practice (Schraudolph et al., 2000).

empty intersection as a unit, and to represent the board by a *common fate graph* containing a node for each unit and an edge between each pair of adjacent units.

4.5.2 Handcrafted Heuristics

In many other classic games, handcrafted heuristic functions have proven highly effective. Basic heuristics such as *material count* and *mobility*, which provide reasonable estimates of goodness in checkers, chess and Othello (Schaeffer, 2000), are next to worthless in Go. Stronger heuristics have proven surprisingly hard to design, despite several decades of endeavour (Müller, 2002).

Until recently, most Go programs incorporated very large quantities of expert knowledge, in a *pattern database* containing many thousands of manually inputted patterns, each describing a rule of thumb that is known by expert Go players. Traditional Go programs used these databases to recommend expert moves in commonly recognised situations, typically in conjunction with local or global alpha-beta search algorithms. In addition, they can be used to encode knowledge about connections, eyes, opening sequences, or promising search extensions. The pattern database accounts for a large part of the development effort in a traditional Go program, sometimes requiring many man-years of effort from expert Go players.

However, pattern databases are hindered by the knowledge acquisition bottleneck: expert Go knowledge is hard to interpret, represent, and maintain. The more patterns in the database, the harder it becomes to predict the effect of a new pattern on the overall playing strength of the program.

4.5.3 Temporal Difference Learning

Reinforcement learning can be used to estimate a value function that predicts the eventual outcome of the game. The learning program can be rewarded by the score at the end of the game, or by a reward of 1 if Black wins and 0 if White wins. Surprisingly, the less informative binary signal has proven more successful (Coulom, 2006), as it encourages the agent to favour risky moves when behind, and calm moves when ahead. Expert Go players will frequently play to minimise the uncertainty in a position once they judge that they are ahead in score; this behaviour cannot be replicated by simply maximising the expected score. Despite this shortcoming, the final score is widely used as a reward signal (Schraudolph et al., 1994; Enzenberger, 1996; Dahl, 1999; Enzenberger, 2003).

Schraudolph et al. (1994) exploit the symmetries of the Go board (see Section 4.5.1) to predict the final territory at an intersection. They train their multilayer perceptron using $TD(0)$, using a reward signal corresponding to the final territory value of the intersection. The network outperformed a commercial Go program, *The Many Faces of Go*, when set to a low playing level in 9×9 Go, after just 3,000 self-play training games.

Dahl's Honte (1999) and Enzenberger's NeuroGo III (2003) use a similar approach to predicting the final territory. However, both programs learn intermediate features that are used to input additional knowledge into the territory evaluation network. Honte has one intermediate network to predict local moves and a second network to evaluate the life and death status of groups. NeuroGo III uses intermediate networks to evaluate connectivity and eyes. Both programs achieved single-digit *kyu* ranks; NeuroGo won the silver medal at the 2003 9×9 Computer Go Olympiad.

Although a complete game of Go typically contains hundreds of moves, only a small number of moves are played within a given local region. Enzenberger (2003) suggests for this reason that $TD(0)$ is a natural choice of algorithm. Indeed, $TD(0)$ has been used almost exclusively in reinforcement learning approaches to position evaluation in Go (Schraudolph et al., 1994; Enzenberger, 1996; Dahl, 1999; Enzenberger, 2003; Runarsson and Lucas, 2005; Mayer, 2007), perhaps because of its simplicity and its proven efficacy in games such as backgammon (Tesauro, 1994).

4.5.4 Comparison Training

If we assume that expert Go players are rational, then it is reasonable to infer the expert's evaluation function V_{expert} by observing their move selection decisions. For each expert move a, rational move selection tells us that $V_{expert}(s \circ a) \geq V_{expert}(s \circ b)$ for any legal move b. This can be used to generate an error metric for training an evaluation function $V(s)$, in an approach known as *comparison training* (Tesauro, 1988). The expert move a is compared to another move b, randomly selected; if the non-expert move evaluates higher than the expert move then an error is generated.

Van der Werf et al. (2002) use comparison training to learn the weights of a multilayer perceptron, using local board features as inputs. Following Enderton (1991), they compute an error function E of the form,

$$E(s, a, b) = \begin{cases} [V(s \circ a) + \epsilon - V(s \circ b)]^2 & \text{if } V(s \circ a) + \epsilon > V(s \circ a) \\ 0 & \text{otherwise,} \end{cases} \tag{4.2}$$

where ϵ is a positive control parameter used to avoid trivial solutions. The trained network was able to predict expert moves with 37% accuracy on an independent test set; the authors estimate its strength to be at strong *kyu* level for the task of local move prediction. The learnt evaluation function was used in the Go program *Magog*, which won the bronze medal in the 2004 9×9 Computer Go Olympiad.

4.5.5 Evolutionary Methods

A common approach is to apply evolutionary methods to learn a heuristic evaluation function, for example by applying genetic algorithms to the weights of a multilayer perceptron. The fitness of a heuristic is typically measured by running a tournament and counting the total number of wins. These approaches have two major sources of inefficiency. First, they only learn from the result of the game, and do not exploit the sequence of positions and moves used to achieve the result. Second, many games must be run in order to produce fitness values with reasonable discrimination. Runarsson and Lucas compare temporal difference learning with coevolutionary learning, using a basic state representation. They find that TD(0) both learns faster and achieves greater performance in most cases (Runarsson and Lucas, 2005). Evolutionary methods have not yet, to our knowledge, produced a competitive Go program.

4.6 Dynamic Evaluation in Computer Go

An alternative method of position evaluation is to construct a search tree from the root position, and dynamically update the evaluation of the nodes in the search tree.

4.6.1 Alpha-Beta Search

Despite the challenging search space, and the difficulty of constructing a static evaluation function, alpha-beta search has been used extensively in computer Go. One of the strongest traditional programs, *The Many Faces of Go*[5], uses a global alpha-beta search to select moves. Each position is evaluated by extensive handcrafted knowledge in combination with local alpha-beta searches to determine the status of individual blocks and groups. The program *GnuGo*[6] uses handcrafted databases of pattern knowledge and specialised search routines to determine local subgoals such as capture, connection, and eye formation. The local status of each subgoal is used to estimate the overall benefit of each legal move.

However, even determining the status of individual blocks can be a challenging problem. In addition, the local searches are not usually independent, and the search trees can overlap significantly. Finally, the global evaluation often depends on more subtle factors than can be represented by simple local subgoals (Müller, 2001).

4.6.2 Monte Carlo Simulation

In contrast to traditional search methods, Monte-Carlo simulation does not require a static evaluation function. This makes it an appealing choice for Go, where as we have seen, position evaluation is particularly challenging.

The first Monte-Carlo Go program, *Gobble* (Bruegmann, 1993), simulated many games of self-play from the current position s. It combined Monte-Carlo evaluation with two novel ideas: the *all-moves-as-first* heuristic, and *ordered simulation*. The all-moves-as-first heuristic assumes that the value of a move is not significantly affected by changes elsewhere on the board. The value of playing move a immediately is estimated by the average outcome of all simulations in which move a is played *at any time* (see Chapter 8 for an exact definition). *Gobble* also used ordered simulation to sort all moves according to their estimated value. This ordering is randomly perturbed according to an annealing schedule that cools down with additional simulations. Each simulation plays out all moves in the prescribed order. *Gobble* itself played weakly, with an estimated rating of around 25 *kyu*.

[5]http://www.smart-games.com/manyfaces.html
[6]http://www.gnu.org/software/gnugo

Bouzy and Helmstetter developed the first competitive Go programs based on Monte-Carlo simulation (Bouzy and Helmstetter, 2003). Their basic framework simulates many games of self-play from the current position s, for each candidate action a, using a uniform random simulation policy; the value of a is estimated by the average outcome of these simulations. The only domain knowledge is to prohibit moves within eyes; this ensures that games terminate within a reasonable timeframe. Bouzy and Helmstetter also investigated a number of extensions to Monte-Carlo simulation, several of which are precursors to the more sophisticated algorithms used now:

1. *Progressive pruning* is a technique in which statistically inferior moves are removed from consideration (Bouzy, 2005b).

2. The *all-moves-as-first heuristic*, described above.

3. The *temperature* heuristic uses a softmax simulation policy to bias the random moves towards the strongest evaluations. The softmax policy selects moves with a probability $\pi(s,a) = \frac{e^{V(s \circ a)/\tau}}{\sum_{b \in legal} e^{V(s \circ b)/\tau}}$, where τ is a constant temperature parameter controlling the overall level of randomness.[7]

4. The *minimax enhancement* constructs a full width search tree, and separately evaluates each node of the search tree by Monte-Carlo simulation. Selective search enhancements were also tried (Bouzy, 2004).

Bouzy also tracked statistics about the final territory status of each intersection after each simulation (Bouzy, 2006). This information is used to influence the simulations towards disputed regions of the board, by avoiding playing on intersections which are consistently one player's territory. Bouzy also incorporated pattern knowledge into the simulation player (Bouzy, 2005a). Using these enhancements his program *Indigo* won the bronze medal at the 2004 and 2006 19×19 Computer Go Olympiads.

It is surprising that a Monte-Carlo technique, originally developed for stochastic games such as backgammon (Tesauro and Galperin, 1996), Poker (Billings et al., 1999) and Scrabble (Sheppard, 2002) should succeed in Go. Why should an evaluation that is based on random play provide any useful information in the precise, deterministic game of Go? The answer, perhaps, is that Monte-Carlo methods successfully manage the uncertainty in the evaluation. A random simulation policy generates a broad distribution of simulated games, representing many possible futures and the uncertainty in what may happen next. As the search proceeds and more information is accrued, the simulation policy becomes more refined, and the distribution of simulated games narrows. In contrast, deterministic play represents perfect confidence in the future: there is only one possible continuation. If this confidence is misplaced, then predictions based on deterministic play will be unreliable and misleading.

[7]Gradually reducing the temperature, as in simulated annealing, was not beneficial.

4.6.3 Monte-Carlo Tree Search

Within just three years of their introduction, Monte-Carlo tree search algorithms have revolutionised computer Go, leading to the first strong programs that are competitive with human master players. Work in this field is ongoing; in this section we outline some of the key developments.

Monte-Carlo tree search, as described in Chapter 3, was first introduced in the Go program *Crazy Stone* (Coulom, 2006). The true value of each move is assumed to have a Gaussian distribution centred on the current value estimate, $Q^\pi(s,a) \sim \mathcal{N}(Q(s,a), \sigma^2(s,a))$. During the first stage of simulation, the tree policy selects each move according to its probability of being better than the current best move, $\pi(s,a) \approx Pr(\forall b, Q^\pi(s,a) > Q(s,b))$. During the second stage of simulation, the default policy selects moves with a probability proportional to an *urgency* value encoding domain specific knowledge. In addition, *Crazy Stone* used a hybrid backup to update values in the tree, which is intermediate between a minimax backup and a expected value backup. Using these techniques, *Crazy Stone* exceeded 1800 Elo on CGOS, achieving equivalent performance to traditional Go programs such as *GnuGo* and *The Many Faces of Go*. *Crazy Stone* won the gold medal at the 2006 9×9 Computer Go Olympiad.

The Go program *MoGo* introduced the UCT algorithm (see Chapter 3) to computer Go (Gelly et al., 2006; Wang and Gelly, 2007). *MoGo* treats each position in the search tree as a multi-armed bandit. There is one arm of the bandit for each legal move, and the payoff from an arm is the outcome of a simulation starting with that move. During the first stage of simulation, the tree policy selects moves using the UCB1 algorithm. During the second stage of simulation, *MoGo* uses a default policy based on specialised domain knowledge. Unlike the enormous pattern databases used in traditional Go programs, *MoGo*'s patterns are extremely simple. Rather than suggesting the best move in any situation, these patterns are intended to produce local sequences of plausible moves. They can be summarised by four prioritised rules following an opponent move a:

1. If a put some of our stones into atari, play a saving move at random.
2. Otherwise, if one of the 8 intersections surrounding a matches a simple pattern for cutting or *hane*, randomly play one.
3. Otherwise, if any opponent stone can be captured, play a capturing move at random.
4. Otherwise play a random move.

Using these patterns in the UCT algorithm, *MoGo* significantly outperformed all previous 9×9 Go programs, exceeding 2100 Elo on the Computer Go Server.

The UCT algorithm in *MoGo* was subsequently replaced by the heuristic MC–RAVE algorithm (Gelly and Silver, 2007) (see Chapter 8). In 9×9 Go *MoGo* reached 2500 Elo on CGOS, achieved *dan*-level play on the Kiseido Go Server, and defeated a human professional in an even game for the first time (Gelly and Silver, 2008). These enhancements also enabled *MoGo* to perform well on larger boards, winning the gold medal at the 2007 19×19 Computer Go Olympiad.

The default policy used by *MoGo* is handcrafted. In contrast, a subsequent version of *Crazy Stone* uses supervised learning to train the pattern weights for its default policy (Coulom, 2007). The relative strength of patterns is estimated by assigning them Elo ratings, much like a tournament between games players. In this approach, the pattern selected by a human player is considered to have won against all alternative patterns. In general, multiple patterns may match a particular move, in which case this team of patterns is considered to have won against alternative teams. The strength of a team is estimated by the product of the individual pattern strengths. The probability of each team winning is assumed to be proportional to that team's strength, using a generalised Bradley-Terry model (Hunter, 2004). Given a data set of expert moves, the maximum likelihood pattern strengths can be efficiently approximated by the minorisation-maximisation algorithm. This algorithm was used to learn a default policy, by training the strengths of simple 3×3 patterns and simple features such as capture, self-atari, extension, and contiguity to the previous move. A more complicated set of 17,000 patterns, harvested from the data set, was also trained and used to progressively widen the search tree. *Crazy Stone* achieved a rating of 1 *kyu* at 19×19 Go against human players on the Kiseido Go Server.

The *Zen* program has combined ideas from both *MoGo* and *Crazy Stone*, using more sophisticated domain knowledge. *Zen* has achieved a 1 *dan* rating, on full-size boards, against human players on the Kiseido Go Server.

Monte-Carlo tree search can be parallelised much more effectively than traditional search techniques (Chaslot et al., 2008c). Recent work on *MoGo* has focused on full size 19×19 Go, using massive parallelisation (Gelly et al., 2008) and incorporating additional expert knowledge into the search tree. A version of *MoGo* running on 800 processors defeated a 9-*dan* professional player with 7 stones handicap. The latest version of *Crazy Stone* and a new, Monte-Carlo version of *The Many Faces of Go* have also achieved impressive victories against professional players on full size boards. Most recently, the program *Fuego* (Müller and Enzenberger, 2009), based on a parallelised version of heuristic MC–RAVE, defeated a 9-*dan* professional player in an even 9×9 game, and defeated a 6-*dan* amateur player with 4 stones handicap on a full size board.[8]

4.7 Summary

We provide a summary of the current state of the art in computer Go, based on ratings from the Computer Go Server (see Table 4.1) and the Kiseido Go Server (see Table 4.2). The Go programs to which this thesis has directly contributed are highlighted in bold.[9]

[8]Nick Wedd maintains a website of all human versus computer challenge matches: *http://www.computer-go.info/h-c/index.html*.

[9]Many of the top Go programs, including *Crazystone*, *Fuego*, *Greenpeep*, *Zen*, and the Monte-Carlo version of *The Many Faces of Go*, now use variants of the RAVE and heuristic UCT algorithms (see Chapter 8).

Program	*Description*	*Elo*
Indigo	Handcrafted patterns, Monte-Carlo simulation	1400
Magog	Supervised learning, neural network, alpha-beta search	1700
GnuGo, Many Faces	Handcrafted patterns, local search	1800
NeuroGo	Reinforcement learning, neural network, alpha-beta search	1850
RLGO	Dyna-2, alpha-beta search	2150
MoGo, Fuego, Greenpeep	Handcrafted patterns, heuristic MC–RAVE	2500+
CrazyStone, Zen	Supervised learning of patterns, heuristic MC–RAVE	2500+

Table 4.1: Approximate Elo ratings of the strongest 9×9 programs using various paradigms on the 9x9 Computer Go Server.

Program	*Description*	*Rank*
Indigo	Handcrafted patterns, Monte-Carlo simulation	6 kyu
GnuGo, Many Faces	Handcrafted patterns, local search	6 kyu
MoGo, Fuego, Many Faces MC	Handcrafted patterns, heuristic MC–RAVE	2 kyu
CrazyStone, Zen	Supervised learning of patterns, heuristic MC–RAVE	1 kyu, 1 dan

Table 4.2: Approximate Elo ratings of the strongest 19x19 Go programs using various paradigms on the Kiseido Go Server.

Part II

Temporal Difference Learning and Search

Chapter 5

Temporal Difference Learning with Local Shape Features

5.1 Introduction

A number of notable successes in artificial intelligence have followed a straightforward strategy: the state is *represented* by many simple features; states are *evaluated* by a weighted sum of those features, in a high-performance search algorithm; and weights are *trained* by temporal-difference learning. In two-player games as varied as chess, checkers, Othello, backgammon and Scrabble, programs based on variants of this strategy have exceeded human levels of performance.

- In each game, the position is broken down into a large number of *features*. These are usually binary features that recognise a small, local pattern or configuration within the position: material, pawn structure and king safety in chess (Campbell et al., 2002); material and mobility terms in checkers (Schaeffer et al., 1992); configurations of discs in Othello (Buro, 1999); checker counts in backgammon (Tesauro, 1994); and single, duplicate and triplicate letter rack leaves in Scrabble (Sheppard, 2002).
- The position is evaluated by a linear combination of these features with *weights* indicating their value. Backgammon provides a notable exception: *TD-Gammon* evaluates positions with a non-linear combination of features, using a multi-layer perceptron.[1] Linear evaluation functions are fast to compute; easy to interpret, modify and debug; are effective over a wide class of applications; and they have good convergence properties in many learning algorithms.
- Weights are trained from games of self-play, by temporal-difference or Monte-Carlo learning. The world champion checkers program *Chinook* was hand-tuned by experts over 5 years. When weights were trained instead by self-play using temporal difference learning, the program equalled the performance of the original version (Schaeffer et al., 2001). A related approach attained master level play in chess (Veness et al., 2009). *TD-Gammon* achieved world

[1]In fact, Tesauro notes that evaluating positions by a linear combination of backgammon features is a "surprisingly strong strategy" (Tesauro, 1994).

class backgammon performance after training by temporal-difference learning and self-play (Tesauro, 1994). Games of self-play were also used to train the weights of the world champion Othello and Scrabble programs, using least squares regression and a domain specific solution respectively (Buro, 1999; Sheppard, 2002).[2]

- A linear evaluation function is combined with a suitable search algorithm to produce a high-performance game playing program. Alpha-beta search variants have proven particularly effective in chess, checkers, Othello and backgammon (Campbell et al., 2002; Schaeffer et al., 1992; Buro, 1999; Tesauro, 1994), whereas Monte-Carlo simulation has been most successful in Scrabble and backgammon (Sheppard, 2002; Tesauro and Galperin, 1996).

In contrast to these games, the ancient oriental game of Go has proven to be particularly challenging. Handcrafted and machine-learnt evaluation functions have so far been unable to achieve good performance (Müller, 2002). It has often been speculated that position evaluation in Go is uniquely difficult for computers because of its intuitive nature, and requires an altogether different approach from other games.

In this chapter, we return to the strategy that has been so successful in other domains, and apply it to Go. We systematically investigate a representation of Go knowledge. This representation uses features based on simple local 1×1 to 3×3 patterns. We evaluate positions using a linear combination of these features, and learn weights by temporal-difference learning and self-play. This approach requires no prior domain knowledge beyond the grid structure of the board, and could in principle be used to automatically construct an evaluation function for many other games. Finally, we apply our evaluation function in a basic alpha-beta search algorithm, and test its performance on the Computer Go Server.

5.2 Shape Knowledge in Go

The concept of shape is extremely important in Go. A good shape uses local stones efficiently to maximise tactical advantage (Matthews, 2003). Professional players analyse positions using a large vocabulary of shapes, such as *joseki* (corner patterns) and *tesuji* (tactical patterns). The joseki at the bottom left of Figure 5.1a is specific to the white stone on the 4-4 intersection,[3] whereas the tesuji at the top-right could be used at any location. Shape knowledge may be represented at different scales, with more specific shapes able to specialise the knowledge provided by more general shapes (Figure 5.1b). Many Go proverbs exist to describe shape knowledge, for example "*ponnuki* is worth 30 points", "the one-point jump is never bad" and "*hane* at the head of two stones" (Figure 5.1c).

Commercial computer Go programs rely heavily on the use of pattern databases to represent shape knowledge (Müller, 2002). Many man-years have been devoted to hand-encoding profes-

[2]Sheppard reports that temporal-difference learning performed poorly, due to insufficient exploration (Sheppard, 2002).
[3]Intersections are indexed inwards from the corners, starting at 1-1 for the corner intersection itself.

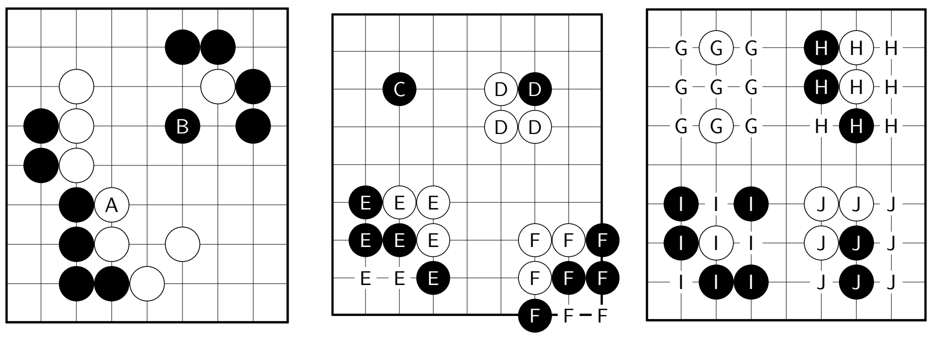

Figure 5.1: a) The pattern of stones near A forms a common *joseki* that is specific to the 4-4 intersection. Black B captures the white stone using a *tesuji* that can occur at any location. b) In general a stone on the 3-3 intersection (C) helps secure a corner. If it is surrounded then the corner is insecure (D), although with sufficient support it will survive (E). However, the same shape closer to the corner is unlikely to survive (F). c) Go players describe positions using a large vocabulary of shapes, such as the *one-point jump* (G), *hane* (H), *net* (I) and *turn* (J).

sional expertise in the form of local pattern rules. Each pattern recommends a move to be played whenever a specific configuration of stones is encountered on the board. The configuration can also include additional features, such as requirements on the liberties or strength of a particular stone. Unfortunately, pattern databases suffer from the knowledge acquisition bottleneck: expert shape knowledge is hard to quantify and encode, and the interactions between different patterns may lead to unpredictable behaviour.

Prior work on learning shape knowledge has focused on predicting expert moves by supervised learning (Stoutamire, 1991; van der Werf et al., 2002; Stern et al., 2006). This approach has achieved a 30–40% success rate in predicting the move selected by a human player, across a large data-set of human expert games. However, it has not led directly to strong play in practice, perhaps due to its focus on mimicking rather than understanding a position by evaluating its long-term consequences.

A second approach has been to train a multi-layer perceptron, using temporal-difference learning by self-play (Schraudolph et al., 1994). The networks implicitly contain some representation of local shape, and utilise weight sharing to exploit the natural symmetries of the Go board. This approach has led to stronger Go playing programs, such as Dahl's *Honte* (Dahl, 1999) and Enzenberger's *NeuroGo* (Enzenberger, 2003) (see Chapter 4). However, these networks utilise a great deal of sophisticated Go knowledge in the network architecture and input features. Furthermore, knowledge learnt in this form cannot be manually interpreted or modified in the manner of pattern databases.

5.3 Local Shape Features

We introduce a much simpler approach for representing shape knowledge, which requires no prior knowledge of the game, except for the basic grid structure of the board.

A state in the game of Go, $s \in \{\cdot, \circ, \bullet\}^{N \times N}$, consists of a state variable for each intersection of a size $N \times N$ board, with three possible values for empty, black and white stones respectively.[4] We define a *local shape* to be a specific configuration of state variables within some square region of the board. We exhaustively enumerate all possible local shapes within all possible square regions up to size $m \times m$. The *local shape feature* $\phi_i(s)$ has value 1 in position s if the board exactly matches the ith local shape, and value 0 otherwise.

The local shape features are combined into a large feature vector $\phi(s)$. This feature vector is very sparse: exactly one local shape is matched in each square region of the board; all other local shape features have value 0.

A vector of weights θ indicates the value of each local shape feature. The value $V(s)$ of a position s is estimated by a linear combination of features and their corresponding weights, squashed into the range $[0, 1]$ by a logistic function $\sigma(x) = \frac{1}{1+e^{-x}}$,

$$V(s) = \sigma(\phi(s) \cdot \theta) \tag{5.1}$$

5.4 Weight Sharing

We use weight sharing to exploit the symmetries of the Go board (Schraudolph et al., 1994). We define an equivalence relationship over local shapes, such that all rotationally and reflectionally symmetric local shapes are placed in the same equivalence class. In addition, each equivalence class includes *inversions* of the local shape, in which all black and white stones are flipped to the opposite colour.

The local shape with the smallest index j within the equivalence class is considered to be the canonical example of that class. Every local shape feature ϕ_i in the equivalence class shares the weight θ_j of the canonical example, but the sign may differ. If the local shape feature has been inverted from the canonical example, then it uses negative weight sharing, $\theta_i = -\theta_j$, otherwise it uses positive weight sharing, $\theta_i = \theta_j$. In certain equivalence classes (for example empty local shapes), an inverted shape is identical to an uninverted shape, so that either positive or negative weight sharing could be used, $\theta_i = \theta_j = -\theta_j \Rightarrow \theta_i = \theta_j = 0$. We describe these local shapes as *neutral*, and assume that they are equally advantageous to both sides. All neutral local shapes are removed from the representation (Figure 5.3 provides one example).

The rotational, reflectional and inversion symmetries define the vector of *location dependent* weights θ^{LD}. The vector of *location independent* weights θ^{LI} also incorporates translation symmetry: all local shapes that have the same configuration, regardless of its location on the board, are included in the same equivalence class. Figure 5.2 shows some examples of both types of weight sharing.

For each size of square up to 3×3, all local shape features are exhaustively enumerated, using both location dependent and location independent weights. This provides a hierarchy of local

[4]Technically the state also includes the full board history, so as to avoid repetitions (known as *ko*).

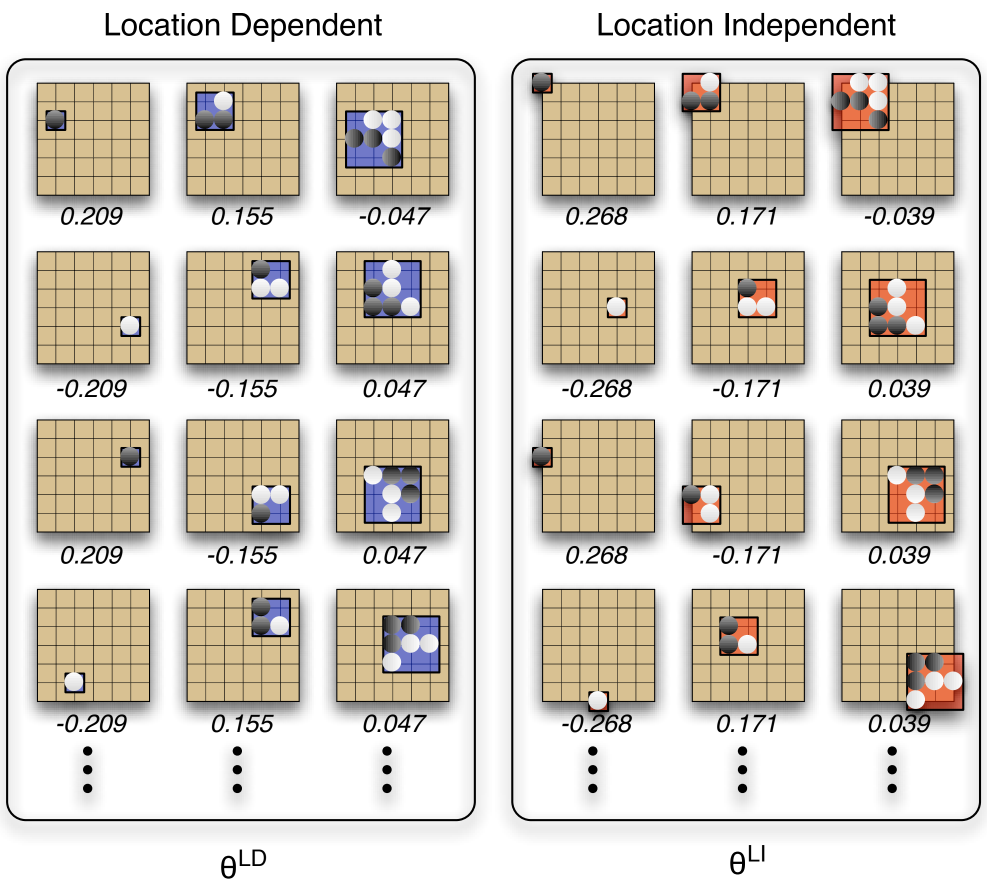

Figure 5.2: Examples of location dependent and location independent weight sharing.

Local shape features	Total features	Unique weights	Max active features
1×1 Location Independent	243	1	81
1×1 Location Dependent		15	81
2×2 Location Independent	5184	8	64
2×2 Location Dependent		344	64
3×3 Location Independent	964467	1418	49
3×3 Location Dependent		61876	49
Total	969894	63303	388

Table 5.1: Number of local shape features of different sizes in 9×9 Go.

shape features, from very general configurations that occur many times each game, to specific configurations that are rarely seen in actual play. Smaller local shape features are more general than larger ones, and location independent weights are more general than location dependent weights. The more general features and weights provide no additional information, but may offer a useful abstraction for rapid learning. Table 5.1 shows, for 9×9 Go, the total number of local shape features of each size; the total number of distinct equivalence classes, and therefore the total number of unique weights; and the maximum number of active features (features with value of 1) in the feature vector.

5.5 Learning Algorithm

Our objective is to win games of Go. This goal can be expressed by a binary reward function, which gives a reward of $r = 1$ if Black wins and $r = 0$ if White wins, with no intermediate rewards. The value function $V^\pi(s)$ is defined to be the expected total reward from board position s when following policy π. This value function is Black's *winning probability* from state s (see Appendix A). Black seeks to maximise his winning probability, while White seeks to minimise it. We approximate the value function by a linear combination of local shape features and both location dependent and location independent weights (see Figure 5.3),

$$V(s) = \sigma\left(\phi(s).\theta^{LI} + \phi(s).\theta^{LD}\right) \tag{5.2}$$

We measure the TD-error between the current value $V(s_t)$, and the value after both player and opponent have made a move, $V(s_{t+2})$. In this approach, which we refer to as a *two-ply update*, the value is updated between successive moves with the same colour to play. The current player is viewed as the agent, and his opponent is viewed as part of the environment. We contrast this approach to a *one-ply update*, used in prior work such as *TD-Gammon* (Tesauro, 1994) and *NeuroGo* (Enzenberger, 2003), that measures the TD-error between Black and White moves.

We update both location dependent and location independent weights by logistic temporal-difference learning (see Appendix A). For each feature ϕ_i, the shared value for the corresponding weights θ_i^{LI} and θ_i^{LD} is updated. This can lead to the same shared weight being updated many times

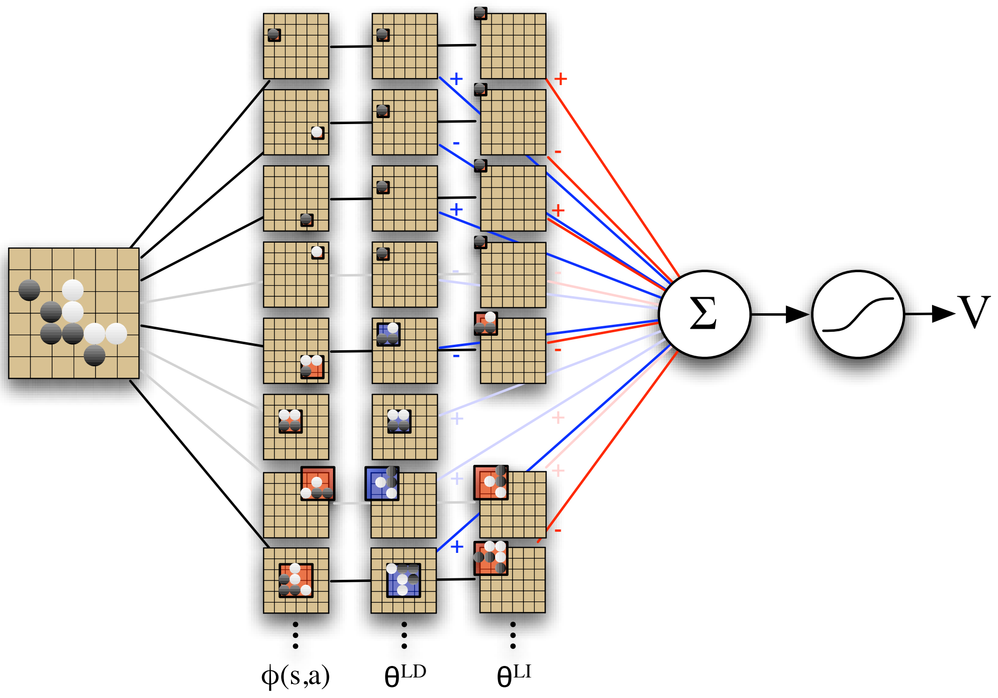

Figure 5.3: Evaluating an example 9×9 Go position using local shape features. The first column shows several local shape features. The dark lines indicate local shape features that are active in the example position, and the grey lines indicate local shape features that are inactive in the example position. The second and third columns show the canonical example of each local shape feature, within the location dependent and location independent equivalence classes respectively. The sixth local shape feature is neutral when using location independent weight sharing; this weight is assumed to be zero and does not contribute to the evaluation. The weights of the canonical examples are combined together for each active feature (indicated by blue lines for location dependent, and red lines for location independent weight sharing). Finally, the linear combination of weights is squashed into a value function that estimates Black's probability of winning in this position.

in a single time-step.[5]

It is well-known that temporal-difference learning, much like the LMS algorithm in supervised learning, is sensitive to the choice of learning rate (Singh and Dayan, 1998). If the features are scaled up or down in value, or if more or less features are included in the feature vector, then the learning rate needs to change correspondingly in magnitude. To address this issue, we divide the step-size by the total number of currently active features, $||\phi(s_t)||^2 = \sum_{i=1}^{n} \phi(s_t)^2$. As in the NLMS algorithm, (Haykin, 1996), this normalises the update by the total signal power of the features,

$$\Delta\theta^{LD} = \Delta\theta^{LI} = \alpha \frac{\phi(s_t)}{||\phi(s_t)||^2}(V(s_{t+2}) - V(s_t)) \tag{5.3}$$

As in the Sarsa algorithm (see Chapter 2) the policy is updated after every move t, by using an ϵ-greedy policy. With probability $1 - \epsilon$ the player selects the move that maximises (Black) or minimises (White) the value function $a = \underset{a'}{\operatorname{argmax}}\, V(s \circ a')$. With probability ϵ the player selects a move with uniform random probability. The learning update is applied whether or not an exploratory move is selected.

Because the local shape features are sparse, only a small subset of features need be evaluated and updated. This leads to an an efficient $O(k)$ implementation, where k is the total number of active features. This requires just a few hundred operations, rather than evaluating or updating a million components of the full feature vector.

The basic algorithm is described in pseudocode in Algorithm 5. This implementation incrementally maintains two sparse sets $\mathcal{F}^{LI}(s)$ and $\mathcal{F}^{LD}(s)$. Each sparse set contains the canonical index i and weight sharing sign d for each active feature in position s.

5.6 Training

We initialise all weights to zero, so that rarely encountered features do not initially contribute to the evaluation. We train the weights by executing a million games of self-play, in 9×9 Go. Both Black and White select moves using an ϵ-greedy policy over the same value function $V(s)$. The same weights are used by both players, and updated after both Black and White moves by Equation 5.3.

All games begin from the empty board position, and terminate when both players pass. To prevent games from continuing for an excessive number of moves, we prohibit moves within single-point eyes, and only allow the pass move when no other legal moves are available. In addition, any game that exceeds 1,000 moves (which occasionally happens when multiple *ko* situations occur) is declared a draw, and both players are given a reward of $r = 0.5$. Games which successfully terminate are scored by Chinese rules, assuming that all stones are alive, and using a *komi* of 7.5.

[5]An equivalent state representation would be to have one feature $\phi_i(s)$ for each equivalence class i, where $\phi_i(s)$ counts the number of occurrences of equivalence class i in position s.

Algorithm 3 TD(0) Self-Play with Binary Features and Weight Sharing

```
procedure TD(0)-SELFPLAY
    while time available do
        $board.Initialise()$
        SELFPLAY($board$)
    end while
    $board.SetPosition(s_0)$
    return $\epsilon$-GREEDY($board, 0$)
end procedure

procedure SELFPLAY($board$)
    $t = 0$
    $V_0, \mathcal{F}_0 = $ EVAL($board$)
    while not $board.Terminal()$ do
        $a_t = \epsilon$-GREEDY($board, \epsilon$)
        $board.Play(a_t)$
        $t$ ++
        $V_t, \mathcal{F}_t^{LI}, \mathcal{F}_t^{LD}, k = $ EVAL($board$)
        if $t \geq 2$ then
            $\delta = V_t - V_{t-2}$
            for all $(i, d) \in \mathcal{F}_{t-2}^{LI}$ do
                $\theta^{LI}[i] \mathrel{+}= \frac{\alpha}{k}\delta d$
            end for
            for all $(i, d) \in \mathcal{F}_{t-2}^{LD}$ do
                $\theta^{LD}[i] \mathrel{+}= \frac{\alpha}{k}\delta d$
            end for
        end if
    end while
end procedure

procedure EVAL($board$)
    if $board.Terminal()$ then
        return $board.BlackWins(), \emptyset, \emptyset, 0$
    end if
    $\mathcal{F}^{\mathcal{LI}} = board.GetActiveLI()$
    $\mathcal{F}^{\mathcal{LD}} = board.GetActiveLD()$
    $v = 0$
    $k = 0$
    for all $(i, d) \in \mathcal{F}^{\mathcal{LI}}$ do
        $v \mathrel{+}= d\theta^{LI}[i]$
        $k$ ++
    end for
    for all $(i, d) \in \mathcal{F}^{\mathcal{LD}}$ do
        $v \mathrel{+}= d\theta^{LD}[i]$
        $k$ ++
    end for
    $V = \frac{1}{1+e^{-v}}$
    return $V, \mathcal{F}^{LI}, \mathcal{F}^{LD}, k$
end procedure

procedure $\epsilon$-GREEDY($board, \epsilon$)
    if $Bernoulli(\epsilon) = 1$ then
        return $Uniform(board.Legal())$
    end if
    $black = board.BlackToPlay()$
    $a^* = Pass$
    $V^* = black$ ? $0 : 1$
    for all $a \in board.Legal()$ do
        $board.Play(a)$
        $V = $ EVAL($board$)
        if ($black$ and $V \geq V^*$)
        or (not $black$ and $V \leq V^*$)
            $V^* = V$
            $a^* = a$
        end if
        $board.Undo()$
    end for
    return $a^*$
end procedure
```

5.7 A Case Study in 9×9 Computer Go

We implemented the learning algorithm and training procedure described above in our computer Go program *RLGO 1.0*.

5.7.1 Computational Performance

On a 2 Ghz processor, using the default parameters and Algorithm 5, *RLGO* evaluates approximately 500,000 positions per second. *RLGO* uses a number of algorithmic optimisations in order to efficiently and incrementally update the value function. Nevertheless, the dominant computational cost in *RLGO* is position evaluation during ϵ-greedy move selection. The temporal-difference learning update itself is relatively inexpensive, and consumes around 15% of the overall computation time.

5.7.2 Experimental Setup

In this case study we compare learning curves for *RLGO 1.0*, using a variety of parameter choices. This requires some means to evaluate the performance of our program for thousands of different combinations of parameters and weights. Measuring performance online against human or computer opposition is only feasible for a small number of programs. Measuring performance against a standardised computer opponent, such as *GnuGo*, is only useful if the opponent is of a similar standard to the program. When Go programs differ in strength by many orders of magnitude, this leads to a large number of matches in which the result is an uninformative whitewash. Furthermore, we would prefer to measure performance robustly against a variety of different opponents.

In each experiment, after training *RLGO* for a million games with several different parameter settings, we ran a tournament between multiple versions of *RLGO*. Each version used the weights learnt after training from N games with a particular parameter setting. Each tournament included a variety of different N, for a number of different parameter settings. In addition, we included the program *GnuGo* 3.7.10 (level 10) in every tournament, to anchor the absolute performance between different tournaments. Each tournament consisted of at least 1,000 games for each version of *RLGO*. After all matches were complete, the results were analysed by the *bayeselo* program to establish an Elo rating for every program. Each figure indicates error bars corresponding to 95% confidence intervals over these Elo ratings.

Unless otherwise specified, we used default parameter settings of $\alpha = 0.1$ and $\epsilon = 0.1$. All local shape features were used for all square regions from 1×1 up to 3×3, using both location dependent and location independent weight sharing. The logistic temporal-difference learning algorithm was used, with two-ply updates (see Equation 5.3). During tournament testing games, moves were selected by a simple one-ply maximisation (Black) or minimisation (White) of the value function, $a = \underset{a'}{\operatorname{argmax}}\, V(s \circ a')$, with no random exploration.

Due to limitations on computational resources, just one training run was executed for each parameter setting. However, Figure 5.4 demonstrates that our learning algorithm is remarkably consis-

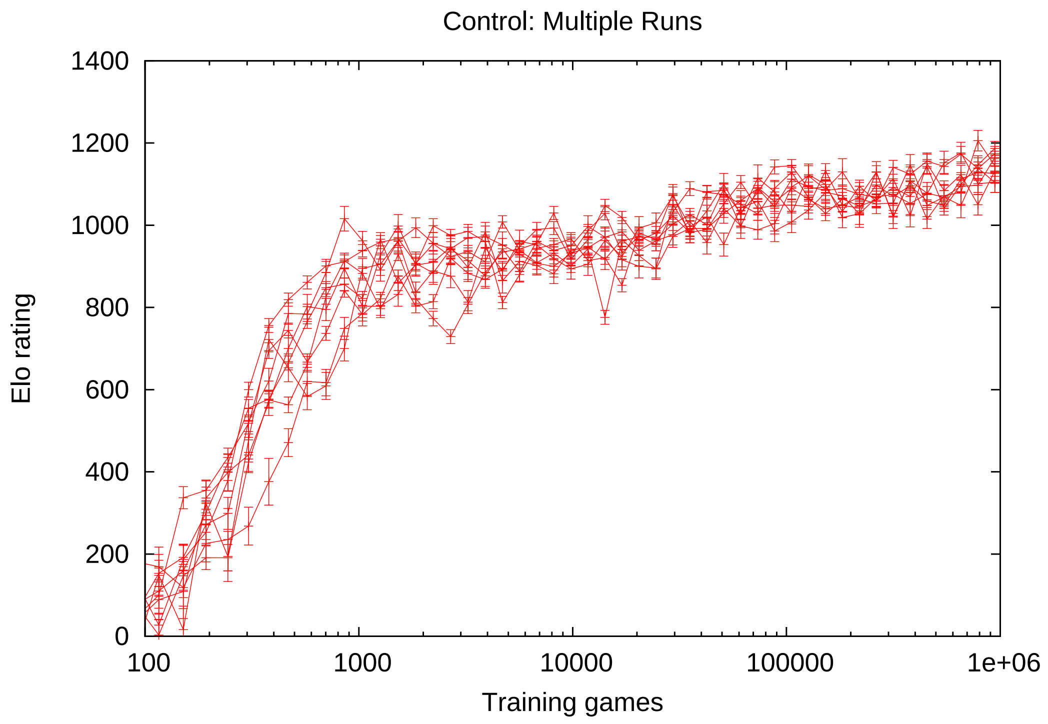

Figure 5.4: Multiple runs using the default learning algorithm and local shape features.

tent, producing very similar performance over the same timescale in 8 different training runs with the same parameters. Thus the conclusions that we draw from single training runs, while not definitive, are very likely to be repeatable.[6]

5.7.3 Local Shape Features in 9×9 Go

Perhaps the single most important property of local shape features is their huge range of generality. To assess this range, we counted the number of times that each equivalence class of feature occurs during training, and plotted a histogram for each size of local shape and for each type of weight sharing (see Figure 5.5). Each histogram forms a characteristic curve in log-log space. The most general class, the location independent 1×1 feature representing the material value of a stone, occurred billions of times during training. At the other end of the spectrum, there were tens of thousands of location dependent 3×3 features that occurred just a few thousand times, and 2,000 that were never seen at all. In total, each class of feature occurred approximately the same amount overall, but these occurrences were distributed in very different ways. Our learning algorithm must cope with this varied data: high-powered signals from small numbers of general features, and low-powered signals from a large number of specific features.

We ran several experiments to analyse how different combinations of local shape features affect

[6]The error bars in each figure correspond to variance in the Elo rating for the tested program, and do not indicate the variance over repeated runs.

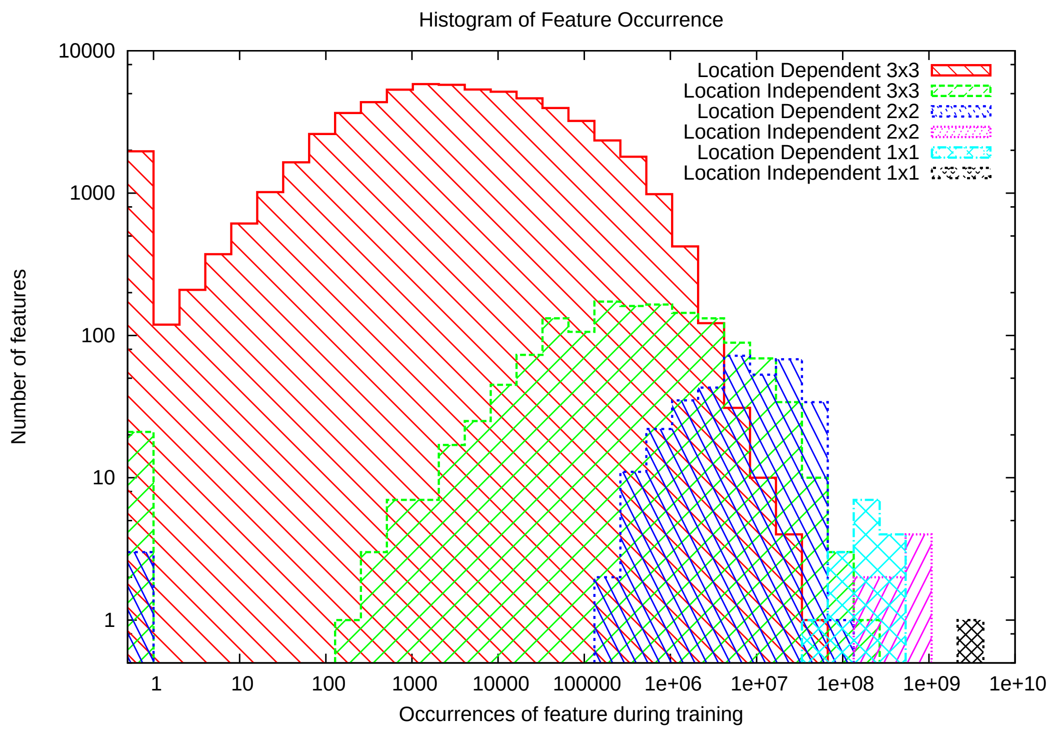

Figure 5.5: Histogram of feature occurrences during a training run of 1 million games.

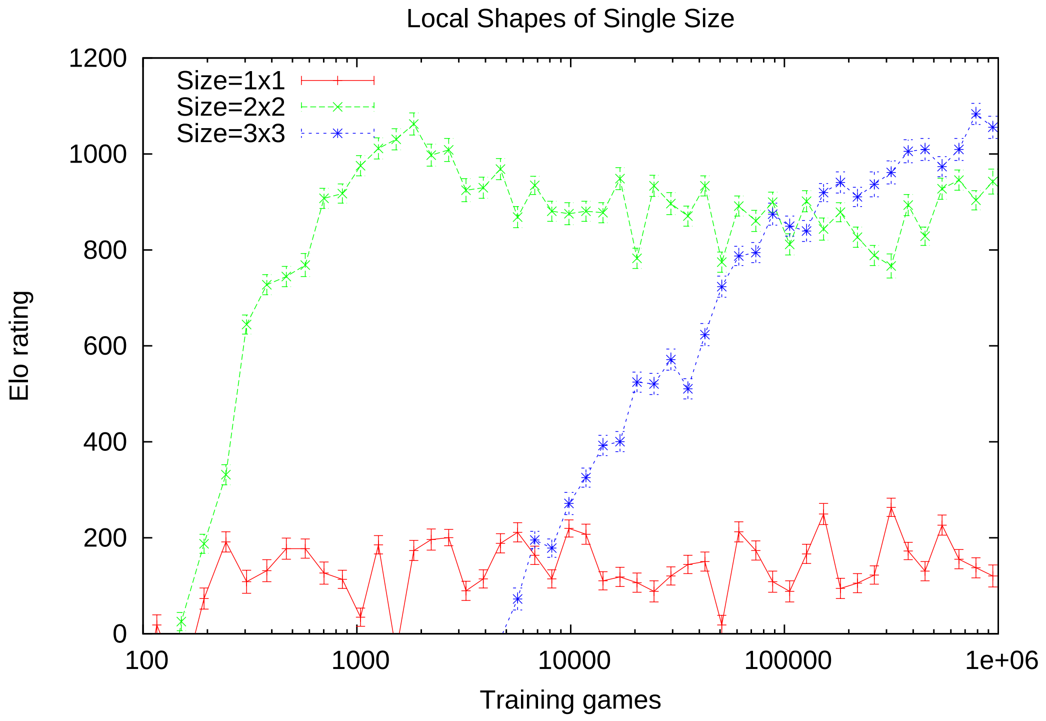

Figure 5.6: Learning curve for one size of local shape feature: 1×1, 2×2 and 3×3.

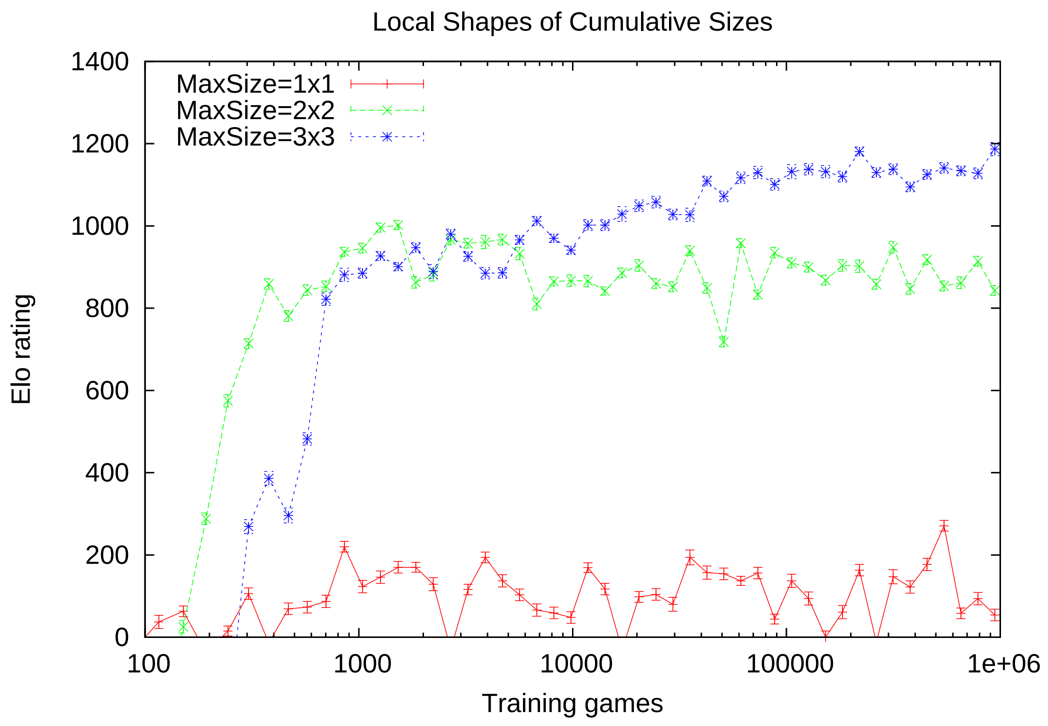

(a) Cumulative sizes: 1×1; 1×1 and 2×2; and 1×1, 2×2 and 3×3

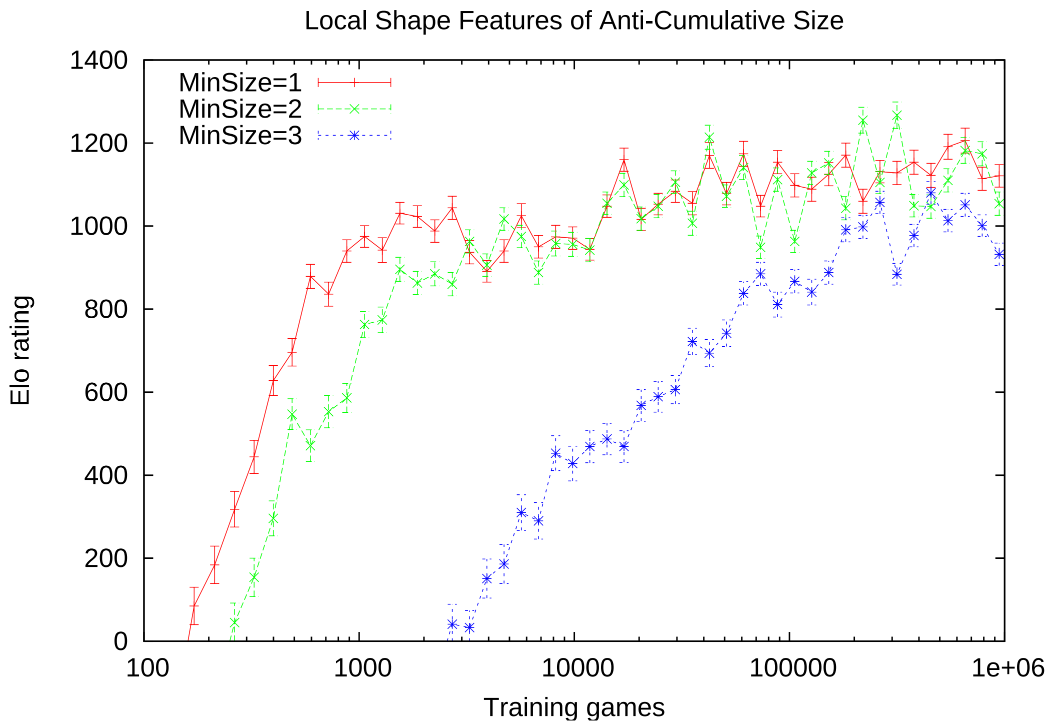

(b) Anti-cumulative sizes: 1×1, 2×2 and 3×3; 1×1 and 2×2; and 3×3

Figure 5.7: Learning curves for cumulative and anti-cumulative sizes of local shape feature.

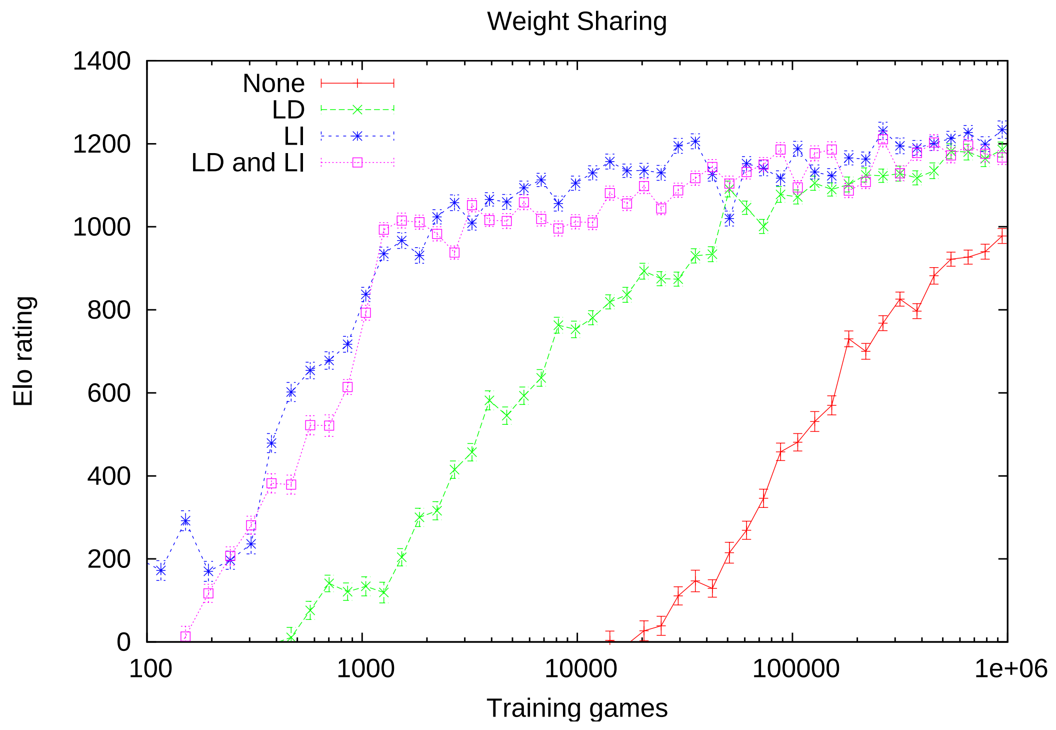

Figure 5.8: Learning curves for different weight sharing rules

the learning rate and performance of *RLGO 1.0*. In our first experiment, we used a single size of square region (see Figure 5.6). The 1×1 local shape features, unsurprisingly, performed poorly. The 2×2 local shape features learnt very rapidly, but their representational capacity was saturated at around 1000 Elo after approximately 2,000 training games. Surprisingly, performance appeared to decrease after this point, although this may be an artifact of a single training run. The 3×3 local shape features learnt very slowly, but exceeded the performance of the 2×2 features after around 100,000 training games.

In our next experiment, we combined multiple sizes of square region (see Figure 5.7). Using all features up to 3×3 effectively combined the rapid learning of the 2×2 features with the better representational capacity of the 3×3 features; the final performance was better than for any single shape set, reaching 1200 Elo, and apparently still improving slowly. In comparison, the 3×3 features alone learnt much more slowly at first, taking more than ten times longer to reach 1100 Elo, although the final rate of improvement may be greater. We conclude that a redundant representation, in which the same information is represented at multiple levels of generality, confers a significant advantage for at least a million training games.

In our final experiment with local shape features, we compared a variety of different weight sharing schemes (see Figure 5.8). Without any weight sharing, learning was very slow, eventually achieving 1000 Elo after a million training games. Location dependent weight sharing provided an intermediate rate of learning, and location independent weights provided the fastest learning. The eventual performance of the location independent weights was equivalent to the location dependent weights, and combining both types of weight sharing together offered no additional benefits. This suggests that the additional knowledge offered by location dependent shapes, for example patterns that are specific to edge or corner situations, was either not useful or not successfully learnt within the training time of these experiments.

5.7.4 Weight Evolution

Figure 5.9 shows the evolution of several feature weights during a single training run. Among the location independent 2×2 features, the efficient *turn* and *hane* shapes were quickly identified as the best, and the inefficient *dumpling* as the worst. The location dependent 1×1 features quickly established the value of stones in central board locations over edge locations. The 3×3 weights took several thousand games to move away from zero, but appeared to have stabilised towards the end of training.

Figure 5.10 shows how the mean cross-entropy TD-error (see Appendix A) decreases with training. In addition, the mean squared error between the value function and the final outcome is also plotted. Both error measures show a similar downward trend that gradually flattens out with additional training.

5.7.5 Logistic Temporal-Difference Learning

In Figure 5.11 we compare our logistic temporal-difference learning algorithm to linear temporal-difference learning algorithm, for a variety of different step-sizes α. In the latter approach, the value function is represented directly by a linear combination of features, with no logistic function; the weight update equation is otherwise identical to Equation 5.3.

Logistic temporal-difference learning is considerably more robust to the choice of step-size. It achieved good performance across three orders of magnitude of step-size, and improved particularly quickly with an aggressive learning rate. With a large step-size, the value function steps up or down the logistic function in giant strides. This effect can be visualised by zooming out of the logistic function until it looks much like a step function. In contrast, linear temporal-difference learning was very sensitive to the choice of step-size, and diverged when the step-size was too large.

Logistic temporal-difference learning also achieved better eventual performance. This suggests that, much like logistic regression for supervised learning (Jordan, 1995), the logistic representation is better suited to representing probabilistic value functions. However, the performance of logistic temporal-difference learning, which minimises a cross-entropy objective, was almost identical to the performance of non-linear temporal-difference learning (see Appendix A), which minimises a mean-squared error objective.

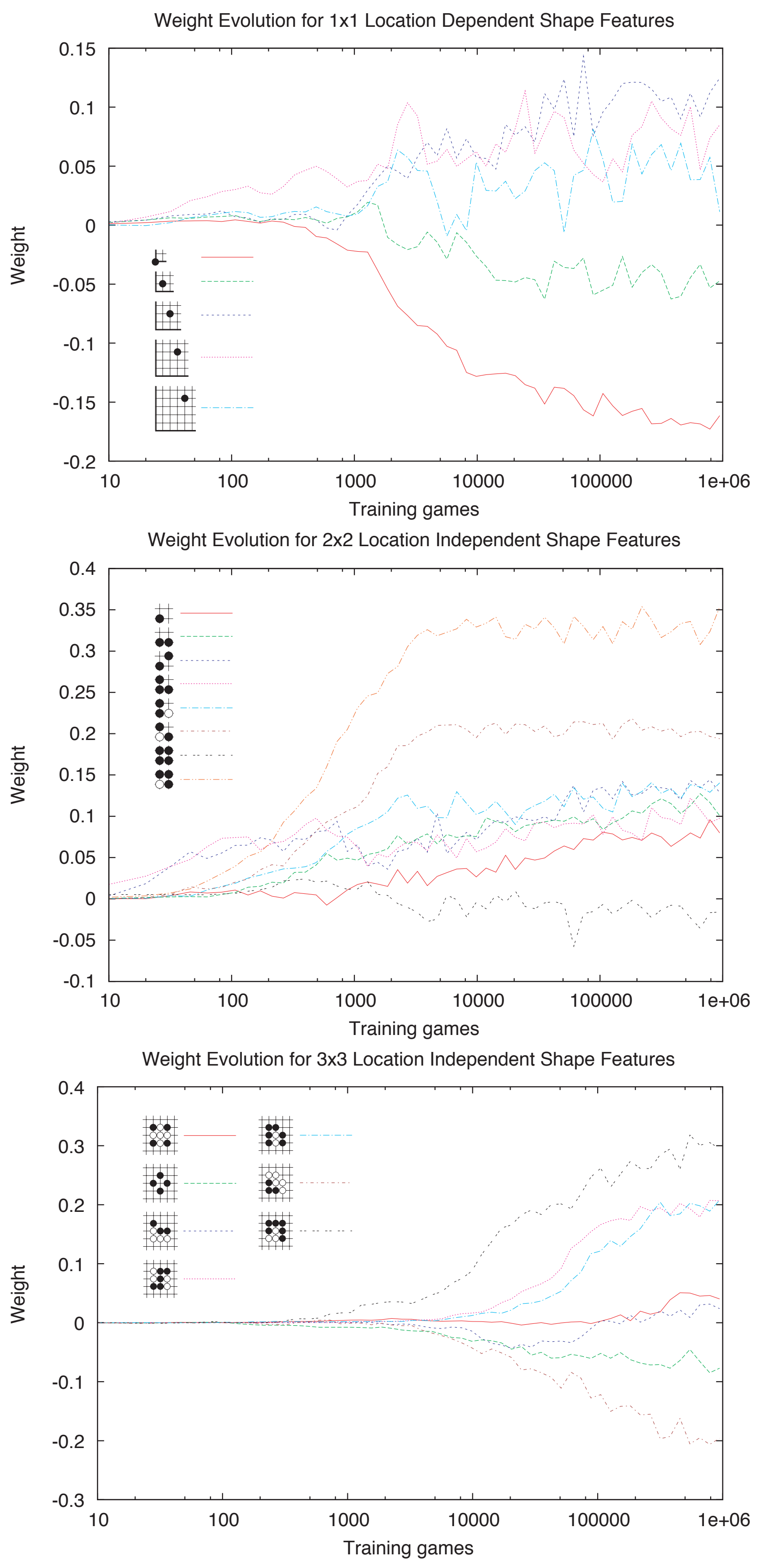

Figure 5.9: Evolution of weights for several different local shape features during training.

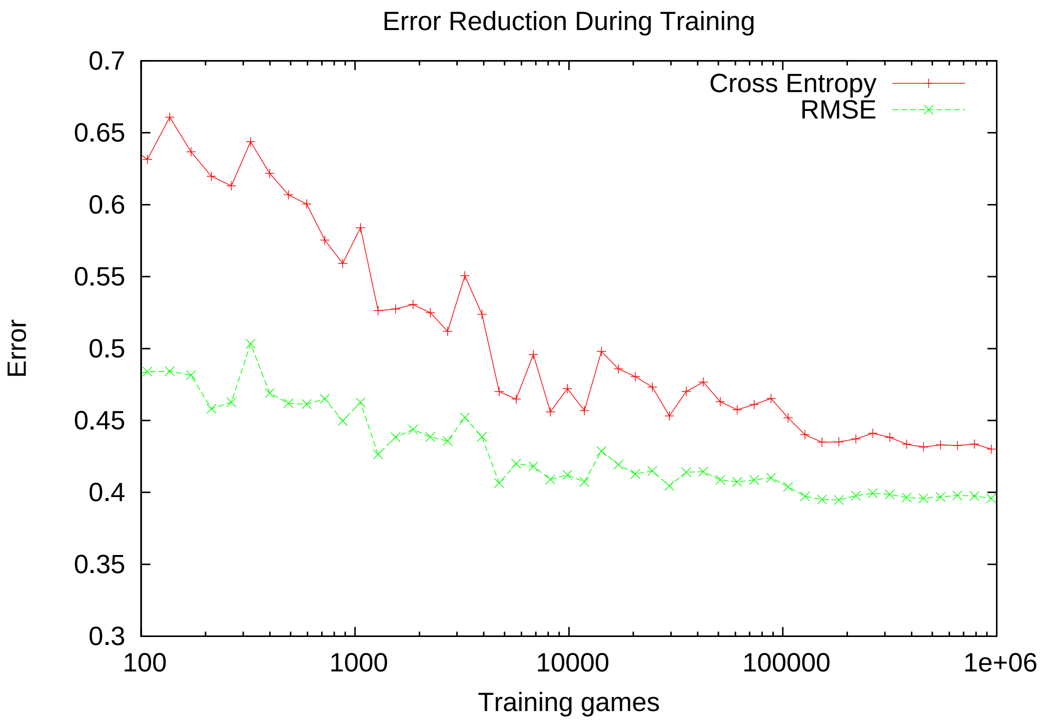

Figure 5.10: Reduction of cross entropy TD-error during training (red) and root mean squared error with respect to the actual outcomes (green).

5.7.6 Self-Play

When training from self-play, temporal-difference learning can use either one-ply or two-ply updates (see Section 5.5). We compare the performance of these two updates in Figure 5.12. Surprisingly, one-ply updates, which were so effective in *TD-Gammon*, performed very poorly in *RLGO*. This is due to our more simplistic representation: *RLGO* does not differentiate the colour to play. Because of this, whenever a player places down a stone, the value function is improved for that player. This leads to a large TD-error corresponding to the current player's advantage, which cannot ever be corrected. This error signal overwhelms the information about the relative strength of the move, compared to other possible moves. By using two-ply updates, this problem can be avoided altogether.[7]

Figure 5.13 compares the performance of different exploration rates ϵ. As might be expected, the performance decreases with increasing levels of exploration. However, without any exploration learning was much less stable, and $\epsilon > 0$ was required for robust learning. This is particularly important when training from self-play: without exploration the games are perfectly deterministic, and the learning process may become locked into local, degenerate solutions.

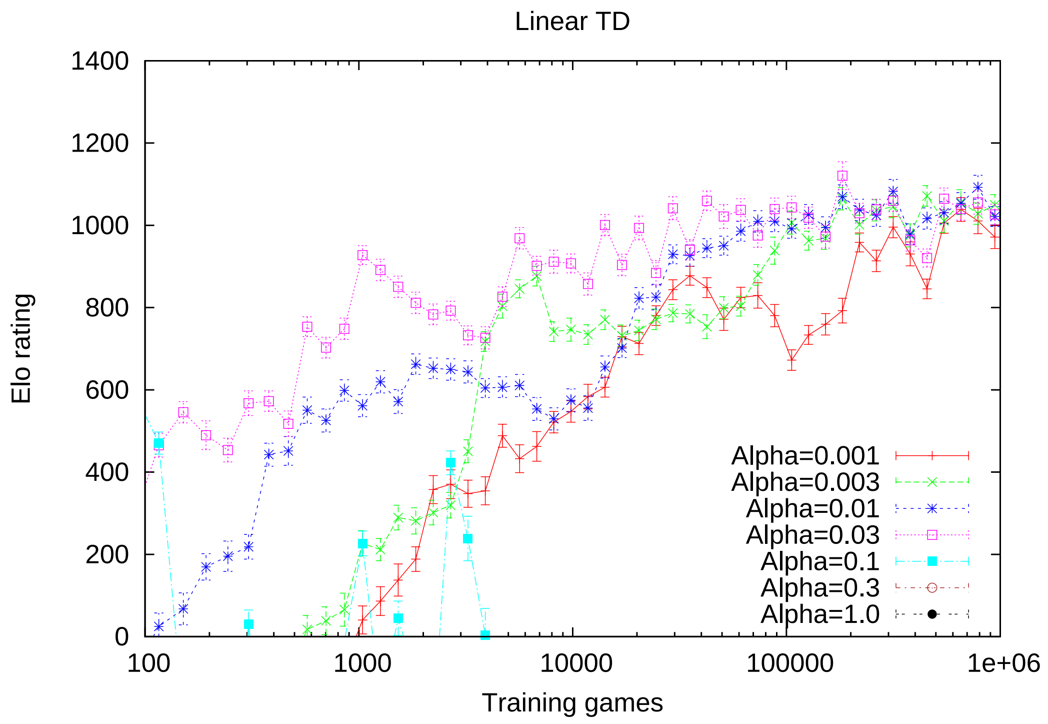

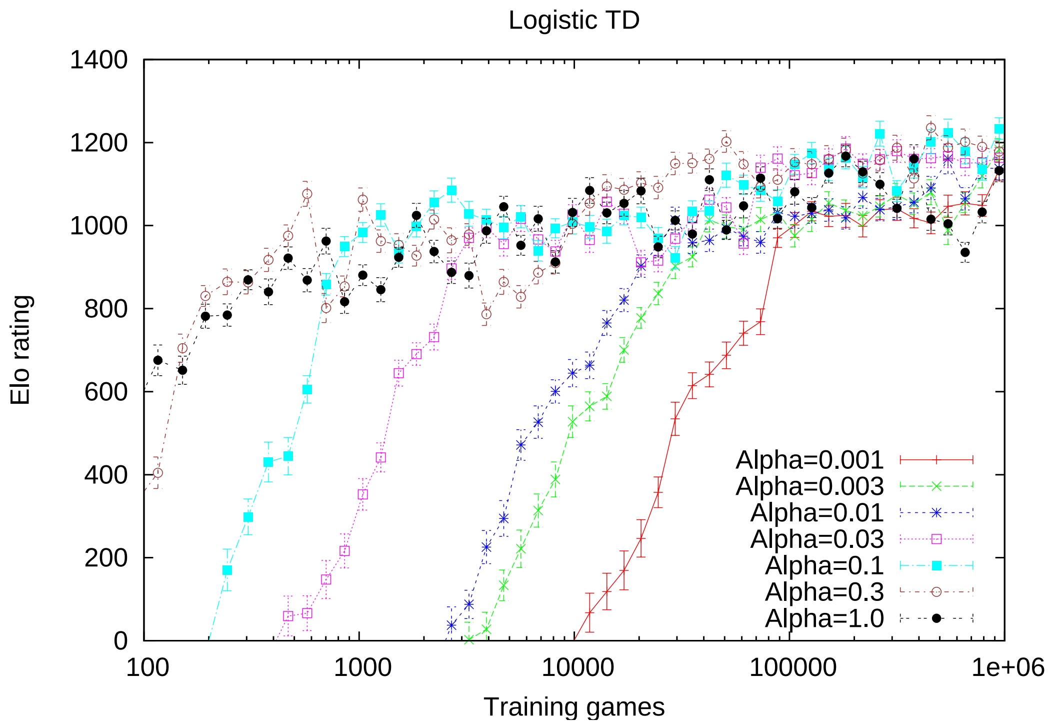

Figure 5.11: Comparison of linear (top) and logistic-linear (bottom) temporal-difference learning. Linear temporal-differencing learning diverged for step-sizes of $\alpha \geq 0.1$.

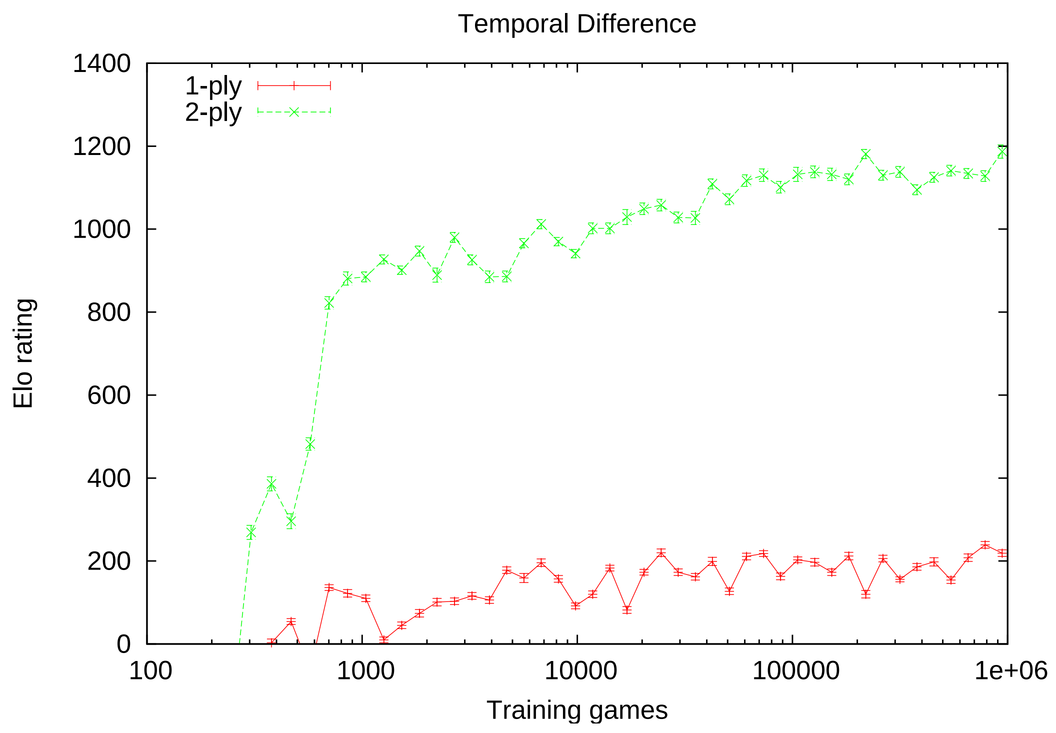

Figure 5.12: Learning curves for one-ply and two-ply updates.

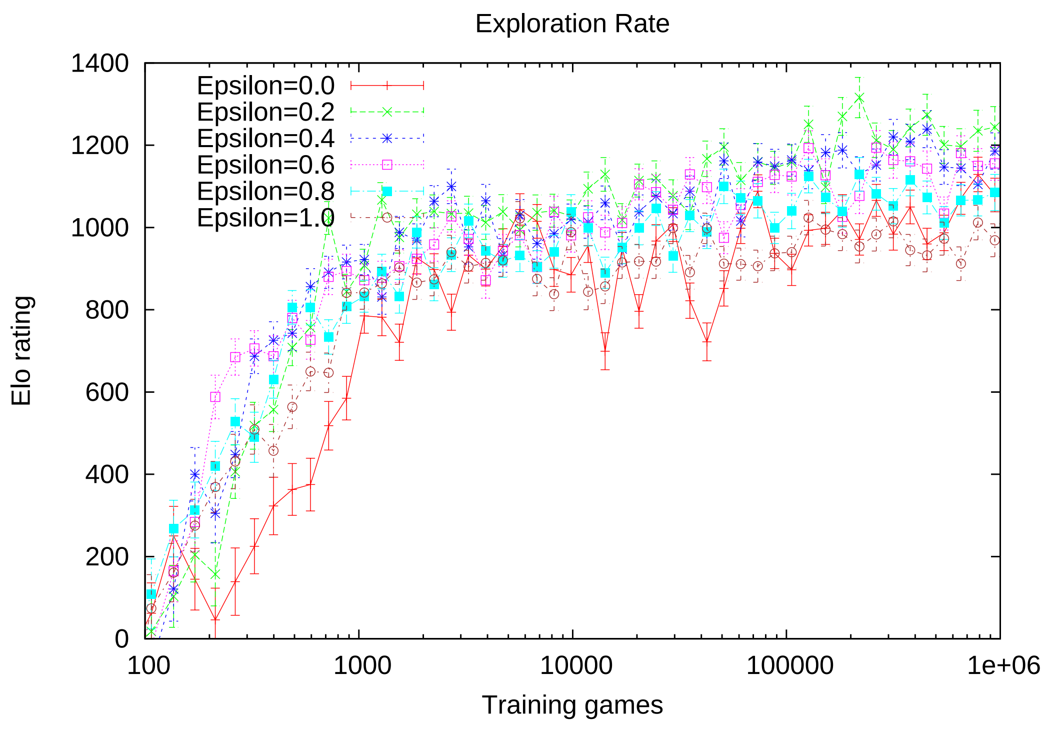

Figure 5.13: Learning curves for different exporation rates ϵ.

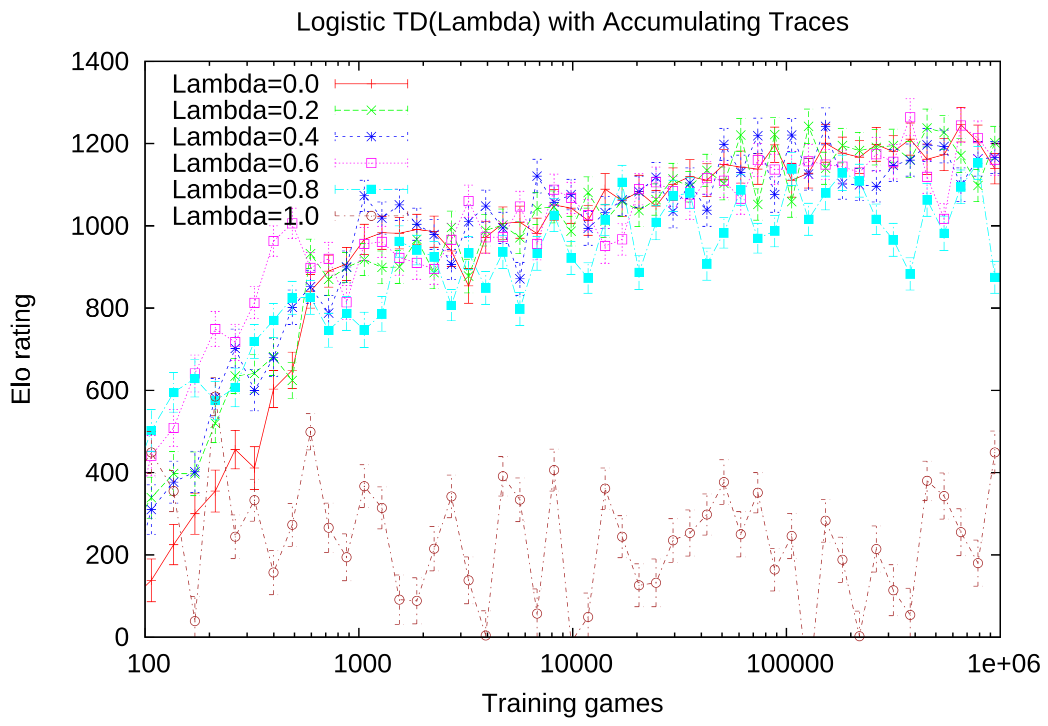

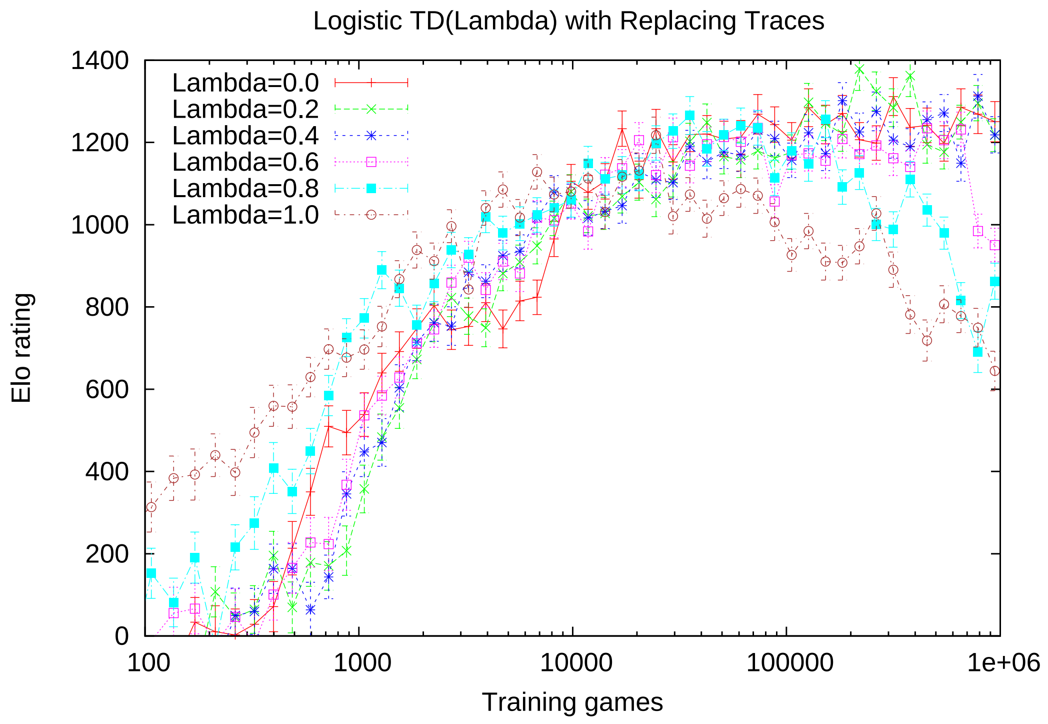

Figure 5.14: Learning curves for different values of λ, using accumulating traces (top) and replacing traces (bottom).

5.7.7 Logistic TD(λ)

The logistic temporal-difference learning algorithm can be extended to incorporate a λ parameter that determines the time-span of the temporal difference. When $\lambda = 1$, learning updates are based on the final outcome of the complete game, which is equivalent to logistic Monte-Carlo (see Appendix A). When $\lambda = 0$, learning updates are based on a one-step temporal difference, which is equivalent to the basic logistic temporal-difference learning update. We implement logistic TD(λ) by maintaining a vector of eligibility traces z that measures the credit assigned to each feature during learning (see Chapter 2), and is initialised to zero at the start of each game. We consider two eligibility update equations, based on accumulating and replacing eligibility traces,

$$z_{t+1} \leftarrow \lambda z_t + \frac{\phi(s_t)}{||\phi(s_t)||^2} \qquad \text{using accumulating traces} \qquad (5.4)$$

$$z_{t+1} \leftarrow (1 - \phi(s_t))\lambda z_t + \frac{\phi(s_t)}{||\phi(s_t)||^2} \qquad \text{using replacing traces} \qquad (5.5)$$

$$\Delta\theta_t = \alpha(V(s_{t+2}) - V(s_t))z_t \qquad (5.6)$$

We compared the performance of logistic TD(λ) for different settings of λ. High values of λ, especially $\lambda = 1$, performed substantially worse with accumulating traces. With replacing traces, high values of λ were initially beneficial, but the performance dropped off with more learning, suggesting that the high variance of the updates was less stable in the long run. The difference between lower values of λ, with either type of eligibility trace, was not significant.

5.7.8 Extended Representations in 9×9 Go

Local shape features are sufficient to represent a wide variety of intuitive Go knowledge. However, this representation of state is very simplistic: it does not represent which colour is to play, and it does not differentiate different stages of the game.

In our first experiment, we extend the local shape features so as to represent the colour to play. Three vectors of local shape features are used: $\phi^B(s)$ only match local shapes when Black is to play, $\phi^W(s)$ only match local shapes when White is to play, and $\phi^{BW}(s)$ matches local shapes when either colour is to play. We append these feature vectors together in three combinations:

1. $[\phi^{BW}(s)]$ is our basic representation, and does not differentiate the colour to play.
2. $[\phi^B(s); \phi^W(s)]$ differentiates the colour to play.
3. $[\phi^B(s); \phi^W(s); \phi^{BW}(s)]$ combines features that differentiate colour to play with features that do not.

[7]Mayer also reports an advantage to two-ply TD(0) when using a simple multi-layer perceptron architecture (Mayer, 2007).

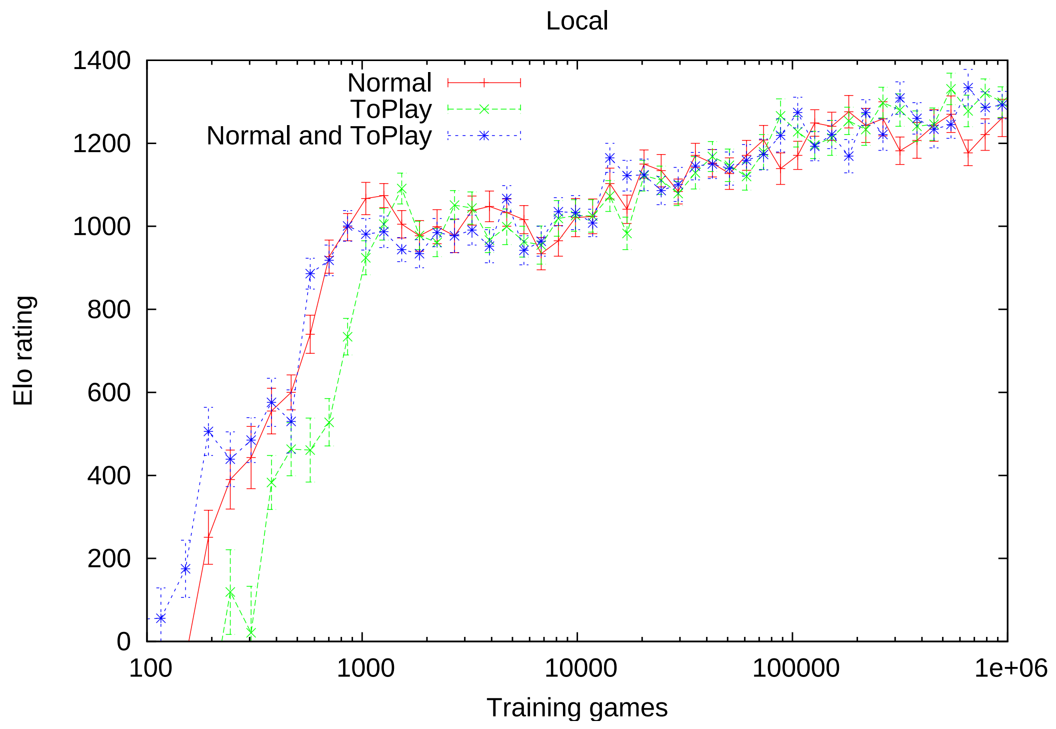

Figure 5.15: Extending the representation by differentiating the colour to play.

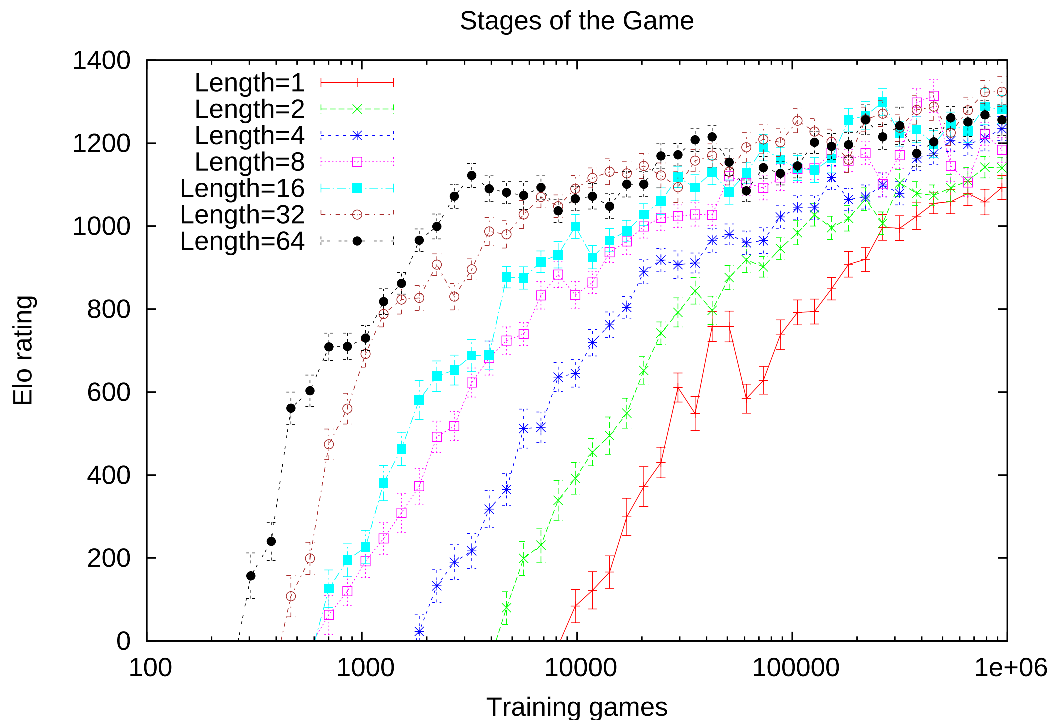

Figure 5.16: Extending the representation by differentiating the stage of the game. Stages are defined to have a variety of different lengths, measured in number of moves.

Search depth	Elo rating	Error
Depth 1	859	$\pm$ 23
Depth 2	1067	$\pm$ 20
Depth 3	1229	$\pm$ 18
Depth 4	1226	$\pm$ 20
Depth 5	1519	$\pm$ 19
Depth 6	1537	$\pm$ 19

Table 5.2: Performance of full width, fixed depth, alpha-beta search, using the learnt weights as an evaluation function. Weights were trained using default settings for 1 million training games. Elo ratings were established by a tournament amongst several players using the same weights. Each player selected moves by an alpha-beta search of the specified depth.

Figure 5.15 compares the performance of these three approaches, showing no significant differences.

In our second experiment, we extend the local shape features so as to represent the stage of the game. Each local shape feature $\phi^Q(s_t)$ only matches local shapes when the current move t is within the Qth stage of the game. Each stage of the game lasts for T moves, and the Qth stage lasts from move QT until $(Q+1)T$. We consider a variety of different timescales T for the stages of the game, and analyse their performance in Figure 5.16.

Surprisingly, differentiating the stage of the game was strictly detrimental. The more stages that are used, the slower learning proceeds. The additional representational capacity did not offer any benefits within a million training games.

These experiments suggest that a richer representation does not necessarily lead to better overall performance. There is a complex interplay between the representation, the learning algorithm, and the training data. Our basic representation already spans a wide range of levels of detail (see Figure 5.5). Ideally, a richer representation would help rather than hinder early learning, and would also help asymptotic performance. In order to achieve this goal, it may be necessary to dynamically adapt the representation, or to dynamically adapt the learning rate for each individual feature. It may also be important to balance exploration and exploitation so as to ensure that uncertain and significant features are explored more frequently.

5.7.9 Alpha-Beta Search

To complete our study of position evaluation in 9×9 Go, we used the learnt value function $V(s)$ as a heuristic function to evaluate the leaf positions in a fixed-depth alpha-beta search. We ran a tournament between several versions of *RLGO 1.0*, including *GnuGo* as a benchmark player, using an alpha-beta search of various fixed depths; the results are shown in Figure 5.2.

Alpha-beta search tournaments with the same program often exaggerate the performance differences between depths. To gain some additional insight into the performance of our program, *RLGO* played online in tournament conditions against a variety of different opponents on the Computer Go Server. The Elo rating established by *RLGO 1.0* is shown in Table 5.3.

Search depth	**Elo rating on CGOS**
1	1050
5	1350

Table 5.3: Elo ratings established by *RLGO 1.0* on the first version of the Computer Go Server (2006).

5.8 Discussion

The approach used by *RLGO* represents a departure from the search methods used in many previous computer Go programs (see Chapter 4). Programs such as *The Many Faces of Go* and *GnuGo* favour a heavyweight, knowledge intensive evaluation function, which can typically evaluate a few hundred positions with a shallow global search. In contrast, *RLGO 1.0* combines a fast, lightweight evaluation function with a deeper, global search that evaluates millions of positions. Using a naive, fixed-depth alpha-beta search, *RLGO 1.0* was not able to compete with the heavyweight knowledge used in previous approaches. However, a fast, simple evaluation function can be exploited in many ways. Later in this thesis we explore other search algorithms that can utilise a lightweight evaluation function much more effectively (see Chapters 6, 7 and 8).

The knowledge learnt using local shape features represents a broad library of common-sense Go intuitions. Figure 5.17 displays the weights with the highest absolute magnitude within each class, after training for a million games. The 1×1 shapes encode the basic material value of a stone. The 2×2 shapes measure the value of connecting and cutting; they encourage efficient shapes such as the *turn*, and discourage inefficient shapes such as the *empty triangle*. The 3×3 shapes represent several ways to split the opponent's stones, and three different ways to form two eyes in the corner.

However, the whole is greater than the sum of its parts. Weights are learnt for tens of thousands of shapes, and *RLGO 1.0* exhibits global behaviours beyond the scope of any single shape, such as territory building and control of the corners. Its principal weakness is its myopic view of the board; it will frequently play moves that look beneficial locally but miss the overall direction of the game, for example adding stones to a group that has no hope of survival (see Figure 5.18). By themselves, local shape features have no knowledge of the global context.

Context could be represented by a more sophisticated set of features, for example by incorporating the rich variety of Go concepts that have proven useful in other programs (see Chapter 4). However, the quality of additional information needs to be weighted against its cost of computation, especially in the context of online search. Furthermore, as we saw in Section 5.7.8, a richer representation does not necessarily lead to better overall performance. It may not be feasible to generate enough training data to justify the additional complexity. Furthermore, a fixed learning rate and exploration rate may be inadequate for a very large, diverse set of features (see Chapter 10 for further discussion of this issue).

In Go, the number of possible contexts is vast, and it may be futile to attempt to learn a single

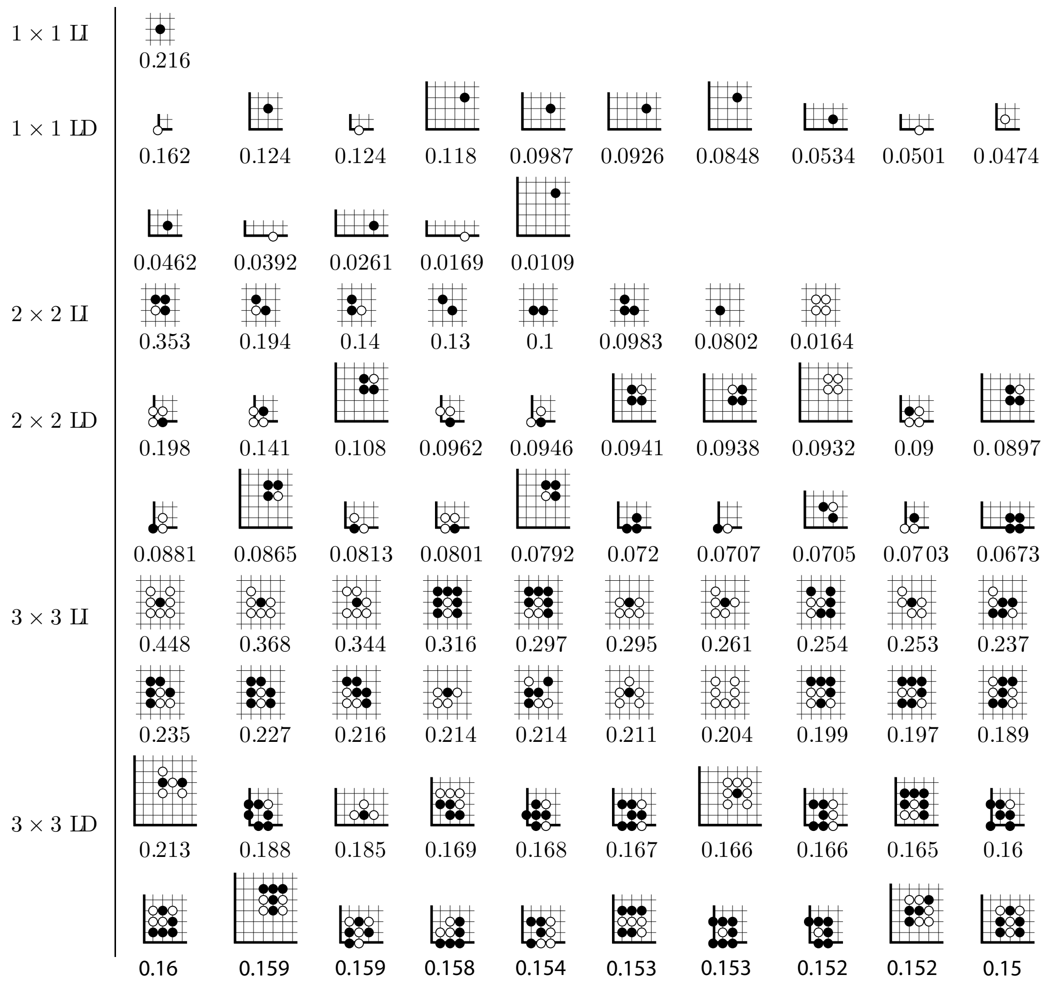

Figure 5.17: The top 20 shapes in each set from 1×1 to 3×3, location independent and location dependent, with the greatest absolute weight after training on a 9×9 board. One example of each set is shown, chosen to have a positive weight.

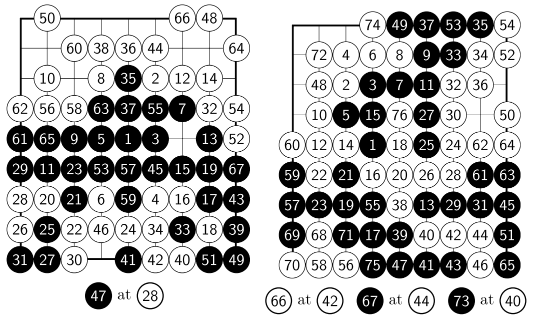

Figure 5.18: a) A game on the first version of the Computer Go Server (2006) between *RLGO 1.0* (white) and DingBat-3.2 (rated at 1577 Elo). RLGO plays a nice opening and develops a big lead. Moves 48 and 50 make good eye shape locally, but for the wrong group. DingBat takes away the eyes from the group at the bottom with move 51 and goes on to win. b) A game between *RLGO 1.0* (white) and the search based Liberty-1.0 (rated at 1110 Elo). RLGO plays good attacking shape from moves 24-37. It then extends from the wrong group, but returns later to make two safe eyes with 50 and 62 and ensure the win.

evaluation function that is appropriate for all contexts, regardless of the richness of the representation. In the next chapter, we develop a new paradigm for combining temporal-difference learning and search. In this approach, the evaluation function is re-learnt in every position, specialising to the current context.

Endnotes

An early version of temporal-difference learning with local shape features, using *RLGO 1.0*, was published in IJCAI (Silver et al., 2007). The evaluation methodology and results presented in this chapter supersede the results presented in that paper. I wrote the program *RLGO* using the SmartGame library for computer Go, by Martin Müller and Markus Enzenberger.

Chapter 6

Temporal-Difference Search

6.1 Introduction

Temporal-difference learning (Sutton, 1988) has proven remarkably successful in a wide variety of domains. In two-player games it has been used by the world champion backgammon program *TD-Gammon* (Tesauro, 1994), a version of the world champion checkers program *Chinook* (Schaeffer et al., 2001), the master-level chess program *Bodo* (Veness et al., 2009), and the strongest machine learnt evaluation function in Go (Enzenberger, 2003). In every case, an evaluation function was learnt offline, by training from thousands of games of self-play, and no further learning was performed online during actual play.

In this chapter we develop a very different paradigm for temporal-difference learning. In this approach, learning takes place *online*, so as to find the best evaluation function *for the current state*. Rather than training a very general evaluation function offline over many weeks or months, the agent trains a much more specific evaluation function online, in a matter of seconds or minutes.

In a two-player game $\mathcal{G}$, the current position s_t defines a new game, $\mathcal{G}'_t$, that is specific to this position. In the subgame $\mathcal{G}'_t$, the rules are the same, but the game always starts from position s_t. It may be substantially easier to solve or perform well in the subgame $\mathcal{G}'_t$, than to solve or perform well in the original game $\mathcal{G}$: the search space is reduced and a much smaller class of positions will typically be encountered. The subgame can have very different properties to the original game: certain patterns or features will be successful in this particular situation, which may not in general be a good idea. The idea of *temporal-difference search* is to apply temporal-difference learning to $\mathcal{G}'_t$, using subgames of self-play that start from the current position s_t.

Temporal-difference search can also be applied to any MDP $\mathcal{M}$, assuming that a generative model of $\mathcal{M}$ is provided, or can be learnt from experience. The current state s_t defines a sub-MDP $\mathcal{M}'_t$ that is identical to $\mathcal{M}$ except that the initial state is s_t. Again, the sub-MDP $\mathcal{M}'_t$ may be much easier to solve or approximate than the full MDP $\mathcal{M}$. Temporal-difference search applies temporal-difference learning to $\mathcal{M}'_t$, by generating episodes of experience that start from the current state s_t.

Rather than trying to learn a policy that covers every possible eventuality, temporal-difference search focuses on the subproblem that arises from the current state: how to perform well *now*. Life is full of such situations: you don't need to know how to climb every mountain in the world; but you'd better have a good plan for the one you are scaling right now.

6.2 Temporality

The nature of experience is that there is a special moment called *now*. The past is gone, the future is yet to arrive, and the agent's goal is to select the best action in the subproblem it faces right *now*. We refer to this concept as *temporality*.

Traditional machine learning, including much of supervised and unsupervised learning, often ignores temporality. Many current machine learning algorithms can be characterised by the search for a single, static, optimal solution. Once found, it is presumed that this solution no longer needs be changed. This is epitomised by the training phase / testing phase dichotomy, which assumes that all learning should be completed before the system is ever used in practice.

In reinforcement learning, time is explicit in the problem description: there is a temporal sequence of states, actions and rewards. However, even in reinforcement learning, temporality is frequently ignored. Batch methods optimise the agent's performance over all time-steps, and explicitly seek the best single value function, or single policy, over all of the agent's experience. Online methods, such as temporal-difference learning, are often applied offline in a separate training phase, with no further learning taking place during testing.

Sometimes, a single, static solution is sufficient to produce exceptional results. For example, when temporal-difference learning was used in the world's best backgammon player TD-Gammon (Tesauro, 1994), the objective was to find a single, static, high-quality evaluation function. When reinforcement learning was applied to helicopter flight (Ng et al., 2004), the search for the best policy was conducted in simulation and no further learning took place during actual flight.

However, if the environment can change over time, and the agent does not have sufficient resources to learn about all possible environments, then no single, stationary solution can ever be enough. Rather, the agent's solution must be continually be updated so as to perform well in the environment as it is *now*. When the environment changes, mistakes will be made and, if learning does not continue, they will be repeated again and again.

Temporality can be equally important in stationary problems. In very large environments, the agent encounters different regions of the state space at different times. In this case, it may be advantageous for the agent to adapt to the temporally local environment – the specific part of the state space it finds itself encountering right *now*. Usually, the agent has limited learning resources compared to the complexity of the problem, for example a fixed set of parameters for value function approximation, or a limited memory model of the environment. In this case, the agent can perform better by adapting those resources to its current subproblem, rather than by spreading those same resources thinly across the entire problem. Simple examples of such environments have been provided by Koop (2007) and Sutton et al. (2007).

6.3 Temporality and Search

Real-time search algorithms (Korf, 1990) exploit temporality by executing a search from the agent's current state s_t. They construct a search tree that is local to the current state s_t, so that both memory and computation are focused on the current state and its successors. The agent searches for as much computation time as is available, selects the best action from the search tree, and proceeds to the next state. Real-time search algorithms can reuse computation from previous time-steps, by retaining memory between searches: open and closed lists in learning real-time A* (Korf, 1990), transposition tables in alpha-beta search (Schaeffer, 2000), and a value function in real-time dynamic programming (Barto et al., 1995).

However, full-width heuristic search algorithms such as A* and alpha-beta utilise a static evaluation function at the leaves of the search tree. Although the search tree is temporally local, the evaluation function is not. In large or non-stationary problems with limited memory, the agent can perform better by specialising its evaluation function to the current subproblem, rather than using a weak heuristic that covers all possibilities.

6.4 Simulation-Based Search

Simulation-based search (see Chapter 3) is a new approach to real-time search that dynamically adapts its evaluation function. At every time-step s_t the agent simulates episodes of experience that start from the current state s_t. Each simulation samples experience from the agent's own policy and from a model of the environment. This samples from the distribution of future experience that would be encountered if the model was correct. By learning from this distribution of future experience, rather than the distribution of all possible experience, the agent exploits the temporality of the environment.[1] It can focus its limited resources on what is likely to happen from *now* onwards, rather than learning about all possible eventualities.

In an MDP, simulation-based search requires a *generative model* of the environment: a black box process for sampling a state transition from $\hat{\mathcal{P}}^a_{ss'}$ and a reward from $\hat{\mathcal{R}}^a_{ss'}$. The effectiveness of simulation-based search depends on the accuracy of the model, and learning a model can in general be a challenging problem. In this thesis we sidestep the model learning problem and assume that an accurate model is provided.

Two-player zero sum games provide an important special case. In these games, the opponent's behaviour can be modelled by the agent's own policy. As the agent's policy improves, so the model

[1]In non-ergodic environments, such as episodic tasks, this distribution can be very different. However, even in ergodic environments, the short-term distribution of experience, generated by discounting or by truncating the simulations after a small number of steps, can be very different from the stationary distribution. This local *transient* in the problem can be exploited by an appropriately specialised policy.

of the opponent also improves. In addition, we assume that the rules of the game are known. By combining the rules of the game with our model of the opponent's behaviour, we can generate complete two-ply state transitions for each possible action. We refer to this state transition model as a *self-play model*. In addition, the rules of the game can be used to generate rewards: a terminal outcome (e.g. winning, drawing or losing), with no intermediate rewards.

By simulating experience from *now*, using a model of the environment, the agent creates a new reinforcement learning problem that starts from the current state s_t. At every computational step u the agent receives a state s_u from the model, executes an action a_u according to its current policy $\pi_u(s, a)$, and then receives a reward r_{u+1} from the model. The idea of simulation-based search is to learn a policy that maximises the total future reward, in this simulation of the environment. Unlike other sample-based planning methods, such as Dyna (Sutton, 1990), simulation-based search seeks the specific policy that maximises expected total reward in the agent's current subproblem.

6.5 Beyond Monte-Carlo Tree Search

Monte-Carlo tree search is the best-known example of a simulation-based search algorithm. It has outperformed previous search algorithms in a variety of challenging problems (see Chapter 3). However, Monte-Carlo tree search is unable to generalise online between related states, and its value estimates have high variance. We introduce a new framework for simulation-based search that addresses these two issues with two new ideas.

In Monte-Carlo tree search, states are represented individually. The search tree is based on table lookup, where each node stores the value of one state. However, unlike table lookup, only some states are stored in the search tree. Once all states have been added, Monte-Carlo tree search is equivalent to Monte-Carlo control using table lookup (see Chapter 2), applied to the subproblem starting from s_t.

Just like table lookup, Monte-Carlo tree search cannot generalise online between related states. Our first idea is to approximate the value function by a linear combination of features, instead of using a search tree. In this approach, the outcome from a single position can be used to update the value function for a large number of similar states. This can lead to a much more efficient search given the same number of simulations. However, the approximate values will not usually be able to represent the optimal values, and unless the features can represent all possible states, asymptotic performance will be reduced.

Furthermore, Monte-Carlo methods must wait many time-steps until the final outcome of the simulation is known. This outcome depends on all of the agent's decisions, and on the environment's uncertain responses to those decisions, throughout the simulation. In our framework, we use temporal-difference learning instead of Monte-Carlo evaluation, so that the value function can bootstrap from subsequent values. In reinforcement learning, bootstrapping often provides a substantial reduction in variance and an improvement in performance. Our second idea is to apply bootstrapping to simulation-based search.

6.6 Temporal-Difference Search

Algorithm 4 Linear TD Search

```
1: $\theta \leftarrow 0$                                  ▷ Initialise parameters
2: procedure SEARCH($s_0$)
3:     while time available do
4:         $e \leftarrow 0$                                ▷ Clear eligibility trace
5:         $s \leftarrow s_0$
6:         $a \leftarrow \epsilon$-greedy$(s; Q)$
7:         while $s$ is not terminal do
8:             $s' \sim \mathcal{P}^a_{ss'}$               ▷ Sample state transition
9:             $r \leftarrow \mathcal{R}^a_{ss'}$          ▷ Sample reward
10:            $a' \leftarrow \epsilon$-greedy$(s'; Q)$
11:            $\delta \leftarrow r + Q(s', a') - Q(s, a)$ ▷ TD-error
12:            $\theta \leftarrow \theta + \alpha\delta e$ ▷ Update weights
13:            $e \leftarrow \lambda e + \phi(s, a)$       ▷ Update eligibility trace
14:            $s \leftarrow s', a \leftarrow a'$
15:        end while
16:    end while
17:    return $\underset{a}{\operatorname{argmax}}\, Q(s_0, a)$
18: end procedure
```

Temporal-difference search is a simulation-based search algorithm in which the value function is updated online, from simulated experience, by temporal-difference learning. Each search begins from a root state s_0. The agent simulates many episodes of experience from s_0, by sampling from its current policy $\pi_u(s, a)$, and from a transition model $\mathcal{P}^a_{ss'}$ and reward model $\mathcal{R}^a_{ss'}$, until each episode terminates.

Instead of using a search tree, the agent approximates the value function by using features $\phi(s, a)$ and adjustable parameters θ_u, using a linear combination $Q_u(s, a) = \phi(s, a) \cdot \theta_u$. After every step u of simulation, the agent updates the parameters by temporal-difference learning, using the TD(λ) algorithm.

The first time a search is performed from s_0, the parameters are initialised to zero. For a subsequent search from s'_0, the parameter values are reused, so that the value function computed by the last search is used as the initial value function for the next search.

The agent selects actions by using an ϵ-greedy policy $\pi_u(s, a)$ that with probability $1 - \epsilon$ maximises the current value function $Q_u(s, a)$, and with probability ϵ selects a random action. As in the Sarsa algorithm, this interleaves policy evaluation with policy improvement, with the aim of finding the policy that maximises expected total reward from s_0, given the current model of the environment.

Temporal-difference search applies the Sarsa(λ) algorithm to the sub-MDP that starts from the state s_0, and thus has the same convergence properties as Sarsa(λ), i.e. continued chattering but no divergence (Gordon, 1996) (see Chapter 2). We note that other online, incremental reinforcement learning algorithms could be used in place of Sarsa(λ), for example policy gradient or actor-critic methods (see Chapter 2), if guaranteed convergence were required. However, the computational simplicity of Sarsa are highly desirable during online search.

6.7 Temporal-Difference Search and Monte-Carlo Search

Temporal-difference search provides a spectrum of different algorithms. At one end of the spectrum, we can set $\lambda = 1$ to give Monte-Carlo search algorithms, or alternatively we can set $\lambda < 1$ to bootstrap from successive values. We can use table lookup features, or we can generalise between states by using abstract features.

In order to reproduce Monte-Carlo tree search, we use $\lambda = 1$ to backup values directly from the final return, without bootstrapping (see Chapter 2). We use one table lookup feature $I^{S,A}$ for each state S and each action A,

$$I^{S,A}(s,a) = \begin{cases} 1 & \text{if } s = S \text{ and } a = A \\ 0 & \text{otherwise.} \end{cases} \tag{6.1}$$

We also use a step-size schedule of $\alpha(s,a) = 1/N(s,a)$, where $N(s,a)$ counts the number of times that action a has been taken from state s. This computes the mean return of all simulations in which action a was taken from state s, in an analogous fashion to Monte-Carlo evaluation (see Chapter 2). Finally, in order to grow the search tree incrementally, in each simulation we add one new feature $I^{S,A}$ for every action A, for the first visited state S that is not already represented by table lookup features.

6.8 Temporal-Difference Search in Computer Go

As we saw in Chapter 5, local shape features provide a simple but effective representation for some intuitive Go knowledge. The value of each shape can be learnt offline, using temporal-difference learning and training by self-play, to provide general knowledge about the game of Go. However, the value function learnt in this way is rather myopic: each square region of the board is evaluated independently, without any knowledge of the global context.

Local shape features can also be used during temporal-difference search. Although the features themselves are very simple, temporal-difference search is able to learn the value of each feature in the current board context. This can significantly increase the representational power of local shape features: a shape may be bad in general, but good in the current situation. By training from simulated experience, starting from the current state, the agent can focus on what works well *now*.

Local shape features provide a simple but powerful form of generalisation between similar positions. Unlike Monte-Carlo tree search, which evaluates each state independently, the value θ_i of a local shape ϕ_i is reused in a large class of related positions $\{s : \phi_i(s) = 1\}$ in which that particular shape occurs. This enables temporal-difference search to learn an effective value function from fewer simulations than is possible with Monte-Carlo tree search.

In Chapter 5 we were able to exploit the symmetries of the Go board by using weight sharing. However, by starting our simulations from the current position, we break these symmetries. The vast majority of Go positions are asymmetric, so that for example the value of playing in the top-left corner will be significantly different to playing in the bottom-right corner. Thus, we do not utilise any form of weight-sharing during temporal-difference search. However, local shape features that consist entirely of empty intersections are assumed to be neutral and are removed from the representation.[2]

We apply the temporal-difference search algorithm to 9×9 computer Go using 1×1 to 3×3 local shape features. We use a self-play model, an ϵ-greedy policy, and default parameters of $\lambda = 0$, $\alpha = 0.1$, and $\epsilon = 0.1$. We use a binary reward function at the end of the game: $r = 1$ if Black wins and $r = 0$ otherwise. We modify the basic temporal-difference search algorithm to exploit the probabilistic nature of the value function, by using logistic temporal-difference learning (see Appendix A). As in Chapter 5 we normalise the step-size by the total number of active features $||\phi(s)||^2$, and use a two-ply temporal-difference update,

$$V(s) = \sigma(\phi(s).\theta) \tag{6.2}$$

$$\Delta\theta = \alpha \frac{\phi(s_t)}{||\phi(s_t)||^2}(V(s_{t+2}) - V(s_t)) \tag{6.3}$$

where $\sigma(x) = \frac{1}{1+e^{-x}}$ is the logistic function.

Once each temporal-difference search is complete, moves are selected greedily so as to maximise (Black) or minimise (White) the value function, $a = \underset{b}{\operatorname{argmax}}\ V(s \circ b)$. The basic algorithm is described in pseudocode in Algorithm 5. This implementation incrementally maintains a sparse set $\mathcal{F}$, which contains the indices of all active features in the current position, $\mathcal{F}(s) = \{i|\phi_i(s) = 1\}$.

6.9 Experiments in 9×9 Go

We implemented the temporal-difference search algorithm in our Go program *RLGO 2.4*. We ran a tournament between different versions of *RLGO*, for a variety of different parameter settings, and a variety of different simulations per move (i.e. varying the search effort). In addition, we included two benchmark programs in each tournament, described below. Each Swiss-style tournament[3] consisted of at least 200 games for each version of *RLGO*. After all matches were complete, the results were analysed by the *bayeselo* program (Coulom, 2008) to establish an Elo rating for every program. Following convention, *GnuGo* was assigned an anchor rating of 1800 Elo in all cases.

[2]If empty shapes are used, then the algorithm is less effective in opening positions, as the majority of credit is assigned to features corresponding to open space.

[3]Matches were randomly selected with a bias towards programs with a similar number of wins.

Algorithm 5 TD Search with TD(0) and Binary Features

```
procedure TD(0)-SEARCH($s_0$)
    $board.Initialise()$
    while time available do
        SELFPLAY($board, s_0$)
    end while
    $board.SetPosition(s_0)$
    return $\epsilon$-GREEDY($board, 0$)
end procedure

procedure EVAL($board$)
    if $board.Terminal()$ then
        return $board.BlackWins(), \emptyset, 0$
    end if
    $\mathcal{F} = board.GetActiveFeatures()$
    $v = 0$
    $k = 0$
    for all $i \in \mathcal{F}$ do
        $v \mathrel{+}= \theta[i]$
        $k$ ++
    end for
    $V = \frac{1}{1+e^{-v}}$
    return $V, \mathcal{F}, k$
end procedure

procedure SELFPLAY($board, s_0$)
    $board.SetPosition(s_0)$
    $t = 0$
    $V_0, \mathcal{F}_0 = $ EVAL($board$)
    while not $board.Terminal()$ do
        if $t \leq T$ then
            $a_t = \epsilon$-GREEDY($board, \epsilon$)
        else
            $a_t = $ DEFAULTPOLICY($board$)
        end if
        $board.Play(a_t)$
        $t$ ++
        $V_t, \mathcal{F}_t, k_t = $ EVAL($board$)
        if $t \geq 2$ then
            $\delta = V_t - V_{t-2}$
            for all $i \in \mathcal{F}_{t-2}$ do
                $\theta[i] \mathrel{+}= \frac{\alpha}{k_t}\delta$
            end for
        end if
    end while
end procedure
```

Two benchmark programs were included in each tournament. First, we included *GnuGo 3.7.10*, set to level 10 (strong, default playing strength). Second, we used an implementation of UCT in *Fuego 0.1* (Müller and Enzenberger, 2009) that we refer to as *vanilla UCT*. This implementation was based on the UCT algorithm, with RAVE and heuristic prior knowledge extensions turned off.[4] Vanilla UCT uses the handcrafted default policy in *Fuego*, which is similar to the rules for *MoGo* described in Chapter 4 (Gelly et al., 2006). The UCT parameters were set to the best reported values for *MoGo* (Gelly et al., 2006): exploration constant $= 1$, first play urgency $= 1$.

6.9.1 Default Policy

The basic temporal-difference search algorithm uses no prior knowledge in its simulation policy. One way to incorporate prior knowledge is to switch to a handcrafted default policy, as in the Monte-Carlo tree search algorithm. We ran an experiment to determine the effect on performance of switching to the default policy from *Fuego 0.1* after a constant number of moves T. The results are shown in Figure 6.2.

Switching policy was consistently most beneficial after 2-8 moves, providing around a 300 Elo improvement over no switching. This suggests that the knowledge contained in the local shape features is most effective when applied close to the root, and that the general domain knowledge

[4]These extensions will be developed and discussed further in Chapter 8.

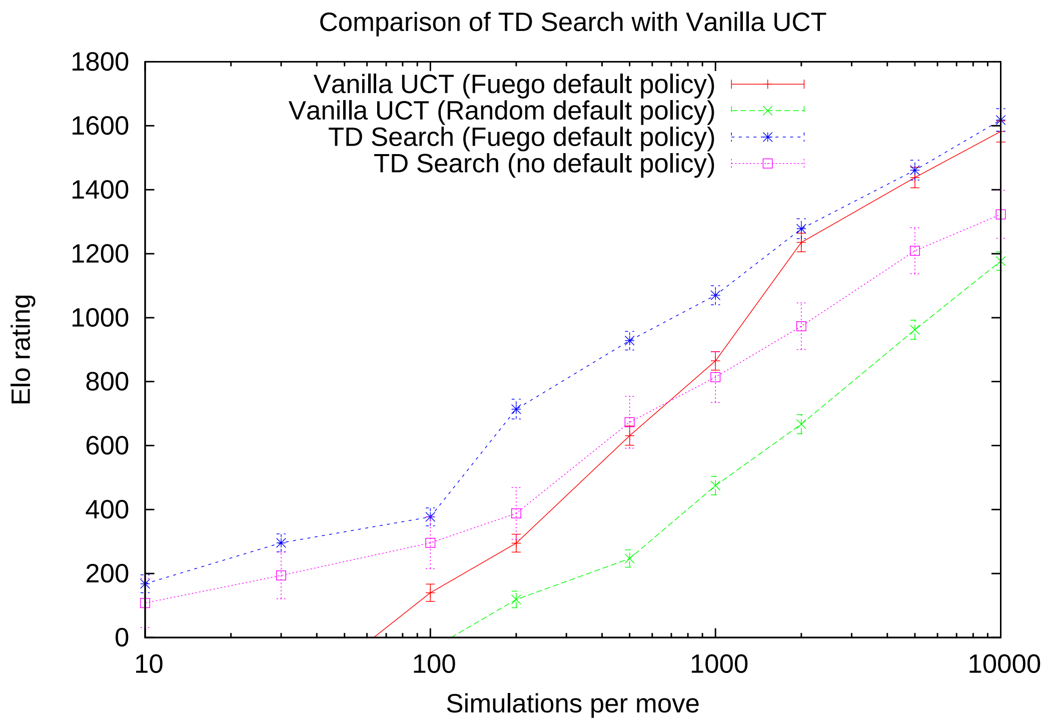

Figure 6.1: Comparison of temporal-difference search and vanilla UCT.

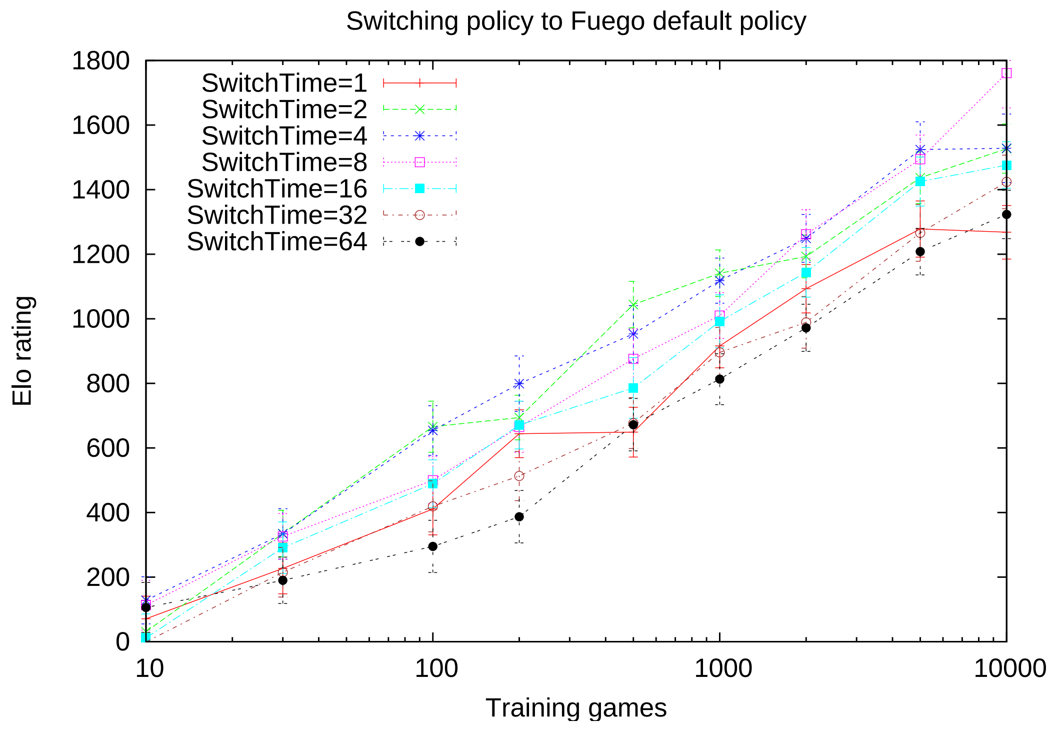

Figure 6.2: Performance of temporal-difference search when switching to the *Fuego* default policy. The number of moves at which the switch occurred was varied between 1 and 64.

encoded by the handcrafted default policy is more effective in positions far from the root.

We also compared the performance of temporal-difference search against the vanilla UCT implementation in *Fuego 0.1*. We considered two variants of each program, with and without a handcrafted default policy. The same default policy from *Fuego* was used in both programs. When using the default policy, the temporal-difference search algorithm switched to the *Fuego* default policy after $T = 6$ moves. When not using the default policy, the ϵ-greedy policy was used throughout all simulations. The results are shown in Figure 6.1.

The basic temporal-difference search algorithm, which utilises minimal domain knowledge based only on the grid structure of the board, significantly outperformed vanilla UCT with a random default policy. When using the *Fuego* default policy, temporal-difference search again outperformed vanilla UCT, although the difference was not significant beyond 2,000 simulations per move.

In our subsequent experiments, we switched to the *Fuego* default policy after $T = 6$ moves. This had the additional benefit of increasing the speed of our program[5] by an order of magnitude, from around 200 simulations/move to 2,000 simulations/move on a 2.4 GHz processor. For comparison, the vanilla UCT implementation in *Fuego 0.1* executed around 6,000 simulations/move.

6.9.2 Local Shape Features

The local shape features that we use in our experiments are quite naive: the majority of shapes and tactics described in Go textbooks span considerably larger regions of the board than 3×3 squares. When used in a traditional reinforcement learning context, the local shape features achieved a rating of around 1200 Elo (see Chapter 5). However, when the same representation was used in temporal-difference search, combining the 1×1 and 2×2 local shape features achieved a rating of almost 1700 Elo with just 10,000 simulations per move, more than vanilla UCT with an equivalent number of simulations (Figure 6.3).

The importance of temporality is aptly demonstrated by the 1×1 features. Using temporal-difference learning, a static evaluation function based only on these features achieved a rating of just 200 Elo (see Chapter 5). However, when the feature weights are adapted dynamically, these simple features are often sufficient to identify the critical moves in the current position. Temporal-difference search increased the performance of the 1×1 features to 1200 Elo, a similar level of performance to temporal-difference learning with a million 1×1 to 3×3 features.

Surprisingly, including the more detailed 3×3 features provided no statistically significant improvement. However, we recall from Figure 5.7, when using the standard paradigm of temporal-difference learning, that there was an initial period of rapid 2×2 learning, followed by a slower period of 3×3 learning. Furthermore we recall that, without weight sharing, this transition took place after many thousands of simulations. This suggests that our temporal-difference search results

[5]An ϵ-greedy search must evaluate all legal moves with probability $1 - \epsilon$. However, a simple rule-based default policy (see Chapter 4) can select a move just by pattern matching.

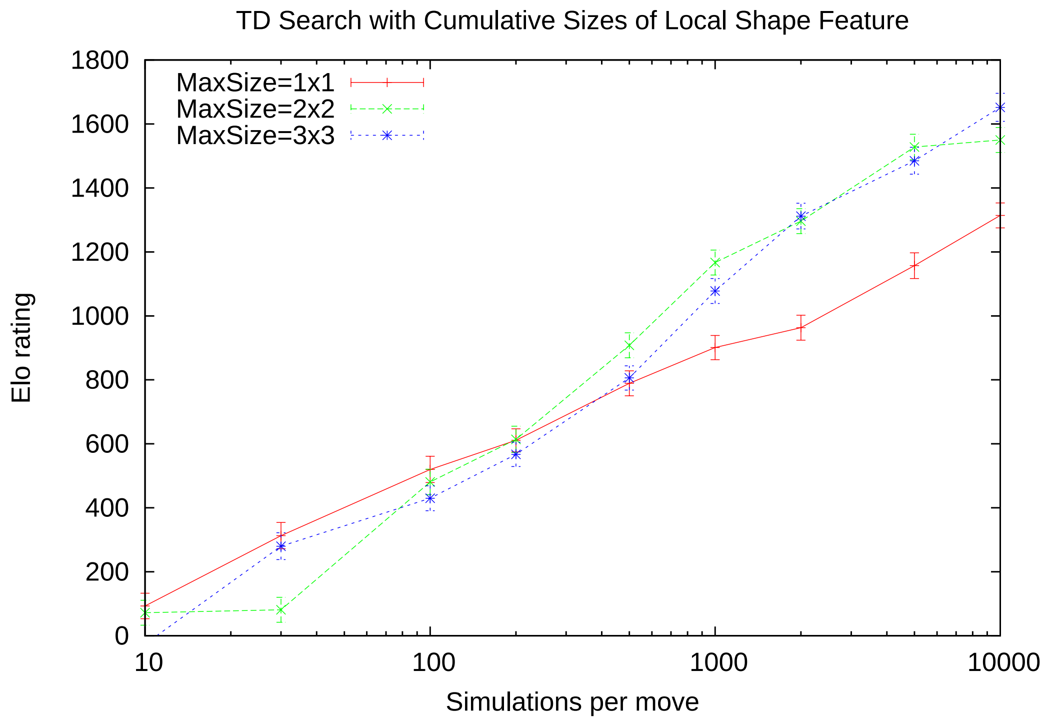

(a) Cumulative sizes: 1×1; 1×1 and 2×2; and 1×1, 2×2 and 3×3

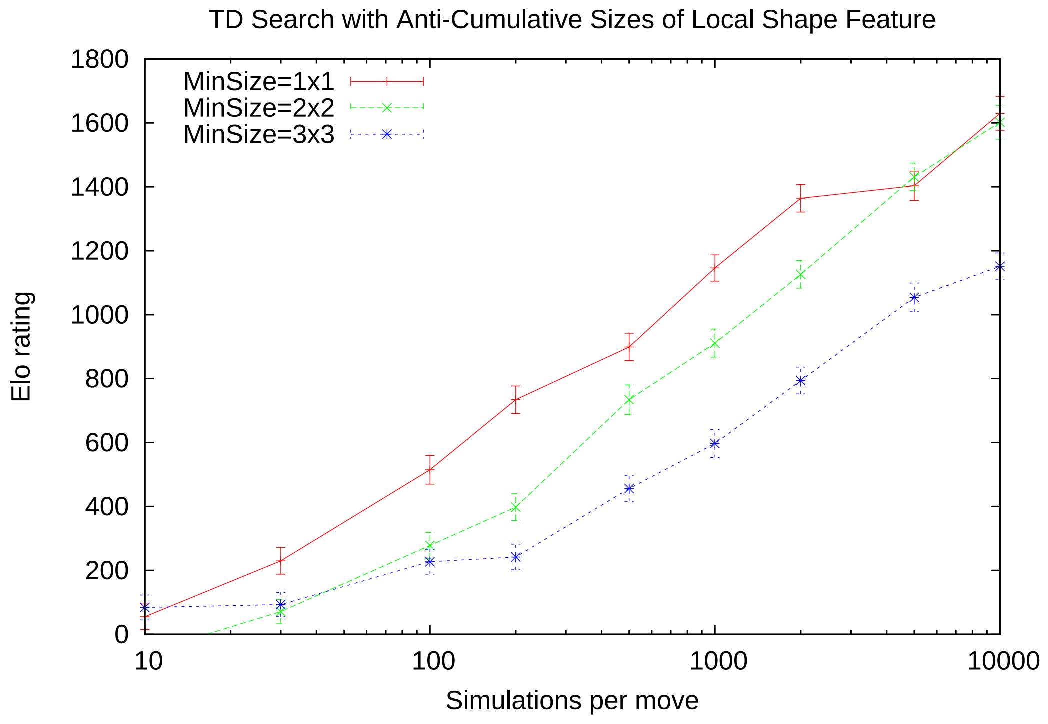

(b) Anti-cumulative sizes: 1×1, 2×2 and 3×3; 1×1 and 2×2; and 3×3

Figure 6.3: Performance of temporal-difference search with cumulative and anti-cumulative sizes of local shape feature.

correspond to the steep region of the learning curve, and that the rate of improvement is likely to flatten out with additional simulations.

6.9.3 Parameter Study

In our next experiment we varied the step-size parameter α (Figure 6.4, top). The results clearly show that an aggressive learning rate is most effective across a wide range of simulations per move, but the rating improvement for the most aggressive learning rates flattened out with additional computation. The rating improvement for $\alpha = 1$ flattened out after 1,000 simulations per move, while the rating improvement for $\alpha = 0.1$ and $\alpha = 0.3$ appeared to flatten out after 5,000 simulations per move.

We also evaluated the effect of the exploration rate ϵ (Figure 6.4, bottom). As in logistic temporal-difference learning (Figure 5.11), the algorithm performed poorly with either no exploratory moves ($\epsilon = 0$), or with only exploratory moves ($\epsilon = 1$). The difference between intermediate values of ϵ was not significant.

6.9.4 TD(λ) Search

We extend the temporal-difference search algorithm to utilise eligibility traces, using the accumulating and replacing traces from Chapter 5. We study the effect of the temporal-difference parameter λ in Figure 6.5. With accumulating traces, bootstrapping ($\lambda < 1$) provided a significant performance benefit. With replacing traces, $\lambda = 1$ performed well for the first 2,000 simulations per move, but its performance dropped off for 5000 or more simulations per move, when bootstrapping again gave better results.

Previous work in simulation-based search has largely been restricted to Monte-Carlo methods (Tesauro and Galperin, 1996; Kocsis and Szepesvari, 2006; Gelly et al., 2006; Gelly and Silver, 2007; Coulom, 2007). Our results suggest that generalising these approaches to temporal- difference learning methods may provide significant benefits when value function approximation is used.

6.9.5 Temporality

Successive positions are strongly correlated in the game of Go. Each position changes incrementally, by just one new stone at every non-capturing move. Groups and fights develop, providing specific shapes and tactics that may persist for a significant proportion of the game, but are unique to this game and are unlikely to ever be repeated in this combination. We conducted two experiments to disrupt this temporal coherence, so as to gain some insight into its effect on temporal-difference search.

In our first experiment, we selected moves according to an old value function from a previous search. At move number t, the agent selects the move that maximises the value function that it computed at move number $t - k$, for some move gap $0 \leq k < t$. The results, shown in Figure 6.6,

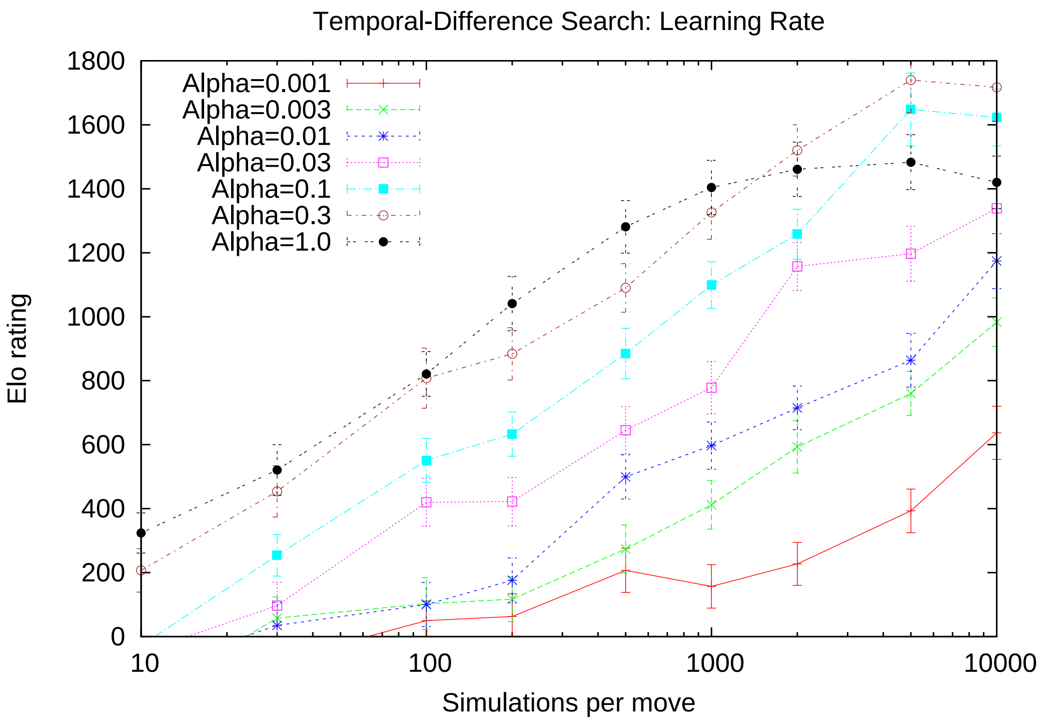

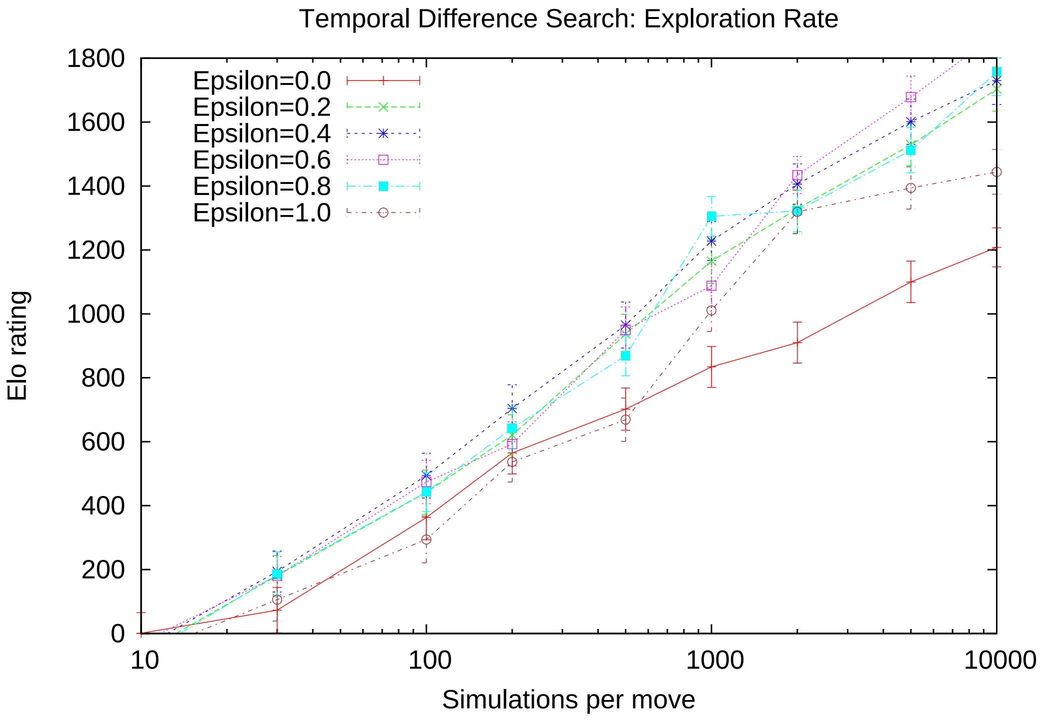

Figure 6.4: Performance of temporal-difference search with different learning rates α (top) and exploration rates ϵ (bottom).

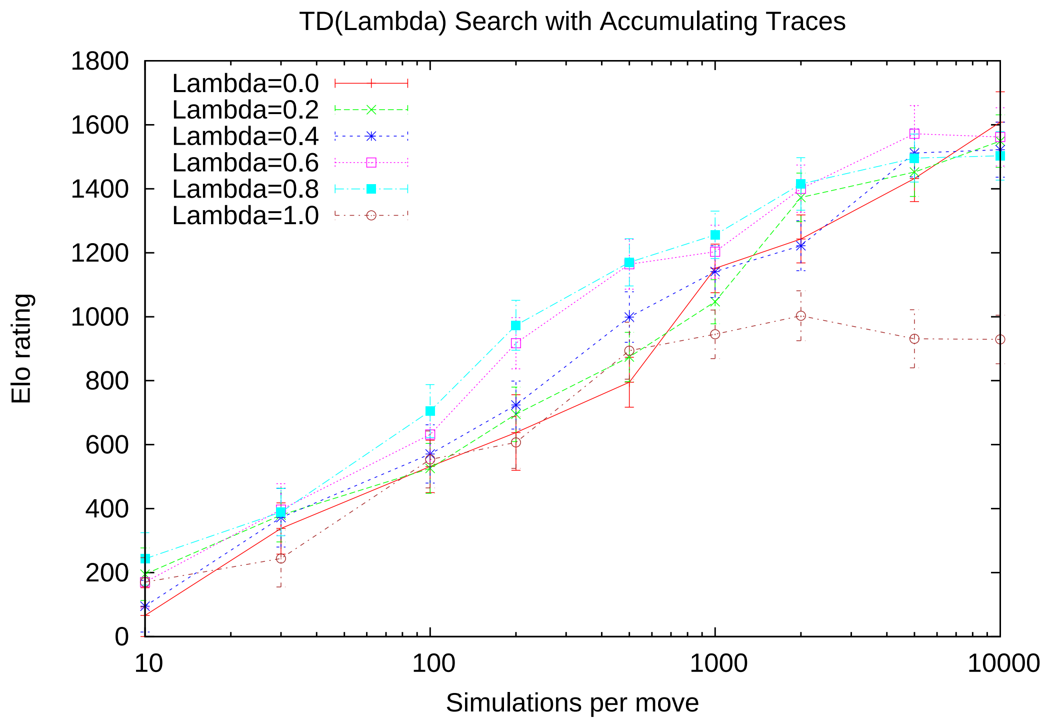

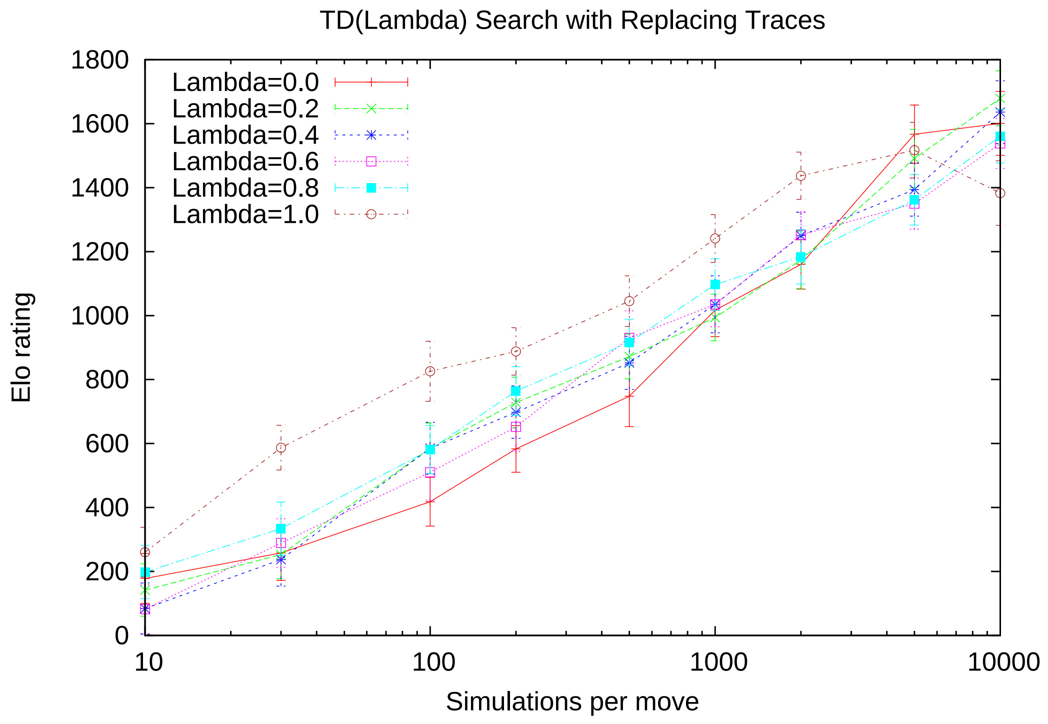

Figure 6.5: Performance of TD(λ) search for different values of λ, using accumulating traces (top) and replacing traces (bottom).

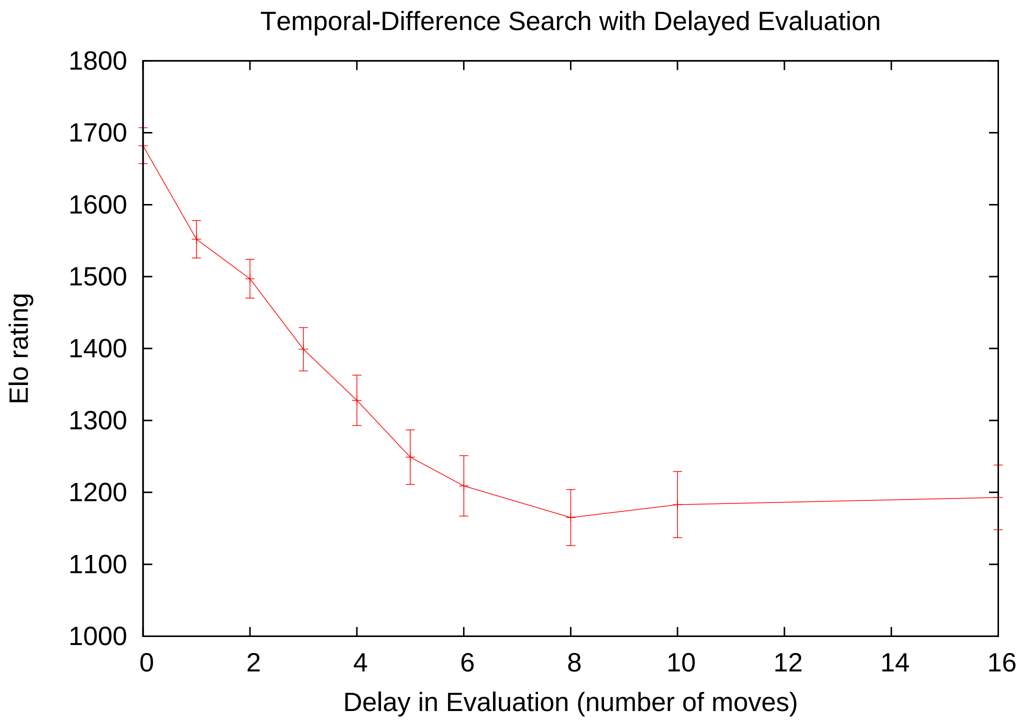

Figure 6.6: Performance of temporal-difference search with 10,000 simulations/move, when the results of the latest search are only used after some additional number of moves have elapsed.

indicate the rate at which the global context changes. The value function computed by the search is highly specialised to the current situation. When it was applied to the position that arose just 6 moves later, the performance of *RLGO*, using 10,000 simulations per move, dropped from 1700 to 1200 Elo, the same level of performance that was achieved by standard temporal-difference learning (see Chapter 5). This also explains why it is beneficial to switch to a handcrafted default policy after around 6 moves (see Figure 6.2).

In our second experiment, instead of reusing the weights from the last search, we reset the weights θ to zero at the beginning of every search, so as to disrupt any transfer of knowledge between successive moves. The results are shown in Figure 6.7. Resetting the weights dramatically reduced the performance of our program by between 400–800 Elo. This suggests that a very important aspect of temporal-difference search is its ability to accumulate knowledge over several successive, highly related positions.

6.9.6 Board Sizes

In our final experiment, we compared the performance of temporal-difference search with vanilla UCT, on board sizes from 5×5 up to 15×15. As before, the same default policy was used in both cases, beyond the search tree for vanilla UCT, and after $T = 6$ moves for temporal-difference search. The results are shown in Figure 6.8.

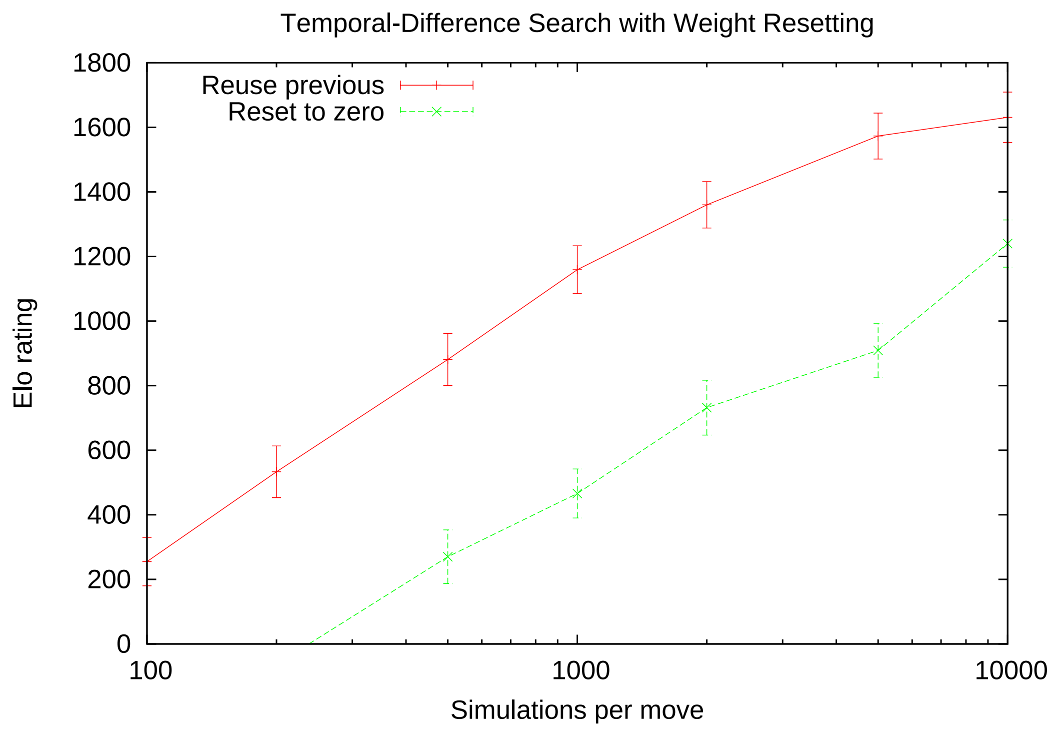

Figure 6.7: Comparison of temporal-difference search when the weights are reset to zero at the start of each search, to when the weights are reused from the previous search.

In 5×5 Go, vanilla UCT was able to play near-perfect Go, and significantly outperformed the approximate evaluation used by temporal-difference search. In 7×7 Go, the results were inconclusive, with both programs performing similarly with 10,000 simulations per move. However, on larger board sizes, temporal-difference search outperformed vanilla UCT by a margin that increased with larger board sizes. In 15×15 Go, using 10,000 simulations per move, temporal-difference search outperformed vanilla UCT by 500 ± 200 Elo. This suggests that the importance of generalising between states increases with larger search spaces.

These experiments used the same default parameters from the 9×9 experiments. It is likely that both temporal-difference search and vanilla UCT could be improved by retuning the parameters to the different board sizes.

6.10 An Illustrative Example

We provide an example of temporal-difference search with local shape features, using a real 9×9 Go position taken from a game between two professional human players (see Figure 6.9a). This position is in many ways a typical, messy middle-game Go position, consisting of several overlapping and unresolved fights.

We executed the temporal-difference search algorithm (see Algorithm 5) for a million training games, using this example position as the root state s_0. The final evaluation of each move $V(s \circ a)$,

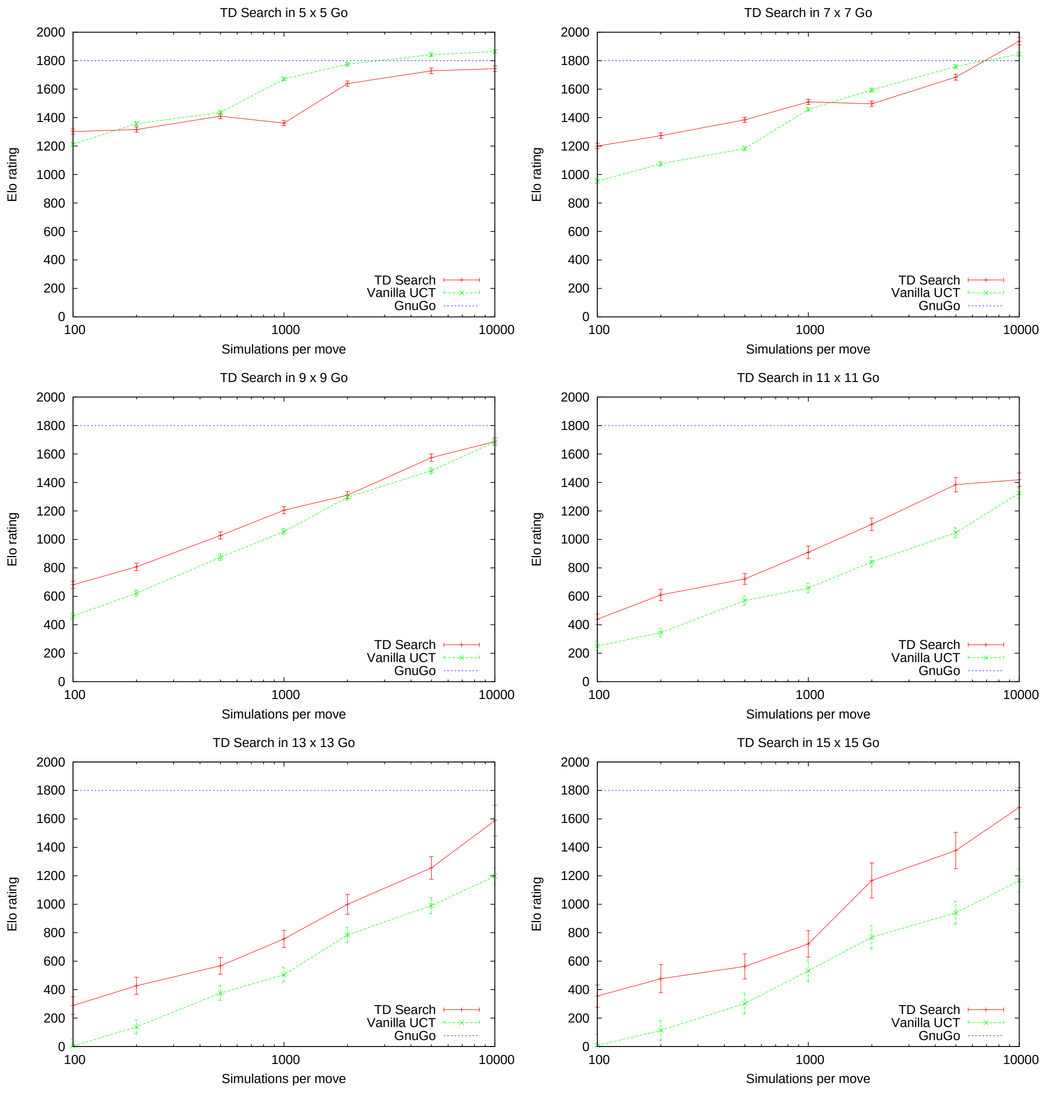

Figure 6.8: Comparison of temporal-difference search and vanilla UCT with different board sizes.

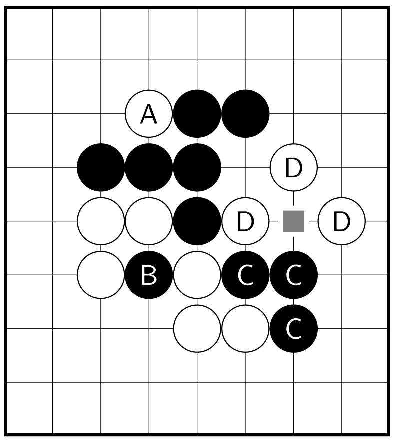

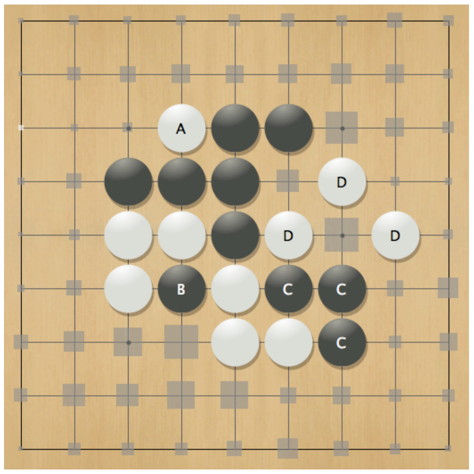

Figure 6.9: (Left) A 9×9 Go position (Black to move) from a game between two 5-*dan* professional players. The position contains several overlapping fights. White A can be captured, but still has the potential to cause trouble. Black B is caught in a ladder, but local continuations will influence black C, which is struggling to survive in the bottom-right. White D is rather weak, and is attempting to survive on the right of the board, in an overlapping battle with black C. The move played by Black is highlighted with a grey square. (Right) The final evaluation of each legal move after executing a temporal-difference search with a million simulations. The size of the square is proportional to the evaluation.

for each legal move a, is shown in Figure 6.9b. The move selected by the professional player was evaluated highest, although extending from Black B was evaluated almost as highly.

6.10.1 Combining Local Search Trees

In the game of Go, the global position can often be approximately decomposed into a set of local regions. Traditional computer Go programs exploit this property, by applying full-width search algorithms to the local positions, and then combining the local results into a global evaluation function (see Chapter 4). In contrast, Monte-Carlo tree search constructs a global search tree, which can duplicate the work of these local searches exponentially many times (see Figure 6.10).

Local shape features provide a simple mechanism for decomposing the global position into overlapping 1×1 to 3×3 local regions. All possible local shape features are enumerated, providing an exhaustive local search tree within each region. Temporal-difference search estimates the value of each local position in each local search tree. This value indicates the contribution of this local position, over all simulations, towards Black winning. The global position is then evaluated by summing the current value of each local search tree.

Like traditional computer Go programs, local shape features decompose the board into local search trees. Like Monte-Carlo tree search, temporal-difference search evaluates positions dynamically, from the outcomes of simulations. Temporal-difference search with local shape features combines these approaches, by reusing local search trees in a simulation-based search.

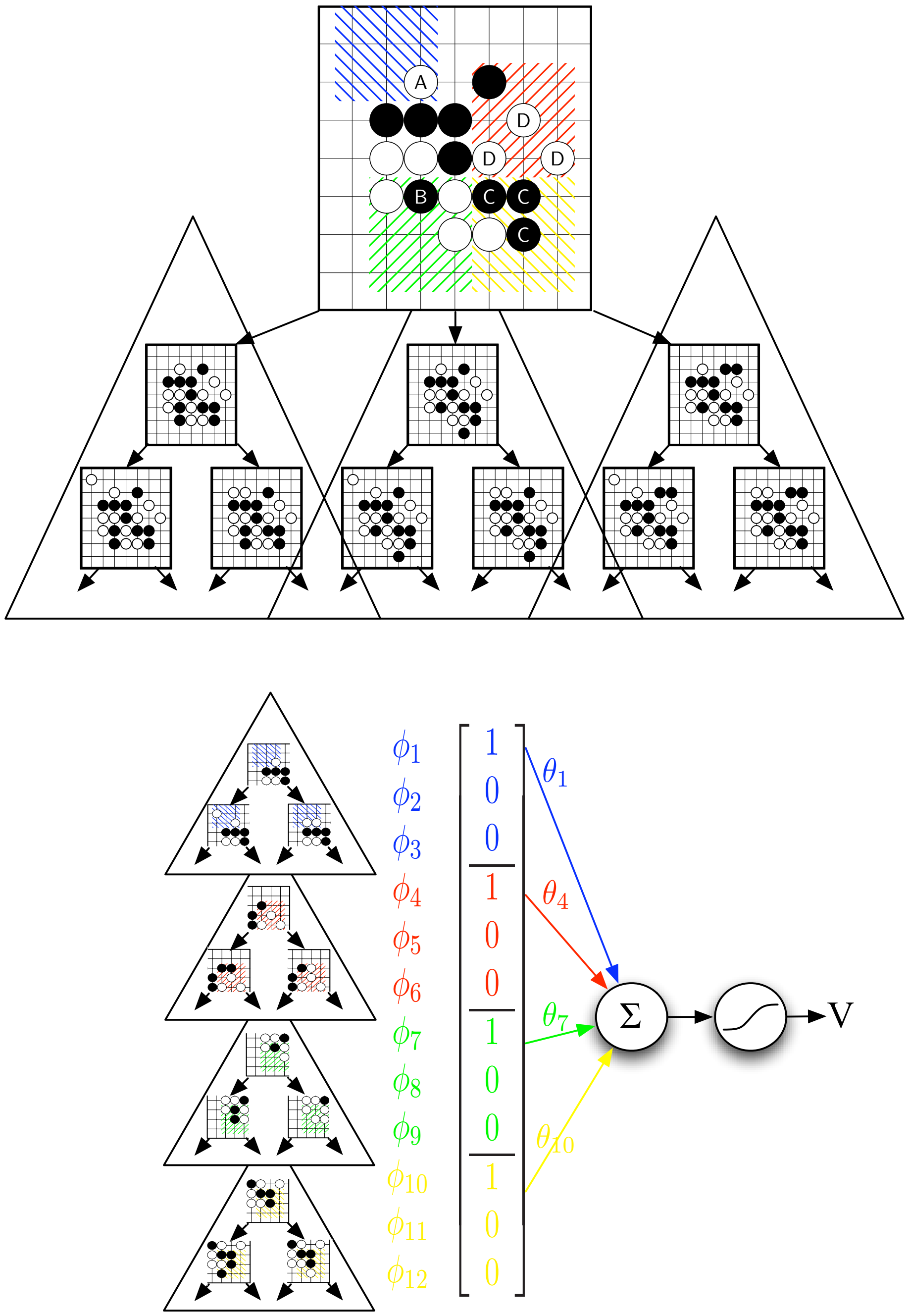

Figure 6.10: (Top) Monte-Carlo tree search constructs a global search tree that duplicates local subtrees. In this position, the global search tree includes several subtrees in which the same moves are played in the blue region. After each move in the red, green and yellow regions, the blue region is re-searched, resulting in an exponential number of duplicated subtrees. (Bottom) Temporal-difference search constructs multiple, overlapping, local search trees. Four 3×3 regions are illustrated in blue, red, green and yellow. The set of possible local shape features in each region forms an exhaustive local search tree for each region. The global value is estimated by summing the value of each local shape feature, and squashing into $[0, 1]$ with a logistic function.

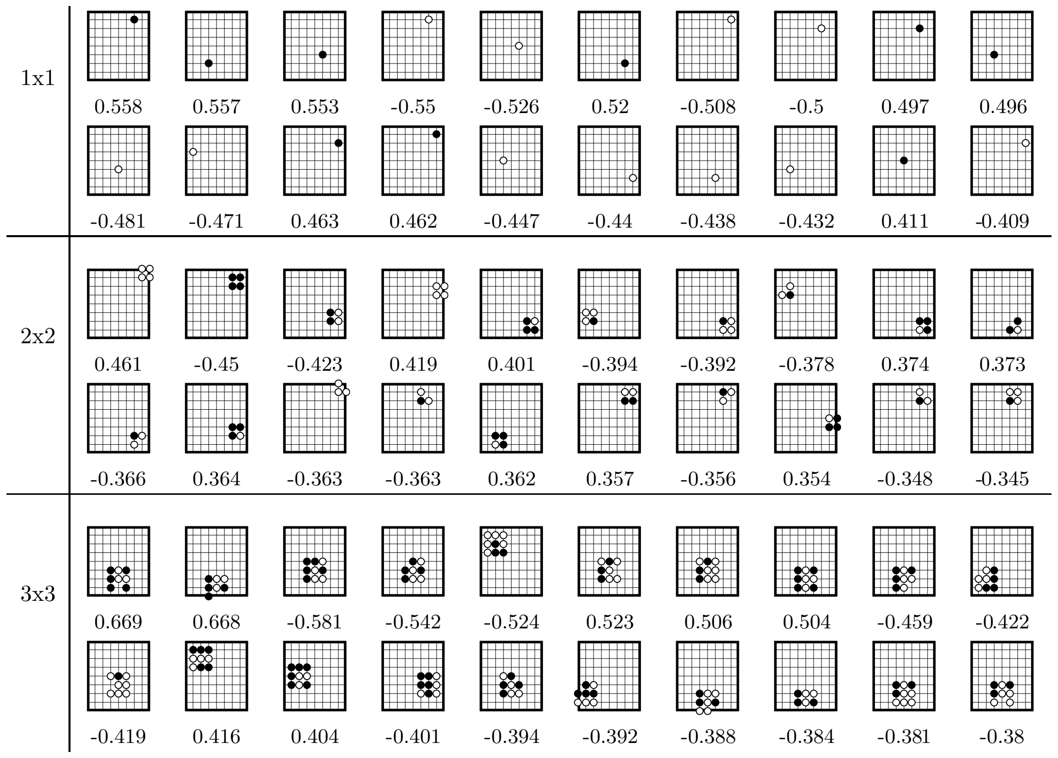

Figure 6.11: The values of local shape features after executing a temporal-difference search from the example position in Figure 6.9. Out of approximately one million features, the top 20 1×1, 2×2, and 3×3 local shape features are shown, measured by absolute weight.

6.10.2 Values of Local Shape Features

After executing a temporal-difference search in the example position for a million simulations, we identified the 1×1, 2×2 and 3×3 local shape features with highest absolute weights (see Figure 6.11).

The 1×1 local shape features give a coarse, first order estimate of the value of each move. In addition, the 1×1 local shape features corresponding to existing stones represent the value of keeping those stones alive. The value of keeping a multi-stone block alive is indicated by the total value of the 1×1 local shape features for each stone in the block.

The 2×2 local shape features were able to represent simple tactical knowledge about the example position. Several of the highest valued 2×2 weights were for local shapes that cut, block or surround Black's weak group C. Several other highly valued 2×2 shapes represent the fight for eye-space in the top-right corner. The *empty triangle* is normally considered a bad or inefficient shape, and received a low weight with temporal-difference learning (see Chapter 5). However, using temporal-difference search in the example position, a White empty triangle in the top-right corner of the board, securing an important eye for White D, was among the highest valued 2×2 shapes.

The local search tree corresponding to the green region in Figure 6.10, and overlapping search trees in neighbouring 3×3 regions, were evaluated highly by temporal-difference search. 9 of the top 10 3×3 local shape features correspond to the life-and-death tactics of Black B. The other local shape feature in the top 10 connects White's weak stone A to the strong group on the bottom-left.

6.11 Conclusion

Reinforcement learning is often considered a slow procedure. Outstanding examples of success have, in the past, learnt a value function from months of offline computation. However, this does not need to be the case. Many reinforcement learning methods, such as Monte-Carlo learning and temporal-difference learning, are fast, incremental, and scalable. When such a reinforcement learning algorithm is applied to experience simulated from the current state, it produces a high performance search algorithm.

Monte-Carlo search algorithms, such as UCT, have recently received much attention. However, this is just one example of a simulation-based search algorithm. There is a spectrum of algorithms that vary from table lookup to highly abstracted state representations, and from Monte-Carlo learning to temporal-difference learning. Value function approximation can provide rapid generalisation in large domains, and bootstrapping can be advantageous in the presence of function approximation. By varying these dimensions in the temporal-difference search algorithm, we have achieved better search efficiency per simulation, in 9×9 Go, than a vanilla UCT search. Furthermore, the advantage of temporal-difference search increased with larger board sizes.

In addition, temporal-difference search offers two potential benefits over Monte-Carlo tree search. First, search knowledge from previous time-steps can be generalised to the current search, simply by using the previous value function to initialise the new search. Unlike Monte-Carlo tree search, this provides an initial value estimate for all positions. Second, simulations never exit the agent's knowledge-base. The value function approximation covers all positions encountered during simulation, so that an ϵ-greedy policy can be used to guide each simulation right up until it terminates, without any requirement for handcrafting a distinct default policy. However, in practice we have found that a handcrafted default policy still provides significant performance benefits.

The UCT algorithm retains several advantages over temporal-difference search. It is faster, simpler, and given unlimited time and memory algorithms it will converge on the optimal policy. In many ways our initial implementation of temporal-difference search is more naive: it uses straightforward features, a simplistic epsilon-greedy exploration strategy, a non-adaptive step-size, and a constant policy switching time. The promising results of this basic strategy suggest that the full spectrum of simulation-based methods, not just Monte-Carlo and table lookup, merit further investigation.

Endnotes

Several aspects of temporality, such as tracking and temporal coherence, were introduced by Anna Koop and

Rich Sutton (Sutton et al., 2007; Koop, 2007). We explored the idea of tracking in computer Go in our ICML paper (Sutton et al., 2007), using an early version of temporal-difference search applied to 5×5 Go. Temporal-difference search is a component of the Dyna-2 algorithm (see Chapter 7). Although the Dyna-2 algorithm was published in ICML (Silver et al., 2008), this is the first time that temporal-difference search has been explicitly identified and investigated. All of the results in this chapter are new material.

Chapter 7

Dyna-2: Integrating Long and Short-Term Memories

7.1 Introduction

In many problems, *learning* and *search* must be combined together in order to achieve good performance. Learning algorithms extract knowledge, from the complete history of training data, that applies very generally throughout the domain. Search algorithms both use and extend this knowledge, so as to evaluate local states more accurately. Learning and search often interact in a complex and surprising fashion, and the most successful approaches integrate both processes together (Schaeffer, 2000; Fürnkranz, 2001).

In computer Go, the most successful learning methods have used reinforcement learning algorithms to extract domain knowledge from games of self-play (Schraudolph et al., 1994; Enzenberger, 1996; Dahl, 1999; Enzenberger, 2003; Silver et al., 2007). The value of a position is approximated by a multi-layer perceptron, or a linear combination of binary features, that forms a compact representation of the state space. Temporal-difference learning is used to update the value function, slowly accumulating knowledge from the complete history of experience.

The most successful search methods in computer Go are simulation based, for example using the Monte-Carlo tree search algorithm (see Chapter 4). This algorithm begins each new move without any domain knowledge, but rapidly learns the values of positions in a temporary search tree. Each state in the tree is explicitly represented, and the value of each state is learnt by Monte-Carlo simulation, from games of self-play that start from the current position.

In this chapter we develop a unified architecture, *Dyna-2*, that combines both reinforcement learning and simulation-based search. Like the Dyna architecture (Sutton, 1990), the agent updates a value function both from real experience, and from simulated experience that is sampled from a model of the environment. The new idea is to maintain two separate memories: a long-term memory that is learnt from real experience; and a short-term memory that is used during search, and is updated from simulated experience. Both memories use linear function approximation to form a compact representation of the state space, and both memories are updated by temporal-difference learning.

7.2 Long and Short-Term Memories

Domain knowledge contains many general rules, but even more special cases. A grandmaster chess player once said, “I spent the first half of my career learning the principles for playing strong chess and the second half learning when to violate them” (Schaeffer, 1997). Long and short-term memories can be used to represent both aspects of knowledge.

We define a *memory* $M = (\phi, \theta)$ to be a vector of features ϕ, and a vector of corresponding parameters θ. The feature vector $\phi(s, a)$ compactly represents the state s and action a, and provides an abstraction of the state and action space. The parameter vector θ is used to approximate the value function, by forming a linear combination $\phi(s, a) \cdot \theta$ of the features and parameters in M.

In our architecture, the agent maintains two distinct memories: a *long-term memory* $M = (\phi, \theta)$ and a *short-term memory* $\overline{M} = (\overline{\phi}, \overline{\theta})$.[1] The agent also maintains two distinct approximations to the value function. The *long-term value function*, $Q(s, a)$, uses only the long-term memory to approximate the true value function $Q^{\pi}(s, a)$. The *short-term value function*, $\overline{Q}(s, a)$, uses *both* memories to approximate the true value function, by forming a linear combination of both feature vectors with both parameter vectors,

$$Q(s, a) = \phi(s, a) \cdot \theta \tag{7.1}$$

$$\overline{Q}(s, a) = \phi(s, a) \cdot \theta + \overline{\phi}(s, a) \cdot \overline{\theta} \tag{7.2}$$

The long-term memory is used to represent *general* knowledge about the domain, i.e. knowledge that is independent of the agent’s current state. For example, in chess the long-term memory could know that a bishop is worth 3.5 pawns. The short-term memory is used to represent *local* knowledge about the domain, i.e. knowledge that is specific to the agent’s current region of the state space. The short-term memory is used to *correct* the long-term value function, representing adjustments that provide a more accurate local approximation to the true value function. For example, in a closed endgame position, the short-term memory could know that the black bishop is worth 1 pawn less than usual. These corrections may actually hurt the global approximation to the value function, but if the agent continually adjusts its short-term memory to match its current state, then the overall quality of approximation can be significantly improved.

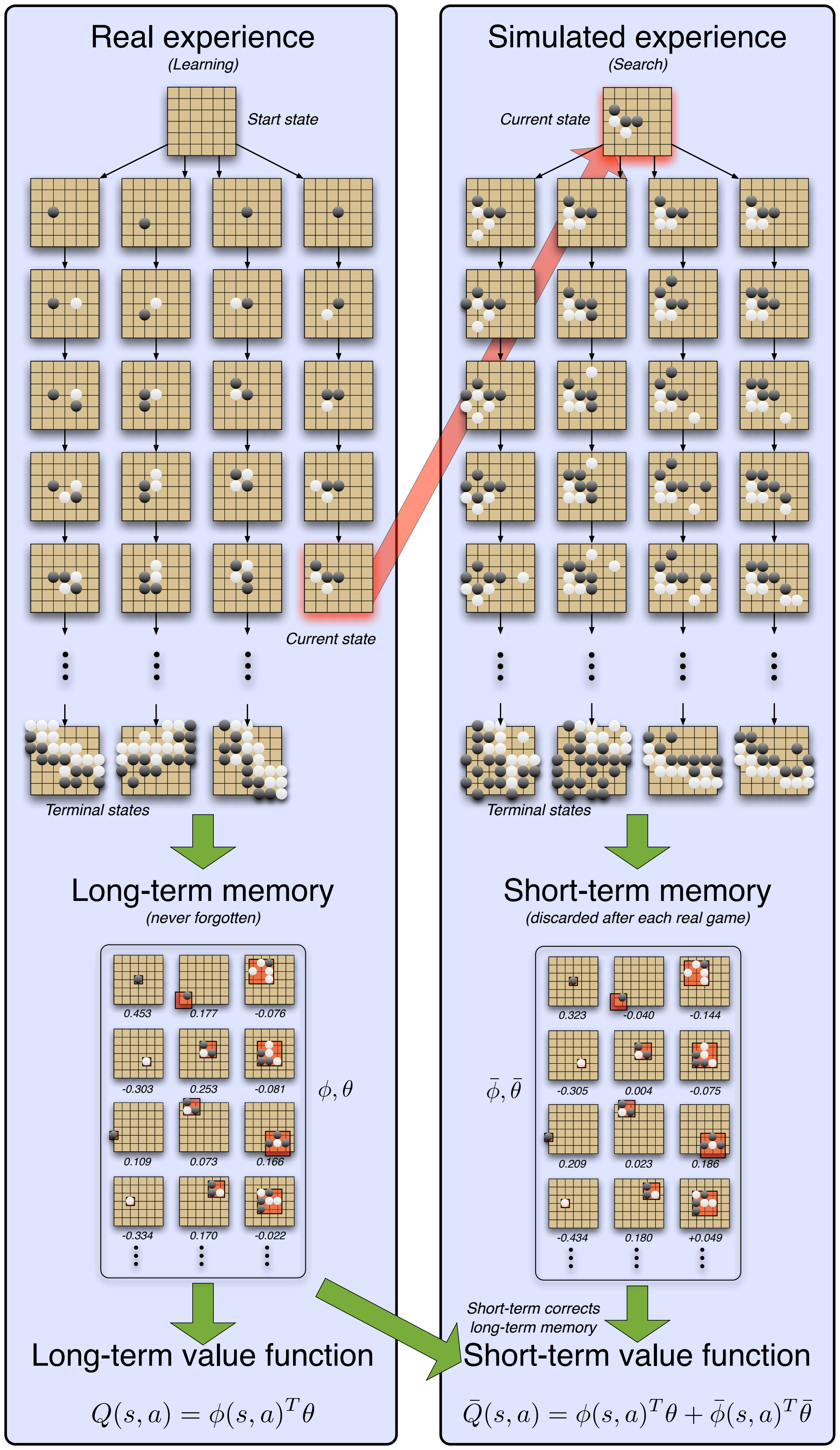

Figure 7.1: The Dyna-2 architecture.

Algorithm 6 Episodic Dyna-2

```
procedure LEARN
    Initialise $\mathcal{P}^a_{ss'}, \mathcal{R}^a_{ss'}$                ▷ State transition and reward models
    $\theta \leftarrow 0$                                                  ▷ Clear long-term memory
    loop
        $s \leftarrow s_0$                                                 ▷ Start new episode
        $\overline{\theta} \leftarrow 0$                                   ▷ Clear short-term memory
        $e \leftarrow 0$                                                   ▷ Clear eligibility trace
        SEARCH($s$)
        $a \leftarrow \epsilon$-greedy$(s; \overline{Q})$
        while $s$ is not terminal do
            Execute $a$, observe reward $r$, state $s'$
            $\mathcal{P}^a_{ss'}, \mathcal{R}^a_{ss'} \leftarrow$ UPDATEMODEL$(s, a, r, s')$
            SEARCH($s'$)
            $a' \leftarrow \epsilon$-greedy$(s'; \overline{Q})$
            $\delta \leftarrow r + Q(s', a') - Q(s, a)$                    ▷ TD-error
            $\theta \leftarrow \theta + \alpha\delta e$                    ▷ Update weights
            $e \leftarrow \lambda e + \phi$                                ▷ Update eligibility trace
            $s \leftarrow s', a \leftarrow a'$
        end while
    end loop
end procedure

procedure SEARCH($s$)
    while time available do
        $\overline{e} \leftarrow 0$                                        ▷ Clear eligibility trace
        $a \leftarrow \overline{\epsilon}$-greedy$(s; \overline{Q})$
        while $s$ is not terminal do
            $s' \sim \mathcal{P}^a_{ss'}$                                  ▷ Sample state transition
            $r \leftarrow \mathcal{R}^a_{ss'}$                             ▷ Sample reward
            $a' \leftarrow \overline{\epsilon}$-greedy$(s'; \overline{Q})$
            $\overline{\delta} \leftarrow r + \overline{Q}(s', a') - \overline{Q}(s, a)$        ▷ TD-error
            $\overline{\theta} \leftarrow \overline{\theta} + \overline{\alpha}\overline{\delta}\overline{e}$   ▷ Update weights
            $\overline{e} \leftarrow \overline{\lambda}\overline{e} + \overline{\phi}$          ▷ Update eligibility trace
            $s \leftarrow s', a \leftarrow a'$
        end while
    end while
end procedure
```

7.3 Dyna-2

The core idea of Dyna-2 is to combine temporal-difference learning with temporal-difference search, using long and short-term memories. The long-term memory is updated from real experience, and the short-term memory is updated from simulated experience, in both cases using the TD(λ) algorithm. We denote short-term parameters with a bar $\overline{x}$, and long-term parameters with no bar x.

At the beginning of each real episode, the contents of the short-term memory are cleared, $\overline{\theta} = 0$. At each real time-step t, before selecting its action a_t, the agent executes a simulation-based search. Many simulations are launched, each starting from the agent's current state s_t. After each step of computation u, the agent updates the weights of its short-term memory from its simulated experience $(s_u, a_u, r_{u+1}, s_{u+1}, a_{u+1})$, using the TD($\lambda$) algorithm. The TD-error is computed from the short-term value function, $\overline{\delta}_u = r_{u+1} + \overline{Q}(s_{u+1}, a_{u+1}) - \overline{Q}(s_u, a_u)$. Actions are selected using an $\overline{\epsilon}$-greedy policy that maximises the short-term value function $a_u = \operatorname*{argmax}_b \overline{Q}(s_u, b)$. This search procedure continues for as much computation time as is available.

When the search is complete, the short-term value function represents the agent's best local approximation to the optimal value function. The agent then selects a real action a_t using an ϵ-greedy policy that maximises the short-term value function $a_t = \operatorname*{argmax}_b \overline{Q}(s_t, b)$. After each time-step, the agent updates its long-term value function from its real experience $(s_t, a_t, r_{t+1}, s_{t+1}, a_{t+1})$, again using the TD($\lambda$) algorithm. This time, the TD-error is computed from the long-term value function, $\delta_t = r_{t+1} + Q(s_{t+1}, a_{t+1}) - Q(s_t, a_t)$. In addition, the agent uses its real experience to update its state transition model $\mathcal{P}^a_{ss'}$ and its reward model $\mathcal{R}^a_{ss'}$. The complete algorithm is illustrated in Figure 7.1 and described in pseudocode in Algorithm 6.

The Dyna-2 architecture learns from both the past and the future. The long-term memory is updated from the agent's actual past experience. The short-term memory is updated from sample episodes of what could happen in the future. Combining both memories together provides a much richer representation than is possible with a single memory.

A particular instance of Dyna-2 must specify learning parameters: a set of features ϕ for the long-term memory; a temporal-difference parameter λ; an exploration rate ϵ and a learning rate α. Similarly, it must specify the equivalent search parameters: a set of features $\overline{\phi}$ for the short-term memory; a temporal-difference parameter $\overline{\lambda}$; an exploration rate $\overline{\epsilon}$ and a learning rate $\overline{\alpha}$.

The Dyna-2 architecture subsumes a large family of learning and search algorithms. If there is no short-term memory, $\overline{\phi} = \emptyset$, then the search procedure has no effect and may be skipped. This results in the linear Sarsa algorithm (see Chapter 2). If there is no long-term memory, $\phi = \emptyset$, then Dyna-2 reduces to the temporal-difference search algorithm. As we saw in Chapter 6, this algorithm itself subsumes a variety of simulation-based search algorithms such as Monte-Carlo tree search.

[1]These names are suggestive of each memory's function, but are not related to biological long and short-term memory systems. There is also no relationship to the Long Short-Term Memory algorithm for training recurrent neural networks (Hochreiter and Schmidhuber, 1997).

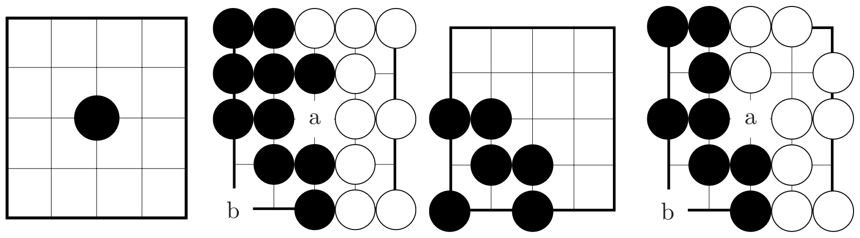

Figure 7.2: a) A 1×1 local shape feature with a central black stone. This feature acquires a strong positive value in the long-term memory. b) In this position, move b is the winning move. Using only 1×1 local shape features, the long-term memory suggests that move a should be played. The short-term memory will quickly learn to correct this misevaluation, reducing the value of a and increasing the value of b. c) A 3×3 local shape feature making two eyes in the corner. This feature acquires a positive value in the long-term memory. d) Black to play, using Chinese rules, move a is now the winning move. Using 3×3 features, the long-term memory suggests move b, believing this to be a good shape in general. However, the short-term memory quickly realises that move b is redundant in this context (black already has two eyes) and learns to play the winning move at a.

Finally, we note that real experience may be accumulated offline prior to execution. Dyna-2 may be executed on any suitable training environment (e.g. a helicopter simulator) before it is applied to real data (e.g. a real helicopter). The agent's long-term memory is learnt offline during a preliminary training phase. When the agent is placed into the real environment, it uses its short-term memory to adjust to the current state. Even if the agent's model is inaccurate, each simulation begins from its true current state, which means that the simulations are usually fairly accurate for at least the first few steps. This allows the agent to dynamically correct at least some of the misconceptions in the long-term memory.

7.4 Dyna-2 in Computer Go

We have already seen that local shape features can be used with temporal-difference learning, to learn general Go knowledge (see Chapter 5). We have also seen that local shape features can be used with temporal-difference search, to learn the value of shapes in the current situation (see Chapter 6). The Dyna-2 architecture lets us combine the advantages of both approaches, by using local shape features in both the long and short-term memories.

Figure 7.2 gives a very simple illustration of long and short-term memories in 5×5 Go. It is usually bad for Black to play on the corner intersection, and so long-term memory learns a negative weight for this feature. However, Figure 7.2 shows a position in which the corner intersection is the most important point on the board for Black: it makes two eyes and allows the Black stones to live. By learning about the particular distribution of states arising from this position, the short-term memory learns a large positive weight for the corner feature, correcting the long-term memory.

In general, it may be desirable for the long and short-term memories to utilise different features, which are best suited to representing either general or local knowledge. In our computer Go experiments, we focus our attention on the simpler case where both vectors of features are identical,

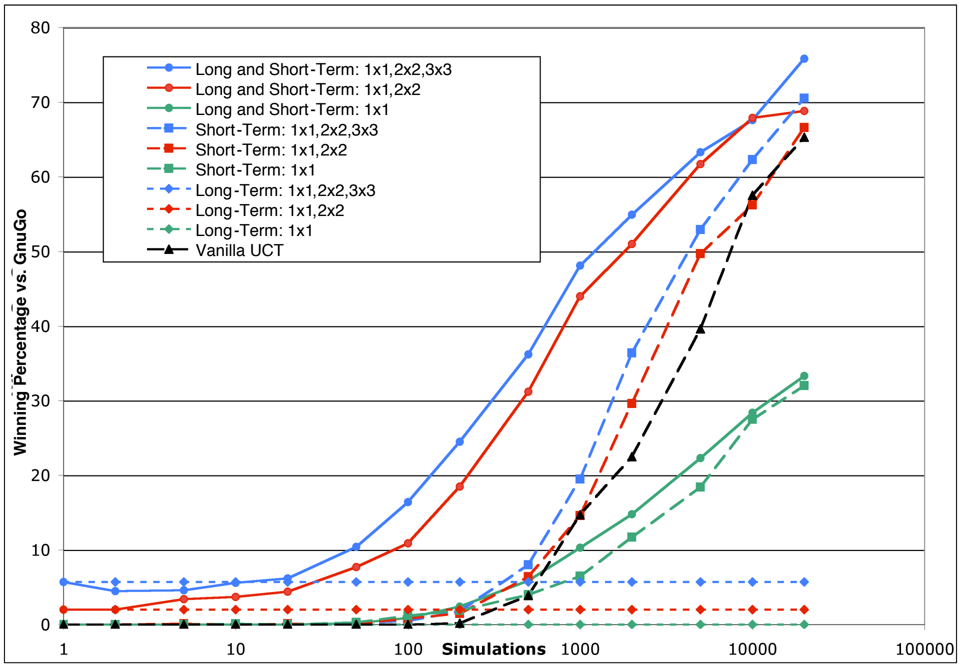

Figure 7.3: Winning rate of *RLGO 2.4* against *GnuGo 3.7.10* (level 0) in 9×9 Go, for different numbers of simulations per move. Local shape features were used in either the long-term memory (dotted lines), the short-term memory (dashed lines), or both memories (solid lines). The long-term memory was trained in a separate offline phase from 100,000 games of self-play. Local shape features varied in size from 1×1 up to 3×3. Each point represents the winning percentage over 1,000 games.

$\phi = \overline{\phi}$. In this special case, the Dyna-2 algorithm can be implemented somewhat more efficiently, using just one memory during search. At the start of each real game, the contents of the short-term memory are initialised to the contents of the long-term memory, $\overline{\theta} = \theta$. Subsequent searches then proceed using only the short-term memory, just as in temporal-difference search.

We applied Dyna-2 to 9×9 computer Go using 1×1 to 3×3 local shape features. We used a self-play model, and default parameters of $\overline{\lambda} = 0$, $\overline{\alpha} = 0.1$, and $\overline{\epsilon} = 0.1$. Just as in Algorithm 5, we utilised logistic temporal-difference learning (see Appendix A) with normalised step-sizes and two-ply updates,

$$\overline{V}(s) = \sigma(\overline{\phi}(s).\overline{\theta}) \tag{7.3}$$

$$\Delta\overline{\theta} = \overline{\alpha}\frac{\overline{\phi}(s_u)}{||\overline{\phi}(s_u)||^2}(\overline{V}(s_{u+2}) - \overline{V}(s_u)) \tag{7.4}$$

where $\sigma(x) = \frac{1}{1+e^{-x}}$ is the logistic function. Pseudocode for the Dyna-2 algorithm, using binary features, is given in Algorithm 7.

An ϵ-greedy simulation policy was used for the first $T = 10$ moves of each simulation; the

Algorithm 7 Dyna-2 with TD(0) and Binary Features

```
procedure DYNA2-SEARCH($s_t, \theta$)
    if $t = 0$ then
        $\overline{\theta} = \theta$
    end if
    $board.Initialise()$
    while time available do
        SELFPLAY($board, s_t$)
    end while
    $board.SetPosition(s_t)$
    return $\epsilon$-GREEDY($board, 0$)
end procedure

procedure EVAL($board$)
    if $board.Terminal()$ then
        return $board.BlackWins(), \emptyset, 0$
    end if
    $\mathcal{F} = board.GetActiveFeatures()$
    $v = 0$
    $k = 0$
    for all $i \in \mathcal{F}$ do
        $v \mathrel{+}= \overline{\theta}[i]$
        $k\,{+}{+}$
    end for
    $\overline{V} = \frac{1}{1+e^{-v}}$
    return $\overline{V}, \mathcal{F}, k$
end procedure

procedure SELFPLAY($board, s_t$)
    $board.SetPosition(s_t)$
    $u = 0$
    $\overline{V}_0, \mathcal{F}_0 =$ EVAL($board$)
    while not $board.Terminal()$ do
        if $u \leq T$ then
            $a_u = \epsilon$-GREEDY($board, \overline{\epsilon}$)
        else
            $a_u =$ DEFAULTPOLICY($board$)
        end if
        $board.Play(a_u)$
        $u\,{+}{+}$
        $\overline{V}_u, \mathcal{F}_u, k_u =$ EVAL($board$)
        if $t \geq 2$ then
            $\overline{\delta} = \overline{V}_u - \overline{V}_{u-2}$
            for all $i \in \mathcal{F}_{u-2}$ do
                $\overline{\theta}[i] \mathrel{+}= \frac{\overline{\alpha}}{k_u}\overline{\delta}$
            end for
        end if
    end while
end procedure
```

Search algorithm	**Memory**	**Elo rating on CGOS**
Alpha-beta	Long-term	1350
Dyna-2	Long and short-term	2030
Dyna-2 + alpha-beta	Long and short-term	2130

Table 7.1: The Elo ratings established by *RLGO 2.4* on the Computer Go Server (October 2007).

Fuego 0.1 default policy was used for the remainder of each simulation. We use weight sharing to exploit symmetries in the long-term memory, but we do not use any weight sharing in the short-term memory. Local shape features consisting of entirely empty intersections were ignored. The long-term memory was trained from 100,000 games of self-play, and was not adjusted further during actual play. After each temporal-difference search was completed, the actual move to play was selected by a simple one-ply maximisation (Black) or minimisation (White) of the value function, $a = \underset{a'}{\operatorname{argmax}}\, V(s \circ a')$, with no random exploration. We implemented this algorithm in our program *RLGO 2.4*, which executed almost 2,000 simulations per second on a 3 GHz processor.

We compared our algorithm to the vanilla UCT implementation from the *Fuego 0.1* program (Müller and Enzenberger, 2009), as described in Section 6.9. Both *RLGO* and vanilla UCT used an identical default policy. We separately evaluated both *RLGO* and vanilla UCT by running 1,000 game matches against *GnuGo 3.7.10* (level 0).[2]

We compared the performance of several different variants of our algorithm. First, we evaluated the performance of the long-term memory by itself, $\overline{\phi} = \emptyset$, which is equivalent to the temporal-difference learning algorithm developed in Chapter 5. Second, we evaluated the performance of the short-term memory by itself, $\phi = \emptyset$, which is equivalent to the temporal-difference search algorithm developed in Chapter 6. Finally, we evaluated the performance of both long and short-term memories, making use of the full Dyna-2 algorithm. In each case we compared the performance of local shape features of different sizes (see Figure 7.3).

Using only a long-term memory, *RLGO 2.4* was only able to achieve a winning rate of around 5% against *GnuGo*. Using only the short-term memory, *RLGO* achieved better performance per simulation than vanilla UCT, by a small margin, for up to 20,000 simulations per move. *RLGO* outperformed *GnuGo* with 5,000 or more simulations. Using both memories, *RLGO* achieved significantly better performance per move than vanilla UCT, by a wide margin for few simulations per move and by a smaller but significant margin for 20,000 simulations per move. Using both memories, it outperformed *GnuGo* with just 2,000 or more simulations.

7.5 Dyna-2 and Heuristic Search

In games such as chess, checkers and Othello, human world-champion level play has been exceeded, by combining a heuristic evaluation function with alpha-beta search. The heuristic function is a

[2]*GnuGo* plays significantly faster at level 0 than at its default level 10, so that results can be collected from many more games. Level 0 is approximately 150 Elo weaker than level 10.

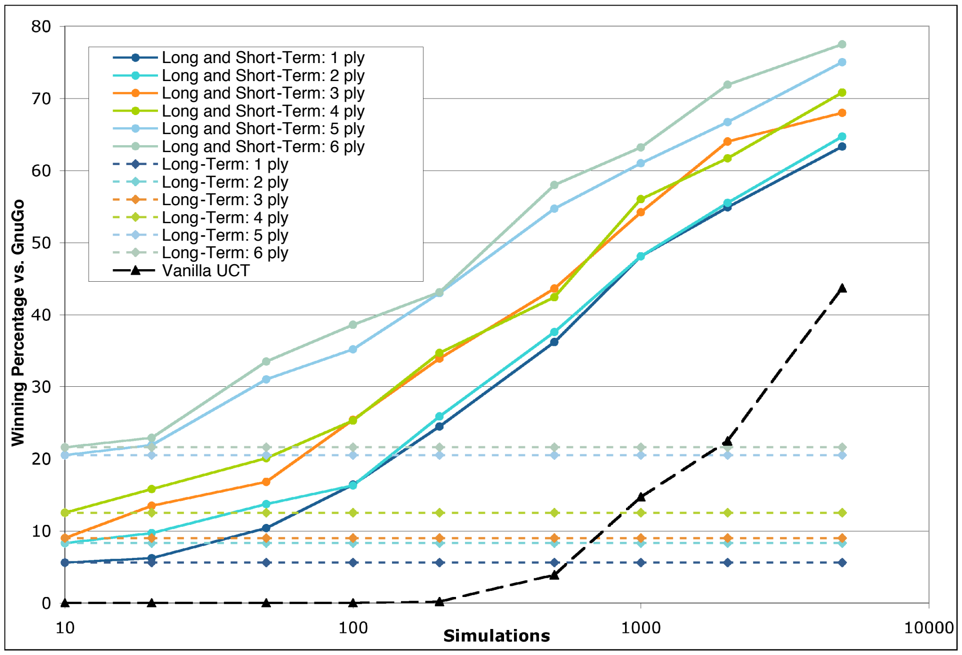

Figure 7.4: Winning rate of *RLGO 2.4* against *GnuGo 3.7.10* (level 0) in 9×9 Go, using a hybrid search based on both Dyna-2 and alpha-beta. A full-width α-β search is used for move selection, using a value function based on either the long-term memory alone (dotted lines), or both long and short-term memories (solid lines). Using only the long-term memory corresponds to a traditional alpha-beta search. Using both memories, but only a 1-ply search, corresponds to the Dyna-2 algorithm. The long-term memory was trained offline from 100,000 games of self-play. Each point represents the winning percentage over 1,000 games.

linear combination of binary features, and can be learnt offline by temporal-difference learning and self-play (Baxter et al., 2000; Schaeffer et al., 2001; Buro, 1999). In Chapter 5, we saw how this approach could be applied to Go, by using local shape features.

In this chapter we have developed a significantly more accurate approximation of the value function, by combining long and short-term memories, using both temporal-difference learning and temporal-difference search. Can this more accurate value function be successfully used in a traditional alpha-beta search?

We describe this approach, in which a simulation-based search is followed by a traditional search, as a *hybrid search*. We extended the Dyna-2 implementation in Algorithm 7 into a hybrid search, by performing an alpha-beta search after each temporal-difference search. As in Dyna-2, after the simulation-based search is complete, the agent selects a real move to play. However, instead of directly maximising the short-term value function, an alpha-beta search is used to find the best move in the depth d minimax tree, where the leaves of the tree are evaluated according to the short-term value function $\overline{Q}(s, a)$.

The hybrid algorithm can also be viewed as an extension to alpha-beta search, in which the evaluation function is dynamically updated. At the beginning of the game, the evaluation function is set to the contents of the long-term memory. Before each alpha-beta search, the evaluation function is re-trained by a temporal-difference search. The alpha-beta search then proceeds as usual, but using the updated evaluation function.

We compared the performance of the hybrid search algorithm to a traditional search algorithm. In the traditional search, the long-term memory $Q(s, a)$ is used as a heuristic function to evaluate leaf positions, as in Chapter 5. The results are shown in Figure 7.3.

Dyna-2 outperformed traditional search by a wide margin. Using only 200 simulations per move, *RLGO* exceeded the performance of a full-width 6-ply search. For comparison, a 5-ply search took approximately the same computation time as 1,000 simulations. When combined with alpha-beta in the hybrid search algorithm, the results were even better. Alpha-beta provided a substantial performance boost of around 15-20% against GnuGo, which remained approximately constant throughout the tested range of simulations per move. With 5,000 simulations per move, the hybrid algorithm achieved a winning rate of almost 80% against GnuGo. These results suggest that the benefits of alpha-beta search are largely complementary to the simulation-based search.

Finally, we implemented a high-performance version of our hybrid search algorithm in *RLGO 2.4*. In this tournament version, time was dynamically allocated, approximately evenly between the two search algorithms, using an exponentially decaying time control. We extended the temporal-difference search to use multiple processors, by sharing the long and short-term memories between processes, and to use pondering, by simulating additional games of self-play during the opponent's thinking time. We extended the alpha-beta search to use several well-known extensions: iterative deepening, transposition table, killer move heuristic, and null-move pruning (Schaeffer, 2000).

RLGO competed on the 9×9 Computer Go Server, which uses 5 minute time controls, for several hundred games in total. The ratings established by RLGO are shown in Table 7.1.

Using only an alpha-beta search, based on the long-term memory alone, RLGO established a rating of 1350 Elo. Using Dyna-2, using both long and short-term memories, but no alpha-beta search, RLGO established a rating of 2030 Elo. Using the hybrid search algorithm, including Dyna-2 and also an alpha-beta search, RLGO established a rating of 2130 Elo.

For comparison, the highest previous rating achieved by any handcrafted, traditional search or traditional machine learning program was around 1850 Elo (see Chapter 4). These previous programs incorporated a great deal of sophisticated handcrafted knowledge about the game of Go, whereas the handcrafted Go knowledge in RLGO is minimal. *RLGO*'s performance on CGOS is comparable to or exceeds the performance of many vanilla UCT programs, but is significantly weaker than the strongest programs, which are based on extensions to Monte-Carlo tree search such as those described in the following chapter.

If we view the hybrid search as an extension to alpha-beta, then we see that dynamically updating the evaluation function offers dramatic benefits, improving the performance of RLGO by 800 Elo. If we view the hybrid search as an extension to Dyna-2, then the performance improves by a more modest, but still significant 100 Elo.

7.6 Conclusion

Learning algorithms accumulate general knowledge about the full problem from real experience within the environment. Search algorithms accumulate specialised knowledge about the local subproblem, using a model of the environment. The Dyna-2 algorithm provides a principled approach to learning and search that effectively combines both forms of knowledge.

Dyna-2 can significantly improve the performance of temporal-difference search. However, the improvement is greatest with limited computation time. Asymptotically, the advantage of the long-term memory is reduced or removed, and the limitations introduced by approximating the value function still apply (see Chapter 6).

In the game of Go, the consequences of a particular move or shape may not become apparent for tens or even hundreds of moves. In a traditional, limited depth search these consequences remain beyond the horizon, and will only be recognised if explicitly represented by the evaluation function. In contrast, Dyna-2 only uses the long-term memory as an initial guide, and learns to identify the consequences of particular patterns in its short-term memory. However, it lacks the precise global lookahead required to navigate the full-board fights that can often engulf a 9×9 board. The hybrid search successfully combines the deep knowledge of Dyna-2 with the precise lookahead of a full-width search. Using this approach, *RLGO* was able to outperform traditional 9×9 Go programs by a wide margin.

Endnotes

A version of this chapter was previously published in ICML (Silver et al., 2008). I wrote the program *RLGO 2.4* using the SmartGame library for computer Go, by Martin Müller and Markus Enzenberger.

Part III

Monte-Carlo Tree Search

Chapter 8

Heuristic MC–RAVE

8.1 Introduction

Simulation-based search has revolutionised computer Go (see Chapter 4) and many other challenging domains (see Chapter 3). As we have seen in previous chapters, simulation-based search can be significantly enhanced: both by generalising between different states, using a short-term memory; and by incorporating general knowledge about the domain, using a long-term memory. In this chapter we apply these two ideas specifically to Monte-Carlo tree search.

Our first extension, the *RAVE* algorithm, uses a very simple generalisation between the nodes of each subtree. The value of each position s_t and move a is estimated using the all-moves-as-first heuristic (see Chapter 3), by averaging the outcome of all simulations in which a was played at any time $u \geq t$. The RAVE algorithm forms a very fast and rough estimate of the value; whereas normal Monte-Carlo is slower but more accurate. The MC–RAVE algorithm combines these two value estimates in a principled fashion, so as to minimise the mean squared error.

Our second extension, *heuristic Monte-Carlo tree search*, uses a heuristic function as a long-term memory. This heuristic is used to initialise the values of new positions in the search tree. As in Chapter 5, we use a heuristic function that has been learnt by temporal-difference learning and self-play; however, in general any heuristic can be provided to the algorithm.

We applied our algorithms in the program *MoGo*, achieving a dramatic improvement to its performance. The resulting program became the first program to achieve *dan*-level at 9×9 Go.

8.2 Monte-Carlo Simulation and All-Moves-As-First

In a two-player game, we define the true action value function $Q^\pi(s, a)$ to be the expected outcome z after playing move a in position s, and then following policy π for both players until termination,

$$Q^\pi(s, a) = \mathbb{E}_\pi[z | s_t = s, a_t = a] \tag{8.1}$$

Monte-Carlo simulation provides a simple method for estimating $Q^\pi(s, a)$. $N(s)$ complete games are simulated by self-play with policy π from position s. The *Monte-Carlo value* (MC value) $Q(s,a)$ is the mean outcome of all simulations in which move a was selected in position s,

$$Q(s,a) = \frac{1}{N(s,a)} \sum_{i=1}^{N(s)} \mathbb{I}_i(s,a) z_i, \tag{8.2}$$

where z_i is the outcome of the ith simulation; $\mathbb{I}_i(s,a)$ is an indicator function returning 1 if move a was selected in position s at any step during the ith simulation, and 0 otherwise; and $N(s,a) = \sum_{i=1}^{N(s)} \mathbb{I}_i(s,a)$ counts the total number of simulations in which move a was selected in position s.

In incremental games such as computer Go, the value of a move is often unaffected by moves played elsewhere on the board. The underlying idea of the *all-moves-as-first* (AMAF) heuristic (Bruegmann, 1993) (see Chapter 4) is to have one general value for each move, regardless of when it is played. We define the true AMAF value function $\tilde{Q}^\pi(s,a)$ to be the expected outcome z from position s, when following policy π for both players, given that move a was selected at some subsequent time,

$$\tilde{Q}^\pi(s,a) = \mathbb{E}_\pi[z | s_t = s, \exists u \geq t \text{ s.t. } a_u = a] \tag{8.3}$$

The true AMAF value function provides a biased estimate of the true action value function. The level of bias, $\tilde{B}(s,a)$, depends on the particular state s and action a,

$$\tilde{Q}^\pi(s,a) = Q^\pi(s,a) + \tilde{B}(s,a) \tag{8.4}$$

Monte-Carlo simulation can be used to approximate $\tilde{Q}^\pi(s,a)$. The *all-moves-as-first value* $\tilde{Q}(s,a)$ is the mean outcome of all simulations in which move a is selected *at any time* after s is encountered,

$$\tilde{Q}(s,a) = \frac{1}{\tilde{N}(s,a)} \sum_{i=1}^{N(s)} \tilde{\mathbb{I}}_i(s,a) z_i, \tag{8.5}$$

where $\tilde{\mathbb{I}}_i(s,a)$ is an indicator function returning 1 if position s was encountered at any step t of the ith simulation, and move a was selected at any step $u >= t$, or 0 otherwise; and $\tilde{N}(s,a) = \sum_{i=1}^{N(s)} \tilde{\mathbb{I}}_i(s,a)$ counts the total number of simulations used to estimate the AMAF value. Note that Black moves and White moves are considered to be distinct actions, even if they are played at the same intersection.

In order to select the best move with reasonable accuracy, Monte-Carlo simulation requires many simulations from every candidate move. The AMAF heuristic provides orders of magnitude more information: every move will typically have been tried on several occasions, after just a handful of simulations. If the value of a move really is unaffected, at least approximately, by moves played elsewhere, then this can result in a much faster rough estimate of the value.

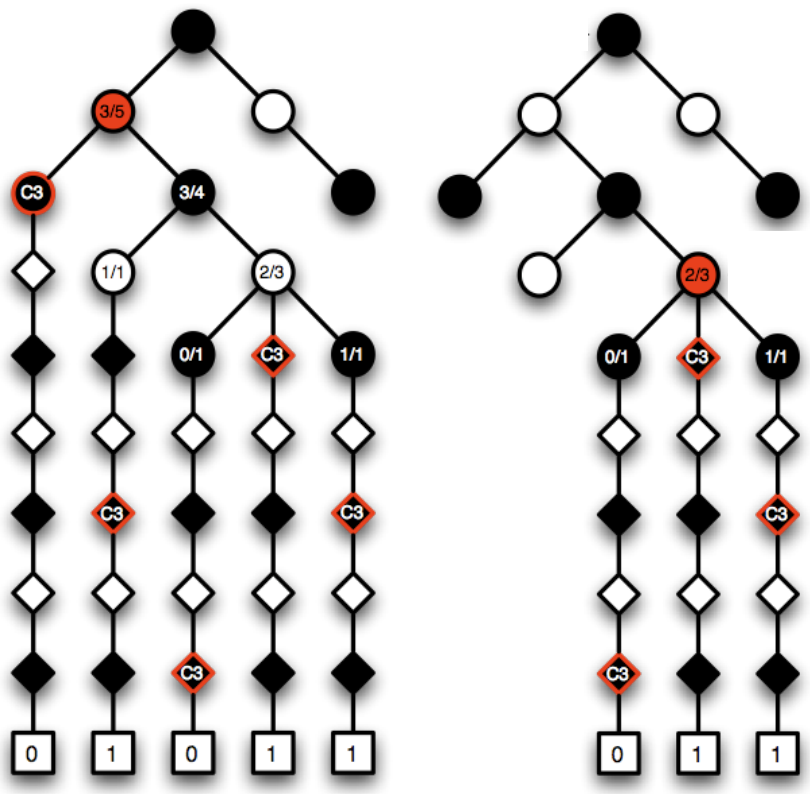

Figure 8.1: An example of using the RAVE algorithm to estimate the value of black c3. Several simulations have already been performed and are shown in the search tree. During the next simulation, black uses RAVE to select his next move to play, first from the solid red node in the left diagram, and then from the solid red node in the right diagram. The AMAF values for Black c3 are shown for the subtree beneath the solid red node. (Left) Black c3 has been played once, and resulted in a loss; its Monte-Carlo value is 0/1. Black c3 has been played 5 times in the subtree beneath the red node, resulting in 3 wins and two losses; its AMAF value is 3/5. (Right) Black c3 has been played once, and resulted in a win; its Monte-Carlo value is 1/1. It has been played 3 times in the subtree, resulting in 2 wins and one loss; its AMAF value is 2/3.

8.3 Rapid Action Value Estimation (RAVE)

Monte-Carlo tree search learns a unique value for each node in the search tree, and cannot generalise between related positions. The RAVE algorithm provides a simple way to share knowledge between related nodes in the search tree, resulting in a rapid, but biased value estimate.

The RAVE algorithm combines Monte-Carlo tree search with the all-moves-as-first heuristic. Instead of computing the MC value (Equation 8.2) of each node of the search-tree, $(s, a) \in \mathcal{T}$, the AMAF value (Equation 8.5) of each node is computed.

Every position in the search tree, $s \in \mathcal{T}$, is the root of a subtree $\tau(s) \subseteq \mathcal{S}$. If a simulation visits position s_t at step t, then all subsequent positions visited in that simulation, s_u such that $u \geq t$, are in the subtree of s_t, $s_u \in \tau(s_t)$. This includes all positions $s_u \notin \mathcal{T}$ visited by the default policy in the second stage of simulation.

The basic idea of RAVE is to generalise over subtrees. The assumption is that the value of move a will be similar from all positions within subtree $\tau(s)$. Thus, the value of a is estimated from all simulations starting from s, regardless of exactly when a is played.

When the AMAF values are used to select a move a_t in position s_t, the most specific subtree is used, $\tau(s_t)$. The move with maximum AMAF value over this subtree is selected, $a = \underset{b}{\operatorname{argmax}}\ \tilde{Q}(s_t, b)$. In our experiments, combining value estimates from more general subtrees did not confer any advantage, although this remains an interesting direction for future work.

RAVE is closely related to the *history heuristic* in alpha-beta search (Schaeffer, 1989). During the depth-first traversal of the search tree, the history heuristic remembers the success[1] of each move at various depths; the most successful moves are tried first in subsequent positions. RAVE is similar, but because the search is not developed in a depth-first manner, it must explicitly store a separate value for each subtree. In addition, RAVE takes account of the success of all moves in the simulation, including moves made by the default policy.

8.4 MC–RAVE

The RAVE algorithm learns very quickly, but it is often wrong. The principal assumption of RAVE, that a particular move has the same value across an entire subtree, is frequently violated. There are many situations, for example during tactical battles, in which nearby changes can completely change the value of a move: sometimes rendering it redundant; sometimes making it even more vital. Even distant moves can significantly affect the value of a move, for example playing a ladder-breaker in one corner can radically alter the value of playing a ladder in the opposite corner.

The *MC–RAVE* algorithm overcomes this issue, by combining the rapid learning of the RAVE algorithm with the accuracy and convergence guarantees of Monte-Carlo tree search.

There is one node $n(s)$ for each state s in the search tree. Each node contains a total count $N(s)$, and for each $a \in \mathcal{A}$, an MC value $Q(s, a)$, AMAF value $\tilde{Q}(s, a)$, MC count $N(s, a)$, and AMAF count $\tilde{N}(s, a)$.

To estimate the overall value of move a in position s, we use a weighted sum $Q_\star(s, a)$ of the MC value $Q(s, a)$ and the AMAF value $\tilde{Q}(s, a)$,

$$Q_\star(s, a) = (1 - \beta(s, a))Q(s, a) + \beta(s, a)\tilde{Q}(s, a) \tag{8.6}$$

where $\beta(s, a)$ is a weighting parameter for state s and action a. It is a function of the statistics for (s, a) stored in node $n(s)$, and provides a schedule for combining the MC and AMAF values. When only a few simulations have been seen, we weight the AMAF value more highly, $\beta(s, a) \approx 1$. When many simulations have been seen, we weight the Monte-Carlo value more highly, $\beta(s, a) \approx 0$.

As with Monte-Carlo tree search, each simulation is divided into two stages. During the first

[1]A successful move in alpha-beta either causes a cut-off, or has the best minimax value.

stage, for positions within the search tree, $s_t \in \mathcal{T}$, moves are selected greedily, so as to maximise the combined MC and AMAF value, $a = \underset{b}{\operatorname{argmax}}\, Q_\star(s_t, b)$. During the second stage of simulation, for positions beyond the search tree, $s_t \notin \mathcal{T}$, moves are selected by a default policy.

After each simulation $s_0, a_0, s_1, a_1, ..., s_T$ with outcome z, both the MC and AMAF values are updated. For every position s_t in the simulation that is represented in the search tree, $s_t \in \mathcal{T}$, the values and counts of the corresponding node $n(s_t)$ are updated,

$$N(s_t) \leftarrow N(s_t) + 1 \tag{8.7}$$

$$N(s_t, a_t) \leftarrow N(s_t, a_t) + 1 \tag{8.8}$$

$$Q(s_t, a_t) \leftarrow Q(s_t, a_t) + \frac{z - Q(s_t, a_t)}{N(s_t, a_t)} \tag{8.9}$$

In addition, the AMAF value is updated for every subtree. For every position s_t in the simulation that is represented in the tree, $s_t \in \mathcal{T}$, and for every subsequent move of the simulation a_u, such that $u \geq t$, the AMAF value of (s_t, a_u) is updated according to the simulation outcome z,

$$\tilde{N}(s_t, a_u) \leftarrow \tilde{N}(s_t, a_u) + 1 \tag{8.10}$$

$$\tilde{Q}(s_t, a_u) \leftarrow \tilde{Q}(s_t, a_u) + \frac{z - \tilde{Q}(s_t, a_u)}{\tilde{N}(s_t, a_u)} \tag{8.11}$$

If the same move is played multiple times during a simulation, then this update is only performed the first time. Moves which are illegal in s_t are ignored.

8.4.1 UCT–RAVE

The tree policy in the MC–RAVE algorithm can be extended to incorporate an exploration term, based on the UCB1 algorithm (see Chapter 1),

$$Q^\oplus_\star(s, a) = Q_\star(s, a) + c\sqrt{\frac{\log N(s)}{N(s, a)}}, \tag{8.12}$$

Moves are selected during the first stage of simulation to maximise the augmented value, $a = \underset{b}{\operatorname{argmax}}\, Q^\oplus_\star(s, b)$. We call this algorithm *UCT–RAVE*.[2]

If the schedule decreases to zero in all nodes, $\forall s \in \mathcal{T}, a \in \mathcal{A}, \lim_{N \to \infty} \beta(s, a) = 0$, then the asymptotic behaviour of UCT–RAVE is equivalent to UCT. The asymptotic convergence properties of UCT (see Chapter 3) therefore also apply to UCT–RAVE. We now describe two different schedules which have this property.

8.4.2 Heuristic Schedule

One possible schedule for MC–RAVE uses an *equivalence parameter* k,

[2]The original UCT-RAVE algorithm also included the RAVE count in the exploration term (Gelly and Silver, 2007). However, it is hard to justify explicit RAVE exploration: many actions will be evaluated by AMAF, regardless of which action is actually selected at time t.

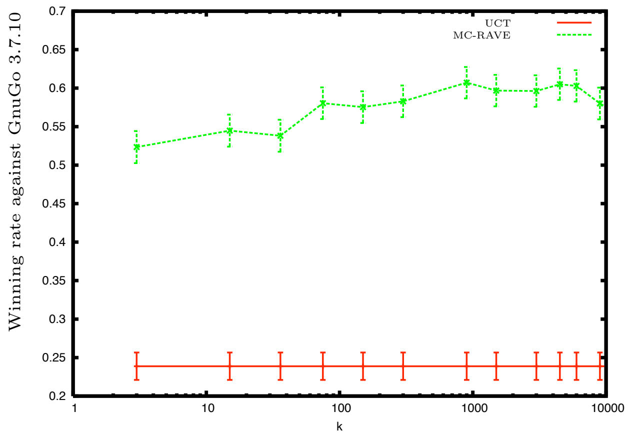

Figure 8.2: Winning rate of MC–RAVE with 3,000 simulations per move against GnuGo 3.7.10 (level 10), for different settings of the equivalence parameter k. The bars indicate the standard error. Each point of the plot is an average over 2300 complete games.

$$\beta(s,a) = \sqrt{\frac{k}{3N(s)+k}} \tag{8.13}$$

where k specifies the number of simulations at which the Monte-Carlo value and the AMAF value should be given equal weight, $\beta(s,a) = \frac{1}{2}$,

$$\frac{1}{2} = \sqrt{\frac{k}{3N(s)+k}} \tag{8.14}$$

$$\frac{1}{4} = \frac{k}{3N(s)+k} \tag{8.15}$$

$$k = N(s) \tag{8.16}$$

We tested MC–RAVE in the Go program *MoGo*, using the heuristic schedule in Equation (8.13) and the default policy described in (Gelly et al., 2006), for different settings of the equivalence parameter k. For each setting, we played a 2300 game match against GnuGo 3.7.10 (level 10). The results are shown in Figure 8.2, and compared to Monte-Carlo tree search, using 3,000 simulations per move for both algorithms. The winning rate using MC–RAVE varied between 50% and 60%, compared to 24% without RAVE. Maximum performance is achieved with an equivalence parameter of 1,000 or more, indicating that the rapid action value estimate is more reliable than standard Monte-Carlo simulation until several thousand simulations have been executed from position s.

8.4.3 Minimum MSE Schedule

The schedule presented in Equation 8.13 is somewhat heuristic in nature. We now develop a more principled schedule, which selects $\beta(s,a)$ so as to minimise the mean squared error in the combined estimate $Q_\star(s,a)$.

Assumptions

To derive our schedule, we make a simplified statistical model of MC–RAVE. Our first assumption is that the policy π is held constant. Under this assumption, the outcome of each Monte-Carlo simulation, when playing move a from position s, is an independent and identically distributed (i.i.d.) Bernoulli random variable. Furthermore, the outcome of each AMAF simulation, when playing move a at any time following position s, is also an i.i.d. Bernoulli random variable,

$$Pr(z = 1|s_t = s, a_t = a) = Q^{\pi}(s, a) \tag{8.17}$$

$$Pr(z = 0|s_t = s, a_t = a) = 1 - Q^{\pi}(s, a) \tag{8.18}$$

$$Pr(z = 1|s_t = s, \exists u \geq t \text{ s.t. } a_u = a) = \tilde{Q}^{\pi}(s, a) \tag{8.19}$$

$$Pr(z = 0|s_t = s, \exists u \geq t \text{ s.t. } a_u = a) = 1 - \tilde{Q}^{\pi}(s, a) \tag{8.20}$$

It follows that the total number of wins, after $N(s, a)$ simulations in which move a was played from position s, is binomially distributed. Similarly, the total number of wins, after $\tilde{N}(s, a)$ simulations in which move a was played at any time following position s, is binomially distributed,

$$N(s, a)Q(s, a) \sim Binomial(N(s, a), Q^{\pi}(s, a)) \tag{8.21}$$

$$\tilde{N}(s, a)\tilde{Q}(s, a) \sim Binomial(\tilde{N}(s, a), \tilde{Q}^{\pi}(s, a)) \tag{8.22}$$

Our second assumption is that these two distributions are independent, so that the MC and AMAF values are uncorrelated. In fact, the same simulations used to compute the MC value are also used to compute the AMAF value, which means that the values are certainly correlated. Furthermore, as the tree develops over time, the simulation policy changes. This means that outcomes are not i.i.d. and that the total number of wins is not in fact binomially distributed. Nevertheless, we believe that these simplifications do not significantly affect the performance of the schedule in practice.

Derivation

To simplify our notation, we consider a single position s and move a. We denote the number of Monte-Carlo simulations by $n = N(s, a)$ and the number of simulations used to compute the AMAF value by $\tilde{n} = \tilde{N}(s, a)$, and abbreviate the schedule by $\beta = \beta(s, a)$. We denote the estimated mean, bias (with respect to $Q^{\pi}(s, a)$) and variance of the MC, AMAF and combined values respectively by $\mu, \tilde{\mu}, \mu_\star$; $b, \tilde{b}, b_\star$ and $\sigma^2, \tilde{\sigma}^2, \sigma^2_\star$, and the mean squared error of the combined value by $e^2_\star$,

$$\mu = Q(s,a) \tag{8.23}$$
$$\tilde{\mu} = \tilde{Q}(s,a) \tag{8.24}$$
$$\mu_\star = Q_\star(s,a) \tag{8.25}$$
$$b = Q^\pi(s,a) - Q^\pi(s,a) = 0 \tag{8.26}$$
$$\tilde{b} = \tilde{Q}^\pi(s,a) - Q^\pi(s,a) = \tilde{B}(s,a) \tag{8.27}$$
$$b_\star = Q_\star^\pi(s,a) - Q^\pi(s,a) \tag{8.28}$$
$$\sigma^2 = \mathbb{E}[(Q(s,a) - Q^\pi(s,a))^2 | N(s,a) = n] \tag{8.29}$$
$$\tilde{\sigma}^2 = \mathbb{E}[(\tilde{Q}(s,a) - \tilde{Q}^\pi(s,a))^2 | \tilde{N}(s,a) = \tilde{n}] \tag{8.30}$$
$$\sigma_\star^2 = \mathbb{E}[(Q_\star(s,a) - Q_\star^\pi(s,a))^2 | N(s,a) = n, \tilde{N}(s,a) = \tilde{n}] \tag{8.31}$$
$$e_\star^2 = \mathbb{E}[(Q_\star(s,a) - Q^\pi(s,a))^2 | N(s,a) = n, \tilde{N}(s,a) = \tilde{n}] \tag{8.32}$$

We start by decomposing the mean squared error of the combined value into the bias and variance of the MC and AMAF values respectively, making use of our second assumption that these values are independently distributed,

$$e_\star^2 = \sigma_\star^2 + b_\star^2 \tag{8.33}$$
$$= (1-\beta)^2\sigma^2 + \beta^2\tilde{\sigma}^2 + (\beta\tilde{b} + (1-\beta)b)^2 \tag{8.34}$$
$$= (1-\beta)^2\sigma^2 + \beta^2\tilde{\sigma}^2 + \beta^2\tilde{b}^2 \tag{8.35}$$

Differentiating with respect to β and setting to zero,

$$0 = 2\beta\tilde{\sigma}^2 - 2(1-\beta)\sigma^2 + 2\beta\tilde{b}^2 \tag{8.36}$$
$$\beta = \frac{\sigma^2}{\sigma^2 + \tilde{\sigma}^2 + \tilde{b}^2} \tag{8.37}$$

We now make use of our first assumption that the MC and AMAF values are binomially distributed, and estimate their variance,

$$\sigma^2 = \frac{Q^\pi(s,a)(1 - Q^\pi(s,a))}{N(s,a)} \approx \frac{\mu_\star(1-\mu_\star)}{n} \tag{8.38}$$
$$\tilde{\sigma}^2 = \frac{\tilde{Q}^\pi(s,a)(1 - \tilde{Q}^\pi(s,a))}{\tilde{N}(s,a)} \approx \frac{\mu_\star(1-\mu_\star)}{\tilde{n}} \tag{8.39}$$
$$\beta = \frac{\tilde{n}}{n + \tilde{n} + n\tilde{n}\tilde{b}^2/\mu_\star(1-\mu_\star)} \tag{8.40}$$

In roughly even positions, $\mu_\star \approx \frac{1}{2}$, we can further simplify the schedule,

$$\beta = \frac{\tilde{n}}{n + \tilde{n} + 4n\tilde{n}\tilde{b}^2} \tag{8.41}$$

This equation still includes one unknown constant: the RAVE bias $\tilde{b}$. This can either be evaluated empirically (by testing the performance of the algorithm with various constant values of $\tilde{b}$), or by machine learning (by learning to predict the error between the AMAF value and the MC value, after many simulations). The former method is simple and effective; but the latter method could allow different biases to be identified for different types of position.

Results

We compared the performance of MC–RAVE using the minimum MSE schedule, using the approximation in Equation 8.41, to the heuristic schedule in Equation 8.13. For the minimum MSE schedule, we first identified the best constant RAVE bias in empirical tests. On a 9×9 board, the performance of MoGo using the minimum MSE schedule increased by around 70 Elo. On a 19×19 board, the improvement was substantially larger.

8.5 Heuristic Prior Knowledge

We now introduce our second extension to Monte-Carlo tree search, *heuristic MCTS*. If a particular position s and move a is rarely encountered during simulation, then its Monte-Carlo value estimate is highly uncertain and very unreliable. Furthermore, because the search tree branches exponentially, the vast majority of nodes in the tree are only experienced rarely. The situation at the leaf nodes is worst of all: by definition each leaf node has been visited only once (otherwise a child node would have been added).

In order to reduce the uncertainty for rarely encountered positions, we incorporate prior knowledge by using a *heuristic evaluation function* $H(s, a)$ and a *heuristic confidence function* $C(s, a)$. When a node is first added to the search tree, it is initialised according to the heuristic function, $Q(s, a) = H(s, a)$ and $N(s, a) = C(s, a)$. The confidence in the heuristic function is measured in terms of *equivalent experience*: the number of simulations that would be required in order to achieve a Monte-Carlo value of similar accuracy to the heuristic value.[3] After initialisation, the value and count are updated as usual, using standard Monte-Carlo simulation.

8.6 Heuristic MC–RAVE

The heuristic Monte-Carlo tree search algorithm can be combined with the MC–RAVE algorithm, described in pseudocode in Algorithm 8. When a new node $n(s)$ is added to the tree, and for all actions $a \in \mathcal{A}$, we initialise both the MC and AMAF values to the heuristic evaluation function, and initialise both counts to heuristic confidence functions C and $\tilde{C}$ respectively,

[3]This is equivalent to a beta prior when binary outcomes are used.

Algorithm 8 Heuristic MC–RAVE

```
procedure MC–RAVE($s_0$)
    $board.SetPosition(s_0)$
    $root = $ NEWNODE($board$)
    while time available do
        SIMULATE($board, s_0, root$)
    end while
    return $\underset{a \in Legal(s_0)}{\text{argmax}}$ EVAL($root, a$)
end procedure

procedure SIMULATE($board, s_0, root$)
    $board.SetPosition(s_0)$
    $moves = []$
    $nodes = []$
    SIMTREE($board, moves, nodes, root$)
    $z = $ SIMDEFAULT($board, moves$)
    BACKUP($z, nodes, moves$)
end procedure

procedure SIMDEFAULT($board, moves$)
    repeat
        $a = $ DEFAULTPOLICY($board$)
        $moves.Append(a)$
        $board.Play(a)$
    until $board.GameOver()$
    return $board.BlackWins()$
end procedure

procedure SIMTREE($board, moves, nodes, root$)
    $n = root$
    loop
        if $board.BlackToPlay()$ then
            $a = \underset{b \in board.Legal()}{\text{argmax}}$ EVAL($n, b$)
        else
            $a = \underset{b \in board.Legal()}{\text{argmin}}$ EVAL($n, b$)
        end if
        $moves.Append(a)$
        $nodes.Append(n)$
        $board.Play(a)$
        if $n.Child[a] = 0$ then
            $n.Child[a] = $ NEWNODE($board$)
            return
        end if
        $n = n.Child[a]$
    end loop
end procedure

procedure EVAL($n, a$)
    $b = $ pretuned constant bias value
    $N = n.MC[a].Count$
    $Q = n.MC[a].Wins/N$
    $\tilde{N} = n.AMAF[a].Count$
    $\tilde{Q} = n.AMAF[a].Wins/\tilde{N}$
    $\beta = \tilde{N}/(N + \tilde{N} + 4N\tilde{N}b^2)$
    return $(1 - \beta)Q + \beta\tilde{Q}$
end procedure

procedure BACKUP($z, nodes, moves$)
    for $t = 0$ to $nodes.Size()$ do
        $n = nodes[t]$
        $a = moves[t]$
        $n.MC[a].Wins \mathrel{+}= z$
        $n.MC[a].Count{+}{+}$
        $touched = \emptyset$
        for $u = t$ to $moves.Size()$ do
            $a = moves[u]$
            if $a \notin touched$ then
                $touched.Insert(a)$
                $n.AMAF[a].Wins \mathrel{+}= z$
                $n.AMAF[a].Count{+}{+}$
            end if
        end for
    end for
end procedure

procedure NEWNODE($board$)
    for all $a \in board.Legal()$ do
        $(H, C, \tilde{C}) = $ HEURISTIC($board$)
        $n.MC[a].Count = C$
        $n.MC[a].Wins = HC$
        $n.AMAF[a].Count = \tilde{C}$
        $n.AMAF[a].Wins = H\tilde{C}$
        $n.Child[a] = 0$
    end for
    return $n$
end procedure
```

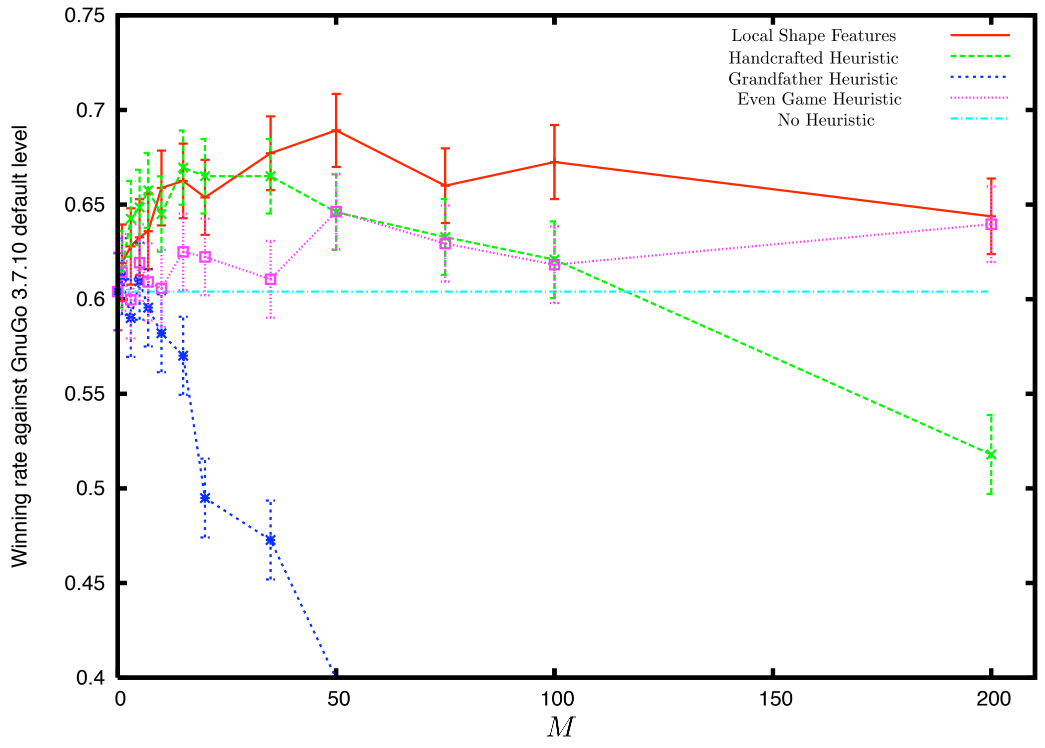

Figure 8.3: Winning rate of *MoGo*, using the heuristic MC–RAVE algorithm, with 3,000 simulations per move against GnuGo 3.7.10 (level 10). Four different forms of heuristic function were used (see text). The bars indicate the standard error. Each point of the plot is an average over 2300 complete games.

$$Q(s,a) \leftarrow H(s,a) \tag{8.42}$$

$$N(s,a) \leftarrow C(s,a) \tag{8.43}$$

$$\tilde{Q}(s,a) \leftarrow H(s,a) \tag{8.44}$$

$$\tilde{N}(s,a) \leftarrow \tilde{C}(s,a) \tag{8.45}$$

$$N(s) \leftarrow \sum_{a \in \mathcal{A}} N(s,a) \tag{8.46}$$

We compare four heuristic evaluation functions in 9×9 Go, using the heuristic MC–RAVE algorithm in the program *MoGo*.

1. The *even-game* heuristic, $Q_{even}(s,a) = 0.5$, makes the assumption that most positions encountered between strong players are likely to be close.

2. The *grandfather* heuristic, $Q_{grand}(s_t,a) = Q(s_{t-2},a)$, sets the value of each node in the tree to the value of its grandfather. This assumes that the value of a Black move is usually similar to the value of that move, last time Black was to play.

3. The *handcrafted* heuristic, $Q_{mogo}(s,a)$, is based on the pattern-based rules that were successfully used in *MoGo's* default policy. The heuristic was designed such that moves matching a "good" pattern were assigned a value of 1, moves matching a "bad" pattern were given value 0, and all other moves were assigned a value of 0.5. The good and bad patterns were identical to those used in *MoGo*, such that selecting moves greedily according to the heuristic, and breaking ties randomly, would exactly produce the default policy π_{mogo}.

4. The *local shape* heuristic, $Q_{rlgo}(s,a)$, is computed from a linear combination of local shape features. This heuristic is learnt offline by temporal difference learning, from games of self-play, exactly as described in Chapter 5.

For each heuristic evaluation function, we assign a heuristic confidence $\tilde{C}(s,a) = M$, for various constant values of equivalent experience M. We played 2300 games between *MoGo* and GnuGo 3.7.10 (level 10). The MC–RAVE algorithm executed 3,000 simulations per move (see Figure 8.3).

The value function learnt from local shape features, Q_{rlgo}, outperformed all the other heuristics and increased the winning rate of *MoGo* from 60% to 69%. Maximum performance was achieved using an equivalent experience of $M = 50$, which indicates that Q_{rlgo} is worth about as much as 50 simulations using all-moves-as-first. It seems likely that these results could be further improved by varying the heuristic confidence according to the particular position, based on the variance of the heuristic evaluation function.

8.7 Exploration and Exploitation

The performance of Monte-Carlo tree search is greatly improved by carefully balancing exploration with exploitation. The UCT algorithm significantly outperforms a greedy tree policy in computer Go (Gelly et al., 2006). Surprisingly, this result does not appear to extend to the heuristic UCT–RAVE algorithm: the optimal exploration rate in our experiments was zero, i.e. greedy MC–RAVE with no exploration in the tree policy.

We believe that the explanation lies in the nature of the RAVE algorithm. Even if a move a is not selected immediately from position s, it will often be played at some later point in the simulation. This greatly reduces the need for explicit exploration, because the values for all moves are continually updated, regardless of the initial move selection.

However, we were only able to run thorough tests with tens of thousands of simulations per move. It is possible that exploration again becomes important when MC–RAVE is scaled up to millions of simulations of move. At this point a substantial number of nodes will be dominated by MC values rather than RAVE values, so that exploration at these nodes should be beneficial.

8.8 Soft Pruning

Computer Go has a large branching factor and several pruning techniques, such as selective search and progressive widening (see Chapter 4), have been developed to reduce the size of the search space. Heuristic MCTS and MC–RAVE can be viewed as *soft pruning* techniques that focus on the highest valued regions of the search space without permanently cutting off any branches of the search tree.

A heuristic function provides a principled way to use prior knowledge to reduce the effective branching factor. Moves favoured by the heuristic function will be initialised with a high value, and tried much more often than moves with a low heuristic value. However, if the heuristic evaluation function is incorrect, then the initial value will drop off at a rate determined by the heuristic confidence function, and other moves will then be explored.

The MC–RAVE algorithm also significantly reduces the effective branching factor. RAVE forms a fast, rough estimate of the value of each move. Moves with high RAVE values will quickly become favoured over moves with low RAVE values, which are soft pruned from the search tree. However, the RAVE values are only used initially, so that MC–RAVE never cuts branches permanently from the search tree.

Heuristic MC–RAVE can often be wrong. The heuristic evaluation function can be inaccurate, and/or the RAVE estimate can be misleading. In this case, heuristic MC–RAVE will prioritise the wrong moves, and the best moves can be soft pruned and not tried again for many simulations. There are no guarantees that these algorithms will help performance. However, in practice they help more than they hurt, and on average over many positions, they provide a very significant performance

Simulations	Wins .v. GnuGo	CGOS rating
3,000	69%	1960
10,000	82%	2110
70,000	92%	2320*

Table 8.1: Winning rate of *MoGo* against GnuGo 3.7.10 (level 10) when the number of simulations per move is increased. *MoGo* competed on CGOS, using heuristic MC–RAVE, in February 2007. The asterisked version used on CGOS modifies the simulations/move according to the available time, from $300,000$ games in the opening to $20,000$.

advantage.

8.9 Performance of *MoGo*

Our two extensions to MCTS, heuristic MCTS and MC–RAVE, increased the winning rate of *MoGo* against GnuGo, from 24% for UCT, up to 69% using heuristic MC–RAVE. However, these results were based on executing just 3,000 simulations per move, using the heuristic schedule in Equation 8.13. When the number of simulations was increased, the overall performance of *MoGo* improved correspondingly. Table 8.1 shows how the performance of heuristic MC–RAVE scales with additional computation.

The 2007 release version of *MoGo* used the heuristic MC–RAVE algorithm, the minimum MSE schedule in Equation 8.41, and an improved, handcrafted heuristic function.[4] The scalability of the release version is shown in Figure 8.4, based on the results of a combined study over many thousands of computer hours (Dailey, 2008). This version of *MoGo* became the first program to achieve *dan*-strength at 9×9 Go; the first program to beat a professional human player at 9×9 Go; the highest rated program on the Computer Go Server for both 9×9 and 19×19 Go; and the gold medal winner at the 2007 Computer Go Olympiad.

8.10 Survey of Subsequent Work on *MoGo*

The results in the previous section were achieved by *MoGo* in 2007. We briefly survey subsequent work on *MoGo* by other researchers.

The heuristic function of *MoGo* was substantially enhanced (Chaslot et al., 2008a), by initialising $H(s, a)$, $C(s, a)$, and $\tilde{C}(s, a)$ to hand-tuned values based on handcrafted rules and patterns. In addition, the handcrafted playout policy was modified to increase the diversity of playouts, by playing in empty regions of the board; and to fix a known issue with life-and-death, by playing in the key point of simple dead shapes, known as *nakade*. Using 100,000 playouts, the improved version of *MoGo* achieved a winning rate of 55% on 9×9 boards, and 53% on 19×19 boards, against the 2007 release version of *MoGo*. A larger winning rate of 66% was achieved when running much

[4]*RLGO* was not used in the release version.

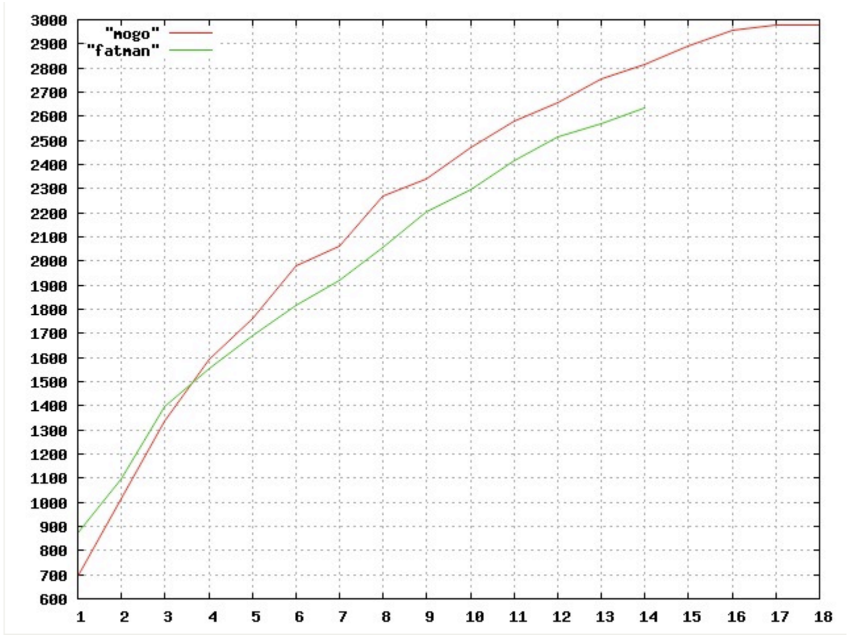

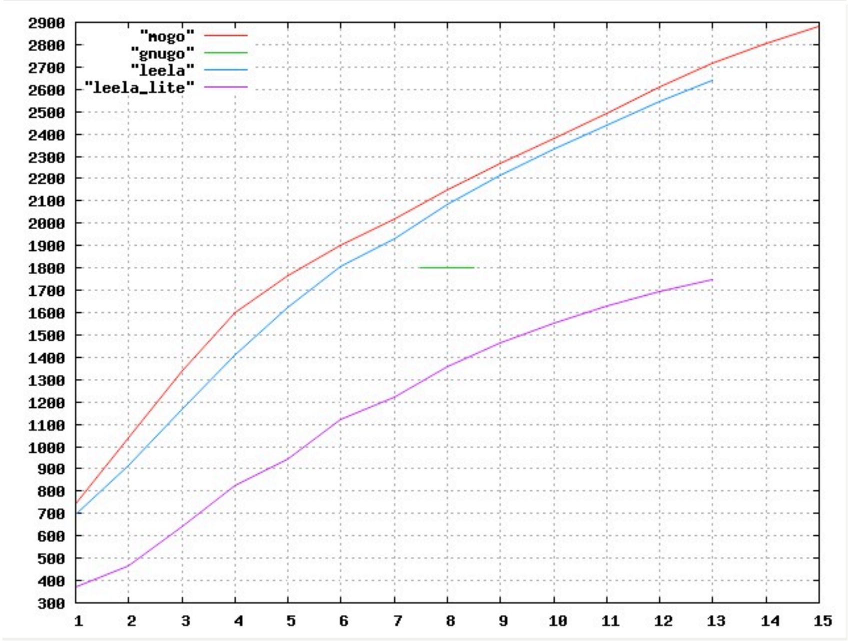

Figure 8.4: Scalability of *MoGo* (2007 release version), reproduced with thanks from (Dailey, 2008). The x-axis represents successive doublings of computation. Elo ratings were computed from a large tournament, consisting of several thousand games for each player, for each program with different levels of computation. a) Scalability of *MoGo* and the UCT program *Fatman* in 9×9 Go. *MoGo* uses 2^{x+5} simulations per move; *Fatman* uses 2^{x+9}. b) Scalability of *MoGo* and another MC–RAVE program *Leela* in 13×13 Go, in a tournament among each program with different levels of computation. *MoGo* and *Leela* both use 2^{x+8} simulations per move.

longer 9×9 games.

MoGo was also modified by massively parallelising the MC–RAVE algorithm to run on a cluster (Gelly et al., 2008). In order to avoid huge communication overheads, memory was only shared between the shallowest nodes in the search tree. The massively parallel version of *MoGo Titan* was run on 800 processors of Huygens, the Dutch national supercomputer. *MoGo Titan* defeated a 9-*dan* professional player, Jun-Xun Zhou, in 19×19 Go with 7 stones handicap.

8.11 Heuristics and RAVE in Dyna-2

In this section we show that the two extensions to Monte-Carlo tree search are special cases of the Dyna-2 architecture (see Chapter 7). We make this connection explicit in order to underline the similarities between the algorithms described in this chapter, and the ideas we have explored in previous chapters. We view the Dyna-2 architecture as a common framework for understanding and improving simulation-based search algorithms, even if the special cases used in *MoGo* can be implemented in a more direct and efficient manner.

8.11.1 Heuristic Monte-Carlo Tree Search in Dyna-2

Heuristic Monte-Carlo tree search can be exactly implemented by the Dyna-2 algorithm, by using different feature vectors in the long and short-term memories. The long-term memory is used to represent the heuristic evaluation function. For example, the heuristic evaluation function $Q_{rlgo}(s, a)$ was learnt by using local shape features in the long-term memory. The short-term memory in Dyna-2 contains the search tree. We use table lookup features, $I^{S,A}$ that match action A in position S (see Chapter 6),

$$I^{S,A}(s, a) = \begin{cases} 1 & \text{if } s = S \text{ and } a = A; \\ 0 & \text{otherwise.} \end{cases} \tag{8.47}$$

The short-term memory uses a state-action feature for every node in the search tree, $\overline{\phi}_i(s, a) = I^{\mathcal{T}_i}(s, a)$, where $\mathcal{T}_i$ denotes the ith node added to the search tree. The search tree is grown incrementally in the usual way, by adding the first new position and action in each simulation.

The temporal difference parameter is set to $\lambda = 1$ so as to replicate Monte-Carlo evaluation.[5] The step-size schedule is set according to the heuristic confidence function $C(s, a)$,

$$\alpha(s, a) = \frac{1}{C(s, a) + N(s, a)}. \tag{8.48}$$

[5]In our experiments with Monte-Carlo tree search, where each state of the search tree is represented individually, bootstrapping slightly reduced performance. When the state is approximated by multiple features, bootstrapping was always beneficial.

8.11.2 RAVE in Dyna-2

A very similar algorithm to RAVE can be implemented by extending the Dyna-2 architecture to use features of the history and not just of the current state.

We define a history h_t to be a sequence of states and actions $h_t = s_0 a_0 ... s_t a_t$, including the current action a_t. We define a *RAVE feature* $\tilde{I}^{S,A}(h)$ that matches move A in the subtree $\tau(S)$. This binary feature has value 1 iff S occurs in the history and A matches the current action a_t,

$$\tilde{I}^{S,A}(s_0 a_0 ... s_t a_t) = \begin{cases} 1 & \text{if } a_t = A \text{ and } \exists i \text{ s.t. } s_i = S; \\ 0 & \text{otherwise.} \end{cases} \tag{8.49}$$

To implement RAVE in Dyna-2, we use a short-term memory consisting of one RAVE feature for every node in the search tree, $\overline{\phi}_i(s, a) = \tilde{I}^{\mathcal{T}_i}(s, a)$. This set of features provides the same abstraction over the search tree as the RAVE algorithm, by generalising over the same move within each subtree. We again set the temporal difference parameter to $\lambda = 1$.

The RAVE algorithm used in *MoGo* makes two additional simplifications, compared to using RAVE features in Dyna-2. First, the value of each RAVE feature is estimated independently. In Dyna-2 the credit for each win or loss is shared among the RAVE features for *all* subtrees visited during that simulation, by linear or logistic regression. Second, *MoGo* selects moves using only the most specific subtree, whereas in Dyna-2 the evaluation function takes account of subtrees of all levels.

In principle it could be advantageous to combine RAVE features from all levels of the tree, either during learning or during move selection. However, in our experiments with *MoGo*, combining value estimates from multiple subtrees did not confer any advantage.

8.12 Conclusions

We have presented two extensions to the Monte-Carlo tree search algorithm. First, we have provided a principled framework for incorporating heuristic knowledge into Monte-Carlo tree search, by initialising the nodes of the search trees to appropriate values and counts.

Second, and perhaps most importantly, we have introduced a method for generalising between related states, by sharing values between subtrees of the search tree. In large problems, such as 19×19 Go, this allows the enormous search space to be searched efficiently, and provides a dramatic reduction in variance. However, this generalisation comes at a cost: the introduction of bias to the value estimates. The minimum MSE schedule for MC–RAVE provides a principled approach to balancing bias and variance.

Using the MC–RAVE algorithm, *MoGo* was able to beat human professional players for the first time, both in even games on 9×9 boards, and in 7 stone handicap games on 19×19 boards. The scalability of *MoGo* suggests that further successes may be achievable with additional computational power.

Endnotes

The original version of *MoGo* was programmed by Sylvain Gelly and Yizao Wang (Gelly et al., 2006). Sylvain Gelly devised and implemented the original MC–RAVE algorithm, using the schedule described in Equation 8.13. I developed the theory for MC–RAVE and the minimum MSE schedule, which was implemented in *MoGo* by Sylvain Gelly, but has not previously been published. I also devised the heuristic MCTS algorithm, in collaboration with Sylvain Gelly, and implemented an interface to *RLGO 1.0* so that it could provide an initial heuristic for *MoGo*. I collaborated with Sylvain Gelly, providing him with numerous bad and occasional good ideas for *MoGo*, until the completion of his Ph.D. in August 2007. *RLGO* was not used in any tournament version of *MoGo*, and I have made no contribution to the subsequent development of *MoGo*. I did not contribute to the scalability study for *MoGo*, which was collated by several members of the computer Go mailing list (Dailey, 2008). The majority of algorithms and results in this chapter have been previously published in ICML (Gelly and Silver, 2007), AAAI (Gelly and Silver, 2008), and Sylvain Gelly's Ph.D. thesis (Gelly, 2007).

Chapter 9

Monte-Carlo Simulation Balancing

9.1 Introduction

The performance of Monte-Carlo search is primarily determined by the quality of the simulation policy. However, a policy that always plays strong moves does not necessarily produce the diverse, well-balanced simulations that are desirable for a Monte-Carlo player. In this chapter we introduce a new paradigm for learning a simulation policy, which explicitly optimises a Monte-Carlo objective.

Broadly speaking, two approaches have previously been taken to improving the simulation policy. The first approach is to directly construct a *strong* simulation policy that performs well by itself, either by hand (Billings et al., 1999), reinforcement learning (Tesauro and Galperin, 1996; Gelly and Silver, 2007), or supervised learning (Coulom, 2007). Unfortunately, a stronger simulation policy can actually lead to a weaker Monte-Carlo search (Gelly and Silver, 2007). One consequence is that human expertise, which typically provides domain knowledge for maximising strength, can be particularly misleading in this context.

The second approach to learning a simulation policy is by trial and error, adjusting parameters and testing for improvements in the performance of the Monte-Carlo player, either by hand (Gelly et al., 2006), or by hill-climbing (Chaslot et al., 2008b). However, each parameter evaluation typically requires many complete games, thousands of positions, and millions of simulations to be executed. Furthermore, hill-climbing methods do note scale well with increasing dimensionality, and fare poorly with complex policy parameterisations.

Handcrafting an effective simulation policy has proven to be particularly problematic in Go. Most of the top Go programs utilise a small number of simple patterns and rules, based largely on the default policy used in *Mogo* (Gelly et al., 2006). Adding further Go knowledge without breaking *Mogo's* "magic formula" has proven to be surprisingly difficult.

We take a new approach to learning a simulation policy. We define an objective function, which we call *balance*, that explicitly measures the performance of a simulation policy for Monte-Carlo evaluation. We introduce two new algorithms that optimise the balance of a simulation policy by gradient descent. These algorithms require very little computation for each parameter update, and are able to learn expressive simulation policies with hundreds of parameters.

We begin with an investigation of simulation policies in 9×9 Go, and demonstrate the paradoxical result that a stronger simulation policy can lead to a weaker Monte-Carlo search. We then introduce our new simulation balancing algorithms, and evaluate them in 5×5 and 6×6 Go. We compare them to reinforcement learning and supervised learning algorithms for maximising strength, and to a well-known simulation policy for this domain, handcrafted by trial and error. The simulation policy learnt by our new algorithms significantly outperforms prior approaches.

9.2 Learning a Simulation Policy in 9×9 Go

In Chapter 5, we learnt an evaluation function for the game of Go, by reinforcement learning and self-play. In the previous chapter, we successfully applied this evaluation function in the search tree of a Monte-Carlo tree search. It is natural to suppose that this same evaluation function, which provides a fast, simple heuristic for playing reasonable Go, might be successfully applied to the default policy of a Monte-Carlo search.

9.2.1 Stochastic Simulation Policies

In a deterministic domain, Monte-Carlo simulation requires a stochastic simulation policy. If there is insufficient diversity in the simulations, then averaging over many simulations provides no additional benefit. We consider three different approaches for generating a stochastic simulation policy from the learnt evaluation function Q_{rlgo}.

First, we consider an ϵ-greedy policy,

$$\pi_\epsilon(s,a) = \begin{cases} 1 - \epsilon + \frac{\epsilon}{|A(s)|} & \text{if } a = \underset{a'}{\operatorname{argmax}}\, Q_{rlgo}(s,a') \\ \frac{\epsilon}{|A(s)|} & \text{otherwise} \end{cases}$$

Second, we consider a greedy policy, where the evaluation function has been corrupted by Gaussian noise $\eta(s,a) \sim N(0,\sigma^2)$,

$$\pi_\sigma(s,a) = \begin{cases} 1 & \text{if } a = \underset{a'}{\operatorname{argmax}}\, Q_{rlgo}(s,a') + \eta(s,a') \\ 0 & \text{otherwise} \end{cases}$$

Third, we select moves using a softmax distribution with an explicit *temperature* parameter τ controlling the level of stochasticity,

$$\pi_\tau(s,a) = \frac{e^{Q_{rlgo}(s,a)/\tau}}{\sum_{a'} e^{Q_{rlgo}(s,a')/\tau}}$$

9.2.2 Strength of Simulation Policies

We compared the performance of each class of simulation policy π_ϵ, π_σ, and π_τ, with *MoGo's* default policy π_{mogo}, and the uniform random policy π_{random}. Figure 9.1 assesses the strength

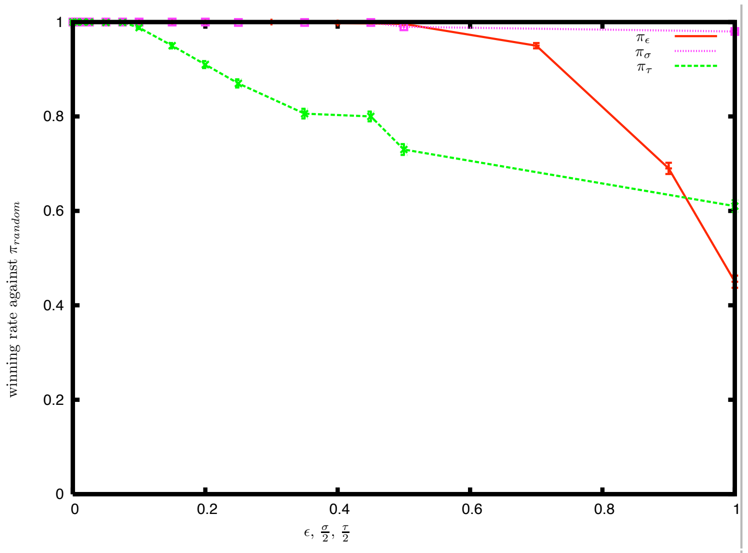

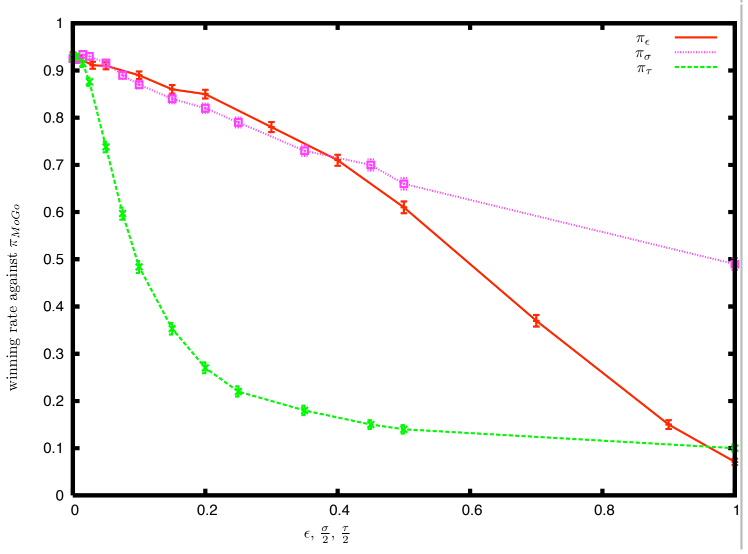

Figure 9.1: The relative strengths of each class of default policy, against the random policy π_{random} (top) and against a handcrafted policy π_{mogo} (bottom). The x axis represents the degree of randomness in each policy.

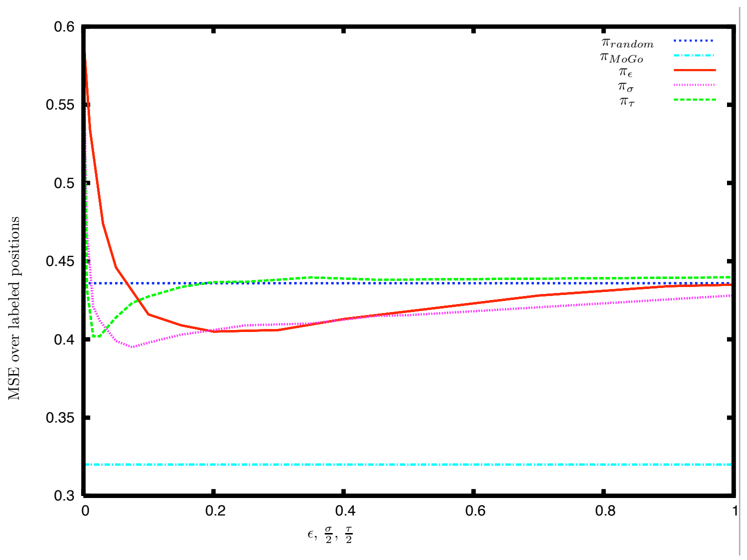

Figure 9.2: The MSE of each policy π when Monte Carlo simulation is used to evaluate a test suite of 200 hand-labelled positions. The x axis indicates the degree of randomness in the policy.

of each policy, directly as a Go player, in a round-robin tournament of 6,000 games between each pair of policies. Without randomisation, the policies based on Q_{rlgo} were by far the strongest, and outperformed both the random policy π_{random} and *MoGo's* handcrafted policy π_{mogo} by a margin of over 90%. As the level of randomisation increased, the policies degenerated towards the random policy π_{random}.

9.2.3 Accuracy of Simulation Policies in Monte-Carlo Simulation

In general, a good simulation policy for Monte-Carlo tree search is one that can evaluate each position accurately, when using Monte-Carlo simulation with no search tree. We measured the performance of Monte-Carlo simulation on a test suite of 200 mid to late-game positions, each of which was hand-labelled as a win or loss by a human expert. 1,000 simulations were played from each test position using each simulation policy. A Monte-Carlo value was estimated by the mean outcome of these simulations. For each simulation policy, we measured the mean-squared error (MSE) between the Monte-Carlo value and the hand-labelled value (see Figure 9.2).[1]

A stronger and appropriately randomised simulation policy achieved a lower MSE than uniform random simulations. However, if the default policy was too deterministic, then Monte-Carlo simulation failed to provide any benefits and the MSE increased dramatically. If the default policy was too random, then it became equivalent to the random policy π_{random}.

Surprisingly, the accuracy of π_ϵ, π_σ and π_τ never come close to the accuracy of the handcrafted policy π_{mogo}, despite the fact that these policies were much stronger Go players. To verify that the default policies based on Q_{rlgo} were indeed stronger in our particular suite of test positions, we

[1]During the development of *MoGo*, the MSE on this test suite was usually a good indicator of overall playing strength.

Default Policy	Wins .v. GnuGo
π_{random}	8.88 $\pm$ 0.4%
π_σ	9.38 $\pm$ 1.9%
π_{mogo}	48.62 $\pm$ 1.1%

Table 9.1: Winning rate of the basic UCT algorithm in *MoGo* against GnuGo 3.7.10 (level 0), given 5,000 simulations per move, using different default policies. The numbers after the $\pm$ correspond to the standard error from several thousand complete games. π_σ was used with $\sigma = 0.15$.

re-ran the round-robin tournament, starting from each of these positions in turn, and found that the relative strengths of the default policies remained very similar. We also compared the performance of a complete Monte-Carlo tree search, using the program *MoGo* and plugging in the simulation policy that minimised MSE as a default policy (see Table 9.1). Again, despite being significantly stronger than π_{mogo}, the simulation policy based on Q_{rlgo} performed much worse overall, performing no better than the uniform random policy.

From these results, we conclude that the spread of outcomes produced by the simulation policy is more important than its strength. Each policy has its own bias, leading it to a particular distribution of simulations. If this distribution is skewed away from the minimax value, then the overall performance can be significantly poorer. In the next section, we develop this intuition into a formal objective function for simulation policies.

9.3 Strength and Balance

We consider deterministic two-player games of finite length with a terminal outcome or score $z \in \mathbb{R}$. During simulation, move a is selected in state s according to a stochastic simulation policy $\pi_p(s, a)$ with parameter vector p, that is used to select moves for both players. The goal is to find the parameter vector p^* that maximises the overall playing strength of a player based on Monte-Carlo search. Our approach is to make the Monte-Carlo evaluations in the search as accurate as possible, by minimising the mean squared error between the estimated values $V(s) = \frac{1}{N}\sum_{i=1}^{N} z_i$ and the minimax values $V^*(s)$.

When the number of simulations N is large, the mean squared error is dominated by the bias of the simulation policy with respect to the minimax value, $V^*(s) - \mathbb{E}_{\pi_p}[z|s]$, and the variance of the estimate (i.e. the error caused by only seeing a finite number of simulations) can be ignored. Our objective is to minimise the mean squared bias, averaged over the distribution of states $\rho(s)$ that are evaluated during Monte-Carlo search.

$$p^* = \operatorname*{argmin}_p \mathbb{E}_\rho \left[\left(V^*(s) - \mathbb{E}_{\pi_p}[z|s] \right)^2 \right] \tag{9.1}$$

where $\mathbb{E}_\rho$ denotes the expectation over the distribution of actual states $\rho(s)$, and $\mathbb{E}_{\pi_p}$ denotes the expectation over simulations with policy π_p.

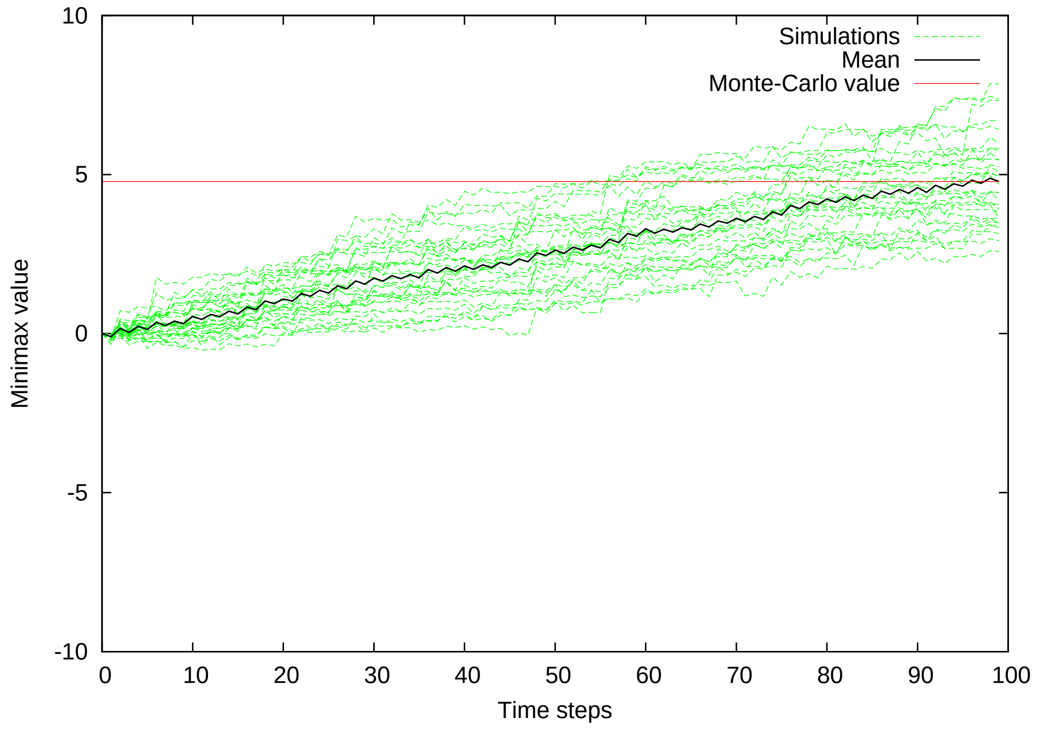

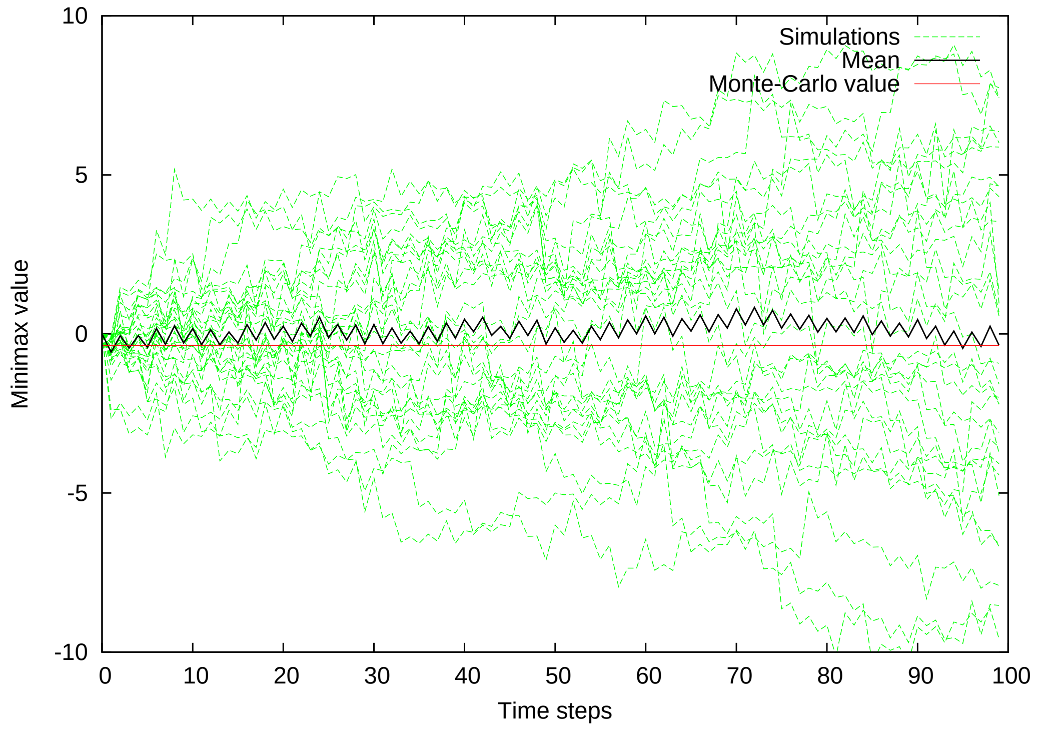

Figure 9.3: Monte-Carlo simulation in an artificial two-player game. 30 simulations of 100 time steps were executed from an initial state with minimax value 0. Each player selects moves imperfectly during simulation, with an error that is exponentially distributed with respect to the minimax value, with rate parameters λ_1 and λ_2 respectively. a) The simulation players are strong but imbalanced: $\lambda_1 = 10, \lambda_2 = 5$, b) the simulation players are weak but balanced: $\lambda_1 = 2, \lambda_2 = 2$. The Monte-Carlo value of the weak, balanced simulation players is significantly more accurate.

In real-world domains, knowledge of the true minimax values is not available. In practice, we use the values $\hat{V}^*(s)$ computed by deep Monte-Carlo tree searches, which converge on the minimax value in the limit (Kocsis and Szepesvari, 2006), as an approximation $\hat{V}^*(s) \approx V^*(s)$.

At every time-step t, each player's move incurs some error $\delta_t = V^*(s_{t+1}) - V^*(s_t)$ with respect to the minimax value $V^*(s_t)$. We will describe a policy with a small error as *strong*, and a policy with a small expected error as *balanced*. Intuitively, a strong policy makes few mistakes, whereas a balanced policy allows many mistakes, as long as they cancel each other out on average. Formally, we define the strength $J(p)$ and k-step imbalance $B_k(p)$ of a policy π_p,

$$J(p) = \mathbb{E}_\rho \left[\mathbb{E}_{\pi_p} \left[\delta_t^2 | s_t = s \right] \right] \tag{9.2}$$

$$\begin{aligned} B_k(p) &= \mathbb{E}_\rho \left[\left(\mathbb{E}_{\pi_p} \left[\sum_{j=0}^{k-1} \delta_{t+j} | s_t = s \right] \right)^2 \right] \qquad (9.3) \\ &= \mathbb{E}_\rho \left[\left(\mathbb{E}_{\pi_p} \left[V^*(s_{t+k}) - V^*(s_t) | s_t = s \right] \right)^2 \right] \end{aligned}$$

We consider two choices of k in this paper. The *two-step imbalance* $B_2(p)$ is specifically appropriate to two-player games. It allows errors by one player, as long as they are on average cancelled out by the other player's error on the next move. The *full imbalance* B_∞ allows errors to be committed at any time, as long as they cancel out by the time the game is finished. It is exactly equivalent to the mean squared bias that we are aiming to optimise in Equation 9.1,

$$\begin{aligned} B_\infty(p) &= \mathbb{E}_\rho \left[\left(\mathbb{E}_{\pi_p} \left[V^*(s_T) - V^*(s) | s_t = s \right] \right)^2 \right] \\ &= \mathbb{E}_\rho \left[\left(\mathbb{E}_{\pi_p} [z | s_t = s] - V^*(s) \right)^2 \right] \qquad (9.4) \end{aligned}$$

where s_T is the terminal state with outcome z. Thus, while the direct performance of a policy is largely determined by its strength, the performance of a policy in Monte-Carlo simulation is determined by its full imbalance.

If the simulation policy is optimal, $\mathbb{E}_{\pi_p}[z|s] = V^*(s)$, then perfect balance is achieved, $B_\infty(p) = 0$. This suggests that optimising the strength of the simulation policy, so that individual moves become closer to optimal, may be sufficient to achieve balance. However, even small errors can rapidly accumulate over the course of long simulations if they are not well-balanced. It is more important to maintain a diverse spread of simulations, which have an average value that is close to optimal, than for the individual moves or simulations to be low in error. Figure 9.3 shows a simple scenario in which the error of each player is i.i.d and exponentially distributed with rate parameters λ_1 and λ_2 respectively. A weak, balanced simulation policy ($\lambda_1 = 2, \lambda_2 = 2$) provides a much more accurate Monte-Carlo evaluation than a strong, imbalanced simulation policy ($\lambda_1 = 10, \lambda_2 = 5$).

In large domains it is not usually possible to achieve perfect strength or perfect balance, and some approximation is required. Our hypothesis is that very different approximations will result from optimising balance as opposed to optimising strength, and that optimising balance will lead to significantly better Monte-Carlo performance.

To test this hypothesis, we implement two algorithms that maximise the strength of the simulation policy, using softmax regression and reinforcement learning respectively. We then develop two new algorithms that minimise the imbalance of the simulation policy by gradient descent. Finally, we compare the performance of these algorithms in 5×5 and 6×6 Go.

9.4 Softmax Policy

We use a *softmax policy* to parameterise the simulation policy,

$$\pi_p(s,a) = \frac{e^{\phi(s,a)\cdot p}}{\sum_b e^{\phi(s,b)\cdot p}} \tag{9.5}$$

where $\phi(s,a)$ is a vector of features for state s and action a, and p is a corresponding parameter vector indicating the preference of the policy for each feature.

The softmax policy can represent a wide range of stochasticity in different positions, ranging from near deterministic policies with large preference disparities, to uniformly random policies with equal preferences. The level of stochasticity is very significant in Monte-Carlo simulation: if the policy is too deterministic then there is no diversity and Monte-Carlo simulation cannot improve the policy; if the policy is too random then the overall accuracy of the simulations is diminished. Existing paradigms for machine learning, such as reinforcement learning and supervised learning, do not explicitly control this stochasticity. One of the motivations for simulation balancing is to tune the level of stochasticity to a suitable level in each position.

We will need the gradient of the log of the softmax policy, with respect to the policy parameters,

$$\begin{aligned}
\nabla_p \log \pi_p(s,a) &= \nabla_p \log e^{\phi(s,a)\cdot p} - \nabla_p \log\left(\sum_b e^{\phi(s,b)\cdot p}\right) \\
&= \nabla_p \left(\phi(s,a)\cdot p\right) - \frac{\nabla_p \sum_b e^{\phi(s,b)\cdot p}}{\sum_b e^{\phi(s,b)\cdot p}} \\
&= \phi(s,a) - \frac{\sum_b \phi(s,b) e^{\phi(s,b)\cdot p}}{\sum_b e^{\phi(s,b)\cdot p}} \\
&= \phi(s,a) - \sum_b \pi_p(s,b)\phi(s,b)
\end{aligned} \tag{9.6}$$

which is the difference between the observed feature vector and the expected feature vector. We denote this gradient by $\psi_p(s,a)$.

Finally, we note that if binary features are used, then the parameters of the softmax policy are equal to the log of the ratings in a generalised Bradley-Terry model, as used in the Go program Crazystone (Coulom, 2007).

9.5 Optimising Strength

We consider two algorithms for optimising the strength of a simulation policy, by supervised learning and reinforcement learning respectively.

9.5.1 Softmax Regression

Our first algorithm optimises the strength of the simulation policy by softmax regression. The aim of the algorithm is simple: to find a simulation policy that behaves as closely as possible to a given expert policy $\mu(s, a)$.

We consider a data-set of L training examples (s_l, a_l^*) of actions a_l^* selected by expert policy μ in positions s_l. The softmax regression algorithm finds parameters maximising the likelihood, $\mathcal{L}(p)$, that the simulation policy $\pi_p(s, a)$ produces the actions a_l^*. This is achieved by gradient ascent of the log likelihood,

$$\begin{aligned}
\mathcal{L}(p) &= \prod_{l=1}^{L} \pi_p(s_l, a_l^*) \\
\log \mathcal{L}(p) &= \sum_{l=1}^{L} \log \pi_p(s_l, a_l^*) \\
\nabla_p \log \mathcal{L}(p) &= \sum_{l=1}^{L} \nabla_p \log \pi_p(s_l, a_l^*) \\
&= \sum_{l=1}^{L} \psi_p(s_l, a_l^*) \qquad (9.7)
\end{aligned}$$

This leads to a stochastic gradient ascent algorithm, in which each training example (s_l, a_l^*) is used to update the policy parameters, with step-size α,

$$\Delta p = \alpha \psi_p(s_l, a_l^*) \qquad (9.8)$$

Softmax regression is a convex optimisation algorithm and is guaranteed to converge to the maximum likelihood solution. We note that this algorithm provides an alternative approach to finding the maximum likelihood ratings in a generalised Bradley-Terry model (Coulom, 2007).

9.5.2 Policy Gradient Reinforcement Learning

Our second algorithm optimises the strength of the simulation policy by reinforcement learning. The objective is to maximise the expected cumulative reward from start state s. *Policy gradient* algorithms adjust the policy parameters p by gradient ascent, so as to find a local maximum for this objective.

We define $\mathcal{X}(s)$ to be the set of possible games $\xi = (s_1, a_1, ..., s_T, a_T)$ of states and actions, starting from $s_1 = s$. The policy gradient can then be expressed as an expectation over game outcomes $z(\xi)$,

$$
\begin{aligned}
\mathbb{E}_{\pi_p}[z|s] &= \sum_{\xi \in \mathcal{X}(s)} Pr(\xi) z(\xi) \\
\nabla_p \mathbb{E}_{\pi_p}[z|s] &= \sum_{\xi \in \mathcal{X}(s)} \nabla_p (\pi_p(s_1, a_1) ... \pi_p(s_T, a_T)) z(\xi) \\
&= \sum_{\xi \in \mathcal{X}(s)} \pi_p(s_1, a_1) ... \pi_p(s_T, a_T) \\
&\quad \left(\frac{\nabla_p \pi_p(s_1, a_1)}{\pi_p(s_1, a_1)} + ... + \frac{\nabla_p \pi_p(s_T, a_T)}{\pi_p(s_T, a_T)} \right) z(\xi) \\
&= \mathbb{E}_{\pi_p} \left[z \sum_{t=1}^{T} \nabla_p \log \pi_p(s_t, a_t) \right] \\
&= \mathbb{E}_{\pi_p} \left[z \sum_{t=1}^{T} \psi_p(s_t, a_t) \right] \qquad (9.9)
\end{aligned}
$$

The policy parameters are updated by stochastic gradient ascent with step-size α, after each game, leading to a REINFORCE algorithm (Williams, 1992),

$$
\Delta p = \frac{\alpha z}{T} \sum_{t=1}^{T} \psi_p(s_t, a_t) \qquad (9.10)
$$

9.6 Optimising Balance

We now introduce two algorithms for minimising the full imbalance and two-step imbalance of a simulation policy. Both algorithms learn from $\hat{V}^*(s)$, an approximation to the minimax value function constructed by deep Monte-Carlo search.

9.6.1 Policy Gradient Simulation Balancing

Our first simulation balancing algorithm minimises the full imbalance B_∞ of the simulation policy, by gradient descent. The gradient breaks down into two terms. The *bias*, $b(s)$, indicates the direction in which we need to adjust the mean outcome from state s: e.g. does black need to win more or less frequently, in order to match the minimax value? The *policy gradient*, $g(s)$, indicates how the mean outcome from state s can be adjusted, e.g. how can the policy be modified, so as to make black win more frequently?

$$
\begin{aligned}
b(s) &= V^*(s) - \mathbb{E}_{\pi_p}[z|s] \\
g(s) &= \nabla_p \mathbb{E}_{\pi_p}[z|s] \\
B_\infty(p) &= \mathbb{E}_\rho \left[b(s)^2 \right] \\
\nabla_p B_\infty(p) &= -2\mathbb{E}_\rho \left[b(s) g(s) \right] \qquad (9.11)
\end{aligned}
$$

We estimate the bias, $\hat{b}(s)$, by sampling M simulations $\mathcal{X}_M(s)$ from state s,

$$\hat{b}(s) = \hat{V}^*(s) - \frac{1}{M} \sum_{\xi \in \mathcal{X}_M(s)} z(\xi) \tag{9.12}$$

We estimate the policy gradient, $\hat{g}(s)$, by sampling N additional simulations $\mathcal{X}_N(s)$ from state s and using Equation 9.9,

$$\hat{g}(s) = \sum_{\xi \in \mathcal{X}_N(s)} \frac{z(\xi)}{NT} \sum_{t=1}^{T} \psi_p(s_t, a_t) \tag{9.13}$$

In general $\hat{b}(s)$ and $\hat{g}(s)$ are correlated, and we need two independent samples to form an unbiased estimate of their product. The size of these samples should be large enough to ensure that the bias (the error due to the simulation policy) dominates the variance (the error due to finite sample size).

The two estimates provide a simple stochastic gradient descent update, $\Delta p = \alpha \hat{b}(s)\hat{g}(s)$. The full procedure is described in pseudocode in Algorithm 9.

Algorithm 9 Policy Gradient Simulation Balancing

```
$p \leftarrow 0$
**for all** $s_1 \in$ training set **do**
    $V \leftarrow 0$
    **for** $i = 1$ to $M$ **do**
        **simulate** $(s_1, a_1, ..., s_T, a_T; z)$ using $\pi_p$
        $V \leftarrow V + \frac{z}{M}$
    **end for**
    $g \leftarrow 0$
    **for** $j = 1$ to $N$ **do**
        **simulate** $(s_1, a_1, ..., s_T, a_T; z)$ using $\pi_p$
        $g \leftarrow g + \frac{z}{NT} \sum_{t=1}^{T} \psi_p(s_t, a_t)$
    **end for**
    $p \leftarrow p + \alpha(\hat{V}^*(s_1) - V)g$
**end for**
```

9.6.2 Two-Step Simulation Balancing

Our second simulation balancing algorithm minimises the two-step imbalance B_2 of the simulation policy, by gradient descent. The gradient can again be expressed as a product of two terms. The *two-step bias*, $b_2(s)$, indicates whether black needs to win more or less games, to achieve balance between time t and time $t + 2$. The *two-step policy gradient*, $g_2(s)$, indicates the direction in which the parameters should be adjusted, in order for black to improve his evaluation at time $t + 2$.

$$\begin{aligned}
b_2(s) &= V^*(s) - \mathbb{E}_{\pi_p}[V^*(s_{t+2})|s_t = s] \\
g_2(s) &= \nabla_p \mathbb{E}_{\pi_p}[V^*(s_{t+2})|s_t = s] \\
B_2(p) &= \mathbb{E}_\rho \left[b_2(s)^2\right] \\
\nabla_p B_2(p) &= -2\mathbb{E}_\rho \left[b_2(s) g_2(s)\right]
\end{aligned} \tag{9.14}$$

The two-step policy gradient can be derived by applying the product rule,

$$\begin{aligned}
g_2(s) &= \nabla_p \mathbb{E}_{\pi_p}[V^*(s_{t+2})|s_t = s] \\
&= \nabla_p \sum_a \sum_b \pi_p(s_t, a)\pi_p(s_{t+1}, b) V^*(s_{t+2}) \\
&= \sum_a \sum_b \pi_p(s_t, a)\pi_p(s_{t+1}, b) V^*(s_{t+2}) \\
&\quad \left(\frac{\nabla_p \pi_p(s_t, a)}{\pi_p(s_t, a)} + \frac{\nabla_p \pi_p(s_{t+1}, b)}{\pi_p(s_{t+1}, b)} \right) \\
&= \mathbb{E}_{\pi_p}\left[V^*(s_{t+2})(\psi_p(s_t, a_t) + \psi_p(s_{t+1}, a_{t+1}))|s_t = s\right]
\end{aligned} \tag{9.15}$$

Both the two-step bias $b_2(s)$ and the policy gradient $g_2(s)$ can be calculated analytically, with no requirement for simulation, leading to a simple gradient descent algorithm (see Algorithm 10), $\Delta p = \alpha b_2(s) g_2(s)$.

Algorithm 10 Two Step Simulation Balancing

```
$p \leftarrow 0$
**for all** $s_1 \in$ training set **do**
    $V \leftarrow 0, g_2 \leftarrow 0$
    **for all** $a_1 \in$ legal moves from $s_1$ **do**
        $s_2 = s_1 \circ a_1$
        **for all** $a_2 \in$ legal moves from $s_2$ **do**
            $s_3 = s_2 \circ a_2$
            $p = \pi_p(s_1, a_1)\pi_p(s_2, a_2)$
            $V \leftarrow V + p\hat{V}^*(s_3)$
            $g_2 \leftarrow g_2 + p\hat{V}^*(s_3)(\psi_p(s_1, a_1) + \psi_p(s_2, a_2))$
        **end for**
    **end for**
    $p \leftarrow p + \alpha(\hat{V}^*(s_1) - V)g_2$
**end for**
```

9.7 Experiments in Computer Go

We applied each of our algorithms to learn a simulation policy for 5×5 and 6×6 Go. For the softmax regression and simulation balancing algorithms, we constructed a data-set of positions from 1,000 games of randomly played games. We used the open source Monte-Carlo Go program *Fuego* to evaluate each position, using a deep search of 10,000 simulations from each position. The results of

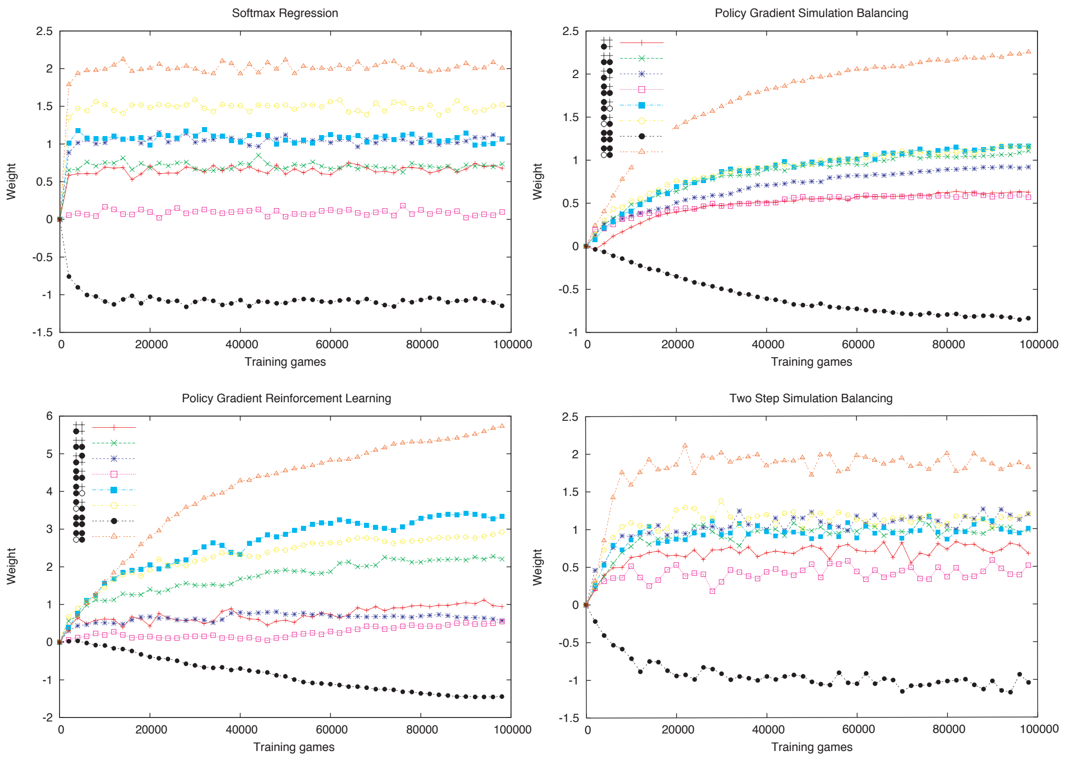

Figure 9.4: Weight evolution for the 2 × 2 local shape features: (top left) softmax regression, (top right) policy gradient simulation balancing, (bottom left) policy gradient reinforcement learning, (bottom right) two-step simulation balancing.

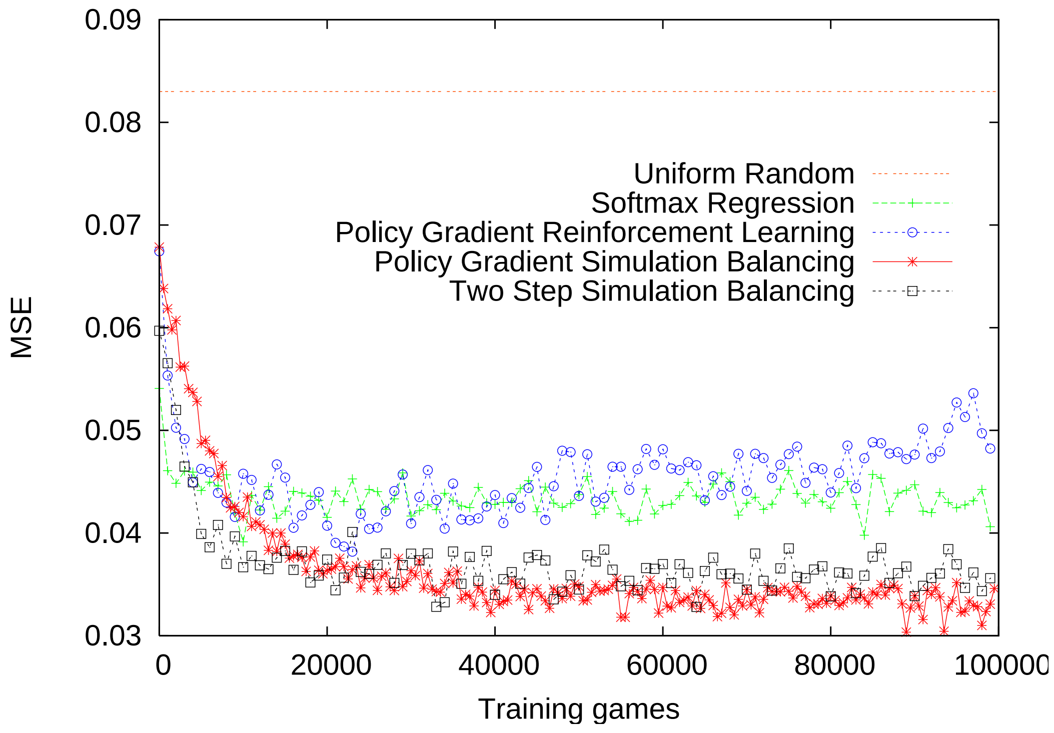

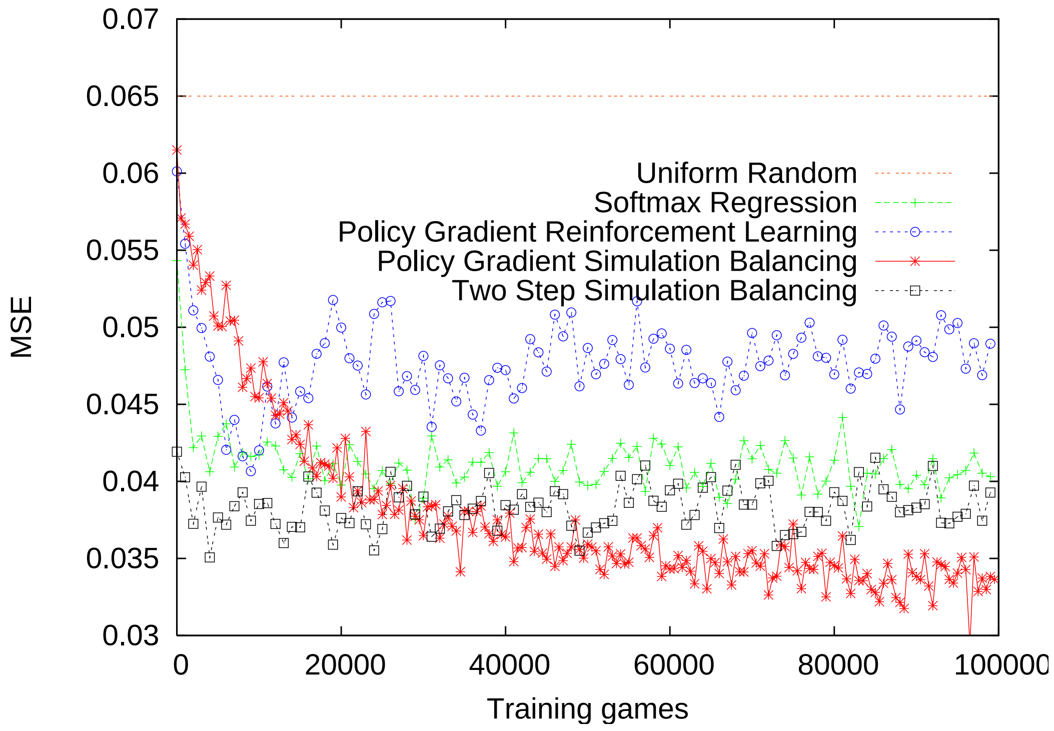

Figure 9.5: Monte-Carlo evaluation accuracy of different simulation policies in 5×5 Go (top) and 6×6 Go (bottom). Each point is the mean squared error over 1,000 positions, between Monte-Carlo values from 100 simulations, and deep rollouts using the Go program *Fuego*.

the search are used to approximate the optimal value $\hat{V}^*(s) \approx V^*(s)$. For the two-step simulation balancing algorithm, a complete tree of depth 2 was also constructed from each position in the data-set, and each leaf position evaluated by a further 2,000 simulations. These leaf evaluations are used in the two-step simulation balancing algorithm, to approximate the optimal value after each possible move and response.

We parameterise the softmax policy (Equation 9.5) with 1×1 and 2×2 local shape features, using location dependent and location independent weight sharing (see Chapter 5). This representation includes 107 unique parameters for the simulation policy, each indicating a preference for a particular pattern.

9.7.1 Balance of Shapes

We trained the simulation policy using 100,000 training games of 5×5 Go, starting with initial weights of zero. The weights learnt by each algorithm are shown in Figure 9.4. All four algorithms converged on a stable solution. They quickly learnt to prefer capturing moves, represented by a positive preference for the location independent 1×1 feature, and to prefer central board intersections over edge and corner intersections, represented by the location dependent 2×2 features. Furthermore, all four algorithms learnt patterns that correspond to basic Go knowledge: e.g. the *turn* shape attained the highest preference, and the *dumpling* and *empty triangle* shapes attained the lowest preference.

In our experiments, the policy gradient reinforcement learning algorithm found the most deterministic policy, with a wide spectrum of weights. The softmax regression algorithm converged particularly quickly, to a moderate level of determinism. The two simulation balancing algorithms found remarkably similar solutions, with the turn shape highly favoured, the dumpling shape highly disfavoured, and a stochastic balance of preferences over other shapes.

9.7.2 Mean Squared Error

We measured the accuracy of the simulation policies every 1,000 training games by selecting 1,000 random positions from an independent test-set, and performing a Monte-Carlo evaluation from 100 simulations. The mean squared error (MSE) of the Monte-Carlo values, compared to the deep search values, is shown in Figure 9.5, for 5×5 and 6×6 Go.

All four algorithms significantly reduced the evaluation error compared to the uniform random policy. The simulation balancing algorithms achieved the lowest error, with less than half the MSE of the uniform random policy. The reinforcement learning algorithm initially reduced the MSE, but then bounced after 20,000 steps and started to increase the evaluation error. This suggests that the simulation policy became too deterministic, specialising to weights that achieve maximum strength, rather than maintaining a good balance. The softmax regression algorithm quickly learnt to reduce the error, but then converged on a solution with significantly higher MSE than the simulation bal-

	5x5		6x6	
Simulation Policy	Direct	MC	Direct	MC
Uniform random	0	1031	0	970
Softmax regression	671	1107	569	1047
Policy gradient RL (20k)	816	1234	531	1104
Policy gradient RL (100k)	**947**	1159	**850**	1023
Policy gradient sim. balancing	719	**1367**	658	**1301**
Two-step simulation balancing	720	1357	444	1109
GnuGo 3.7.10 (level 10)	1376	N/A	1534	N/A
Fuego simulation policy	356	689	374	785

Table 9.2: Elo rating of simulation policies in 5×5 Go and 6×6 Go tournaments. The first column shows the performance of the simulation policy when used directly. The second column shows the performance of a simple Monte-Carlo search using the simulation policy. Each program played a minimum of 8,000 games, and Bayesian Elo ratings were computed from the results, with a 95% confidence interval of approximately +/-10 points.

ancing algorithms. Given a source of expert evaluations, this suggests that simulation balancing can make more effective use of this knowledge, in the context of Monte-Carlo simulation, than a supervised learning approach.

9.7.3 Performance in Monte-Carlo Search

In our final experiment, we measured the performance of each learnt simulation policy in a Monte-Carlo search algorithm. We ran a tournament between players based on each simulation policy, consisting of at least 5,000 matches for every player. Two players were included for each simulation policy: the first played moves directly according to the simulation policy; the second used the simulation policy in a Monte-Carlo search algorithm. Our search algorithm was intentionally simplistic: for every legal move a, we simulated 100 games starting with a, and selected the move with the greatest number of wins. We included two simulation policies for the policy gradient reinforcement learning algorithm, firstly using the parameters that maximised performance (100k games of training), and secondly using the parameters that minimised MSE (20k and 10k games of training in 5×5 and 6×6 Go respectively). The results are shown in Table 9.2.

When the simulation policies were used directly, policy gradient RL (100k) was by far the strongest, around 200 Elo points stronger than simulation balancing. However, when used as a Monte-Carlo policy, simulation balancing was much stronger, 200 Elo points above policy gradient RL (100k), and almost 300 Elo stronger than softmax regression.

The two simulation balancing algorithms achieved similar performance in 5×5 Go, suggesting that it suffices to balance the errors from consecutive moves, and that there is little to be gained by balancing complete simulations. However, in the more complex game of 6×6 Go, Monte-Carlo simulation balancing performed significantly better than two-step simulation balancing.

Finally, we compared the performance of our Monte-Carlo search to GnuGo, a deterministic Go program with sophisticated, handcrafted knowledge and specialised search algorithms. Using the policy learnt by simulation balancing, our simple one-ply search algorithm achieved comparable strength to GnuGo. In addition, we compared the performance of the *Fuego* simulation policy, which is based on the well-known *MoGo* patterns (see Chapter 4) and handcrafted for Monte-Carlo search on larger boards. Surprisingly, the Fuego simulation policy performed poorly, suggesting that handcrafted patterns do not generalise well to smaller board sizes.

9.8 Conclusions

In this chapter we have presented a new paradigm for simulation balancing in Monte-Carlo search. Unlike supervised learning and reinforcement learning approaches, our algorithms can balance the level of stochasticity to an appropriate level for Monte-Carlo search. They are able to exploit deep search values more effectively than supervised learning methods, and they maximise a more relevant objective function than reinforcement learning methods. Unlike hill-climbing or handcrafted trial and error, our algorithms are based on an analytical gradient based only on the current position, allowing parameters to be updated with minimal computation. Finally, we have demonstrated that our algorithms outperform prior methods in small board Go.

We are currently investigating methods for scaling up the simulation balancing paradigm both to larger domains, using *actor-critic* methods to reduce the variance of the policy gradient estimate; and to more sophisticated Monte-Carlo search algorithms, such as UCT (Kocsis and Szepesvari, 2006). In complex domains, the quality of the minimax approximation $\hat{V}^*(s)$ can affect the overall solution. One natural idea is to use the learnt simulation policy in Monte-Carlo search, and generate new deep search values, in an iterative cycle.

One advantage of softmax regression over simulation balancing is that it optimises a convex objective function. This suggests that the two methods could be combined: first using softmax regression to find a global optimum, and then applying simulation balancing to find a local, balanced optimum.

For clarity of presentation we have focused on deterministic two-player games with terminal outcomes. However, all of our algorithms generalise directly to stochastic environments and intermediate rewards.

Endnotes

The experiments with *MoGo* were performed in collaboration with Sylvain Gelly, and were previously published in ICML (Gelly and Silver, 2007). I developed the Monte-Carlo simulation balancing theory and algorithms while visiting IBM Watson, with the help and supervision of Gerry Tesauro, and was supported in part under the DARPA GALE project, contract No. HR0011-08-C-0110. This work was previously published in ICML (Silver and Tesauro, 2009).

Chapter 10

Discussion

In this thesis we have used the game of Go as a case study for reinforcement learning and simulation-based search. However, the basic framework that we have developed is widely applicable, and many avenues remain to be explored, both within Go, and in other applications.

In this chapter we discuss several directions for future work. In particular, we mention many of the ideas that we tried that were not successful in Go. Perhaps this may help other researchers to avoid the same pitfalls, but perhaps also these ideas may prove to be useful in other guises or in other applications. These ideas are presented without detailed results or experimental methodology, and the conclusions that we draw should be considered tentative.

10.1 Representation

Temporal-difference search provides a framework for generalisation in simulation-based search. State abstraction is used to compress the state into features, and the value function is approximated in terms of these features.

Clearly, the choice of features has a large effect on the performance of the algorithm. So far, we have primarily analysed one choice of representation in one application, by using local shape features in Go. However, temporal-difference search can be applied to any MDP, and local shape features are only one of many possible representations.

Local shape features have several important properties: they can be incrementally and efficiently computed, they provide a rich, multi-level state abstraction at several levels of detail, and they correspond to frequently occurring patterns of state variables. We now consider several other classes of representation that have similar properties.

10.1.1 Incremental Representations

Local shape features provide a static representation based on a fixed vector of features. In Chapter 6 we saw that, in large problems with limited memory, a dynamic value function can be more effective than a static value function. Similarly, a dynamic representation can in principle be more effective than a static representation, by specialising the representation to the subproblem occurring *now*.

Monte-Carlo tree search uses a simple mechanism for updating the representation dynamically. It adds the first new state encountered in each simulation into the representation. This same idea can be applied more generally. The first new pattern to occur in each simulation can be added into the representation as a new feature. We refer to this approach as an *incremental representation*. This simple mechanism ensures that the set of features continually grows to cover the situations that actually occur during simulations.[1]

10.1.2 Incremental Representations of Local Shape

Local shape features can be extended into an incremental representation. The board can be partitioned into overlapping regions of any shape or size. A binary feature matches a local configuration of stones and empty intersections within one of these regions. One new feature is added to each region in each simulation, for the first new configuration encountered within that region. Just as Monte-Carlo tree search incrementally grows a global search tree, this procedure incrementally grows multiple local search trees.

We consider three types of incremental representation, based on three different shapes of region,

1. *Incremental shape features* are a direct extension of local shape features. Each simulation, one new shape is added to the representation, for each square region of the board. Growing the representation incrementally allows larger shapes to be used. We have experimented with 1×1 to 5×5 incremental shape features.

2. *Block features* match local configurations within an irregularly shaped region. Several regions are used, one for each block of stones on the board. Each region adapts to the shape of one block, and includes all intersections within Manhattan distance d of that block. We have experimented with block features of Manhattan distance $d = 0$ to 3.

3. *Table lookup features* match full board positions (see Chapter 6), with one new position added in each simulation, just like Monte-Carlo tree search. Table lookup features are also equivalent to 9×9 incremental shape features.

We used these incremental representations in temporal-difference search (see Chapter 6). Surprisingly, none of the incremental representations performed as well as the naive 1×1 to 3×3 local shape features. Incremental shape features were most effective when 1×1 to 3×3 features were used. However, incremental shape features take many simulations to build up their representation, and perform slightly worse than the equivalent sizes of local shape feature. Cumulatively including incremental shape features of 4×4 and 5×5 was strictly detrimental. Block features performed

[1]We assume that there is enough memory to store one feature per simulation. Otherwise it is also necessary to prune the least frequently used features.

worse than incremental shape features, and table lookup features performed worst of all. Combining table lookup features with local shape features was no better than local shape features alone.

10.1.3 Sequence Features

Binary features can in general specify any configuration of stones in the state. They can also specify any configuration of actions in the history. Unlike local shape features, which match spatially contiguous moves that may be played at any time, sequence features match temporally contiguous moves that may be played at any location. They generalise between histories that include common sequences of actions. We define a sequence feature $I^{A_1 \dots A_\tau}(h)$ to be a binary feature of the history h that matches a sequence of τ actions from A_1 to A_τ. The binary feature is on iff the specified sequence has occurred at any point within the history,

$$I^{A_1 \dots A_\tau}(s_1 a_1 ... s_t a_t) = \begin{cases} 1 & \text{if } \exists i \text{ s.t. } \forall j \in [1, \tau], a_{i+j} = A_j; \\ 0 & \text{otherwise.} \end{cases} \tag{10.1}$$

Each simulation, one new sequence of each length τ is added into the representation. We have experimented with sequence features of length $\tau = 1$ to 8. Initial results suggest that the performance of temporal-difference search with sequence features is a little worse than with local shape features. However, sequence features can be computed particularly efficiently. In simulation-based search, they may allow the principal variation discovered in one part of the search tree to be generalised immediately to other parts of the search tree.

10.1.4 Generalisations of RAVE

Local shape features perform well in temporal-difference search (see Chapter 6), and the RAVE algorithm performs well in Monte-Carlo tree search (see Chapter 8). *Extended RAVE* features attempt to combine their advantages together, so that the value of local shape features can be specialised to each subtree.

We have investigated two complementary mechanisms for generalising RAVE features to use local shape features (or other underlying features). First, we propose binary features $\tilde{I}^{s\phi}(h)$ that are on iff s occurs in the history and the local shape feature ϕ matches the current state and action. Second, we propose features $\tilde{I}^{\phi a}(h)$ that are on iff ϕ matches any state in the history, and a matches the current action,

$$\tilde{I}^{s\phi}(s_1 a_1 ... s_t a_t) = \begin{cases} 1 & \text{if } \phi(s_t, a_t) = 1 \text{ and } \exists i \text{ s.t. } s_i = s; \\ 0 & \text{otherwise.} \end{cases} \tag{10.2}$$

$$\tilde{I}^{\phi a}(s_1 a_1 ... s_t a_t) = \begin{cases} 1 & \text{if } a_t = a \text{ and } \exists i \text{ s.t. } \phi(s_i, a_i) = 1; \\ 0 & \text{otherwise.} \end{cases} \tag{10.3}$$

We have not investigated extended RAVE features in any depth, and they provide an interesting avenue for further investigation.

10.2 Combining Dyna-2 with Heuristic MC–RAVE

In this thesis we have developed two separate approaches to computer Go based on the Dyna-2 framework. The first approach uses local shape features and temporal-difference search, and was implemented in the program *RLGO*. The second approach uses the RAVE algorithm and heuristic Monte-Carlo tree search, and was implemented in the program *MoGo*. Although the approach used in *MoGo* is significantly stronger, it is natural to wonder whether the local shape knowledge acquired by temporal-difference search could be combined with the search tree knowledge acquired by MC–RAVE, to further enhance its performance. We briefly consider three different ideas for combining these two approaches together.

The first idea is to combine the two approaches into a hybrid search. Just as we combined temporal-difference search with alpha-beta search in Chapter 7, the idea would be to execute two consecutive searches. A temporal-difference search would compute a value function that is specialised to the current subproblem. Just as in the heuristic MC–RAVE algorithm (see Chapter 8), the value function would then be used as a heuristic function to initialise new nodes in the search tree. Unfortunately, this approach does not appear to work well in practice. This is almost certainly due to the temporality of the short-term memory. In Chapter 6 we saw that the dynamic evaluation function learnt by temporal-difference learning is specialised to positions occurring up to 6 moves in the future; beyond this point it is no better than a static evaluation function learnt by temporal-difference learning. However, MC–RAVE programs such as *MoGo* routinely search to depths of 10 or more moves, where this dynamic evaluation function is no more effective than the local shape heuristic described in Chapter 8.

Another idea is to use the learnt value function as a simulation policy. Unfortunately, as we saw in Chapter 9, even though this provides an objectively stronger simulation policy, it does not improve the performance of the overall program.

Rather than incorporating local shape knowledge into MC–RAVE, an alternative idea is to incorporate search tree knowledge into the Dyna-2 framework. As described in Chapter 6, table lookup features provide the same representation in Dyna-2 as the search tree provides in Monte-Carlo tree search. Similarly, as described in Chapter 8, RAVE features provide the same representation as the search tree in the RAVE algorithm. A natural idea, then, is to combine these features together, along with local shape features or any of the richer representations described above. If temporal-difference search could adapt to this wide array of features effectively, this might be a very effective approach for combining these different sources of knowledge together.

10.2.1 Interpolation Versus Regression

It is perhaps worth highlighting one key difference between the MC–RAVE algorithm and the Dyna-2 architecture. In MC–RAVE, each statistic is computed independently: the MC value is assumed to be independent from the RAVE value. This idea has subsequently been generalised to incorporate additional values, each estimated independently, for example in the programs *Greenpeep* and *Fuego* (Müller and Enzenberger, 2009). In Dyna-2, values are not assumed to be independent, and are combined together additively or multiplicatively, using linear or logistic regression.[2] However, as representations become more sophisticated, combining together many elements of overlapping knowledge, a linear or logistic-linear combination may become preferable.

To illustrate why this might be the case, consider an example from the game of chess, in which Black is ahead by a knight and a bishop. One could estimate the winning probability when Black is ahead by a knight (say 0.7), and independently estimate the winning probability when Black is ahead by a bishop (say 0.8). But a weighted average of these two estimates (say 0.75) would badly underestimate the real winning probability. Instead, a linear evaluation function additively combines the evidence from each feature. In a typical chess program, evidence is accumulated from thousands of overlapping features for material balance, pawn structure and king safety. Naively interpolating between separate value estimates for each feature would provide a very poor evaluation function.

10.3 Adaptive Temporal-Difference Search

In Chapter 5, we saw that enhancing local shape features with additional features does not necessarily produce better performance in temporal-difference learning. In Chapter 6, we saw that the 2×2 local shape features perform surprisingly well in temporal-difference search, and little advantage is gained by using the richer 3×3 features. We have also tried numerous other features based on Go specific knowledge such as liberties, capture, atari, and locality to the previous move, all of which have proven useful in traditional machine learning approaches to Go (see 4). In each case we could produce no significant advantage by incorporating these features.

In practice, we conclude that the naive application of temporal-difference learning and temporal-difference search does not fully exploit a rich representation. To realise the potential of these methods, we believe that two key issues must be addressed. First, the algorithm must adapt its learning rate appropriately to a wide array of features occurring at very different frequencies and levels of generality. Second, the algorithm must adapt its exploration rate so as to improve the policy as efficiently as possible.

10.3.1 Learning Rate Adaptation

Features can occur with a frequency that varies by many orders of magnitude (see Figure 5.5). Without adaptation, the most frequent features provide an overpowering signal that can swamp the rarer and more specific features. To solve this problem, each feature needs a distinct step-size, which reduces over time as the uncertainty in the feature weight diminishes. One possibility is to use a fixed step-size schedule that decays with the number of occurrences of that feature (see George and Powell

[2]The logistic function is linear at its centre, but exponential at its tail. Hence logistic regression combines evidence additively for even positions, but multiplicatively for one-sided positions.

(2006) for a survey). A second possibility is to estimate the variance of the feature weights, and to set the step-sizes in proportion to the variance, for example by using a Kalman filter (Kalman, 1960). A third possibility is to adapt the step-size by gradient descent (Sutton, 1992).

We have investigated a number of these possibilities. A diagonalised approximation to the extended Kalman filter significantly boosted performance for up to 5,000 simulations, and was used in the tournament version of *RLGO 2.4*. However, subsequent experiments suggest that this algorithm actually hurt performance with more simulations. We have not so far found an approach that works as robustly and effectively, across many different board sizes, representations and levels of computation, as a constant step-size, normalised by the number of active features (see Chapters 5 and 6).

10.3.2 Exploration Rate Adaptation

A rich set of features is only effective when sufficient data is experienced to justify the complexity of the representation. However, in reinforcement learning problems the agent is able to control the experience that it sees. It can choose to explore the most significant parts of its state space, so as to learn detailed knowledge about those regions, and intentionally forsake the less significant parts of the state space. Efficient exploration is a crucial aspect of high-performance reinforcement learning.

Perhaps the most successful and widely used principle is optimism in the face of uncertainty (see Chapter 2). The UCT algorithm applies this principle to a table lookup representation, and has achieved great success in several challenging games (see Chapter 3). A natural idea is to generalise this principle to a linear combination of features.

One approach is to track the variance of the features, and to add an exploration bonus that is proportional to the total variance of the value function (Auer, 2002). Another simple idea is to replace the count $N(s, a)$ in the UCT algorithm with a *virtual count* that is based on the number of occurrences of each feature matching state s and action a.

Other approaches to exploration are also possible, for example decaying the exploration rate according to a fixed schedule, using a softmax policy, or applying policy gradient methods (see Chapter 2). Rather than exploring randomly with probability ϵ, it is also possible to use a handcrafted default policy with some probability ϵ'; this provided a small performance improvement in 9×9 Go (at least for low numbers of simulations per move) and was used in the tournament version of *RLGO 2.4*. However, in our experiments nothing has performed as robustly and effectively, over many different contexts, as a naive ϵ-greedy exploration policy with constant ϵ.

10.4 Second Order Reinforcement Learning

Simulation-based search can be viewed as reinforcement learning applied to simulated experience. A large number of reinforcement learning algorithms could be applied to simulation-based search. In this thesis we have focused on first order methods, in particular Monte-Carlo search and temporal-difference learning. However, the effectiveness of simulation-based search is determined in large part by the efficiency of the reinforcement learning algorithm, and it is natural to wonder if second order reinforcement learning methods could be more effective.

Unlike the traditional paradigm of reinforcement learning, experience is cheap and plentiful during simulation-based search. The quantity of learning that takes place is determined by the computational efficiency of the reinforcement learning algorithm, while the quality of the learning is determined by its data efficiency. We desire reinforcement learning algorithms that achieve the best combined computational and data efficiency. First order algorithms, such as TD(0), are computationally efficient, requiring just $O(n)$ computation per time-step for n features. Second order algorithms, such as least-squares temporal-difference learning (LSTD) (Bradtke and Barto, 1996), are generally more data efficient, but are also more computationally expensive, requiring $O(n^2)$ computation per time-step.

In our application, simulations were fast to generate. Furthermore, using a million local shape features, or any of the feature rich representations discussed above, a cost of $O(n^2)$ is simply infeasible. For both these reasons, we have focused on first order methods. However, in other applications such as robotic simulators, where it can be more expensive to simulate experience, second order methods may prove to be desirable.

10.5 Beyond Go

Reinforcement learning has been successful across a broad variety of fields and applications (Sutton and Barto, 1998). Simulation-based search, which applies reinforcement learning to simulated experience, may prove to be equally widely applicable. We briefly consider some of the key issues that must be addressed in order to apply this approach to other settings.

10.5.1 Generative Models

In zero sum, two-player games such as Go, a self-play model can be used to simulate experience (see Chapter 3). To apply simulation-based search algorithms to more general MDPs, other forms of generative model are required.

In many problems, the environment is fully specified as part of the problem. For example, in classical planning, the consequence of each action is deterministic and known, and the challenge is to identify a sequence of actions that achieves a particular goal. Applying stochastic methods to these deterministic problems may seem counter-intuitive. However, as in computer Go, simulation-based search may prove to be an effective method for breaking the curse of dimensionality (Rust, 1997), and managing the uncertainty of the agent's own policy (see Chapter 3). Recently, Monte-Carlo search has achieved promising results in classical planning (Nakhost and Müller, 2009), suggesting that the full spectrum of simulation-based search algorithms may be worth investigating.

Stochastic simulators are widely used in applications from robotics to finance (Asmussen and Glynn, 2007). Sample-based planning methods can use a stochastic simulator as a black-box, to provide a generative model of the environment.

In general, learning an accurate model of an MDP can be a very challenging problem. Nevertheless, there have been several successful examples of model learning in real-world applications, such as robotic helicopter flight (Abbeel et al., 2007). Such models are often based on parametric probability distributions, which can be sampled efficiently, and used to simulate experience.

In summary, there are many applications in which experience can be simulated. The question then is how to make the most effective use of this simulated experience. By generating simulations from the current state, and applying reinforcement learning to the simulated experience, the agent can focus on the subproblem it is facing right now. This broad concept could be equally applied to robotic motion-planning, financial decision-making, or classical planning.

10.5.2 Features

In computer Go, we have primarily used three representations of state: table lookup, local shape features, and subtree features based on RAVE. In some problems, a Monte-Carlo tree search using a simple search tree based on table lookup may be sufficient to achieve good performance. However, as in Go, many real-world problems have an enormous state space and a large branching factor. In these problems, it may also be advantageous to generalise between related states by using features to abstract over the state space. Furthermore, when state abstraction is used, bootstrapping is usually beneficial (see Chapters 2, 5 and 6). In this case, temporal-difference search may provide better performance.

Local shape features can be generalised to other environments, by considering all possible configurations of overlapping subsets of state variables. For example, in a classical planning problem there are typically many state variables, each denoting the logical status of one atomic element of state (e.g. “door=open” or “box=empty”). We may have some prior knowledge of the problem, suggesting that subsets of state variables are related (e.g. the state of several boxes). Temporal-difference search would then learn to evaluate the state in terms of these configurations (e.g. the value of having three adjacent boxes empty). Similarly, in a robotics application, the various sensor inputs could be combined together in different combinations, or partitioned into overlapping tiles (Sutton, 1996).

The state abstraction used by RAVE may be more problematic to apply more widely. The key assumption of RAVE, based on the all-moves-as-first heuristic (see Chapter 4), is that the value of an action remains approximately consistent over several time-steps. However, this assumption depends strongly on the underlying representation of state and actions. For example, in a maze or gridworld, the agent’s actions can be expressed either objectively (north, east, south, west) or subjectively (forward, right, backward, left). In the first case, actions are likely to retain similar values through neighbouring regions of the grid; in the second case, the value of an action will change each time the agent turns to face a new direction. The extended RAVE features suggested above may provide one solution to this problem, by generalising over consistent features within each subtree, rather than generalising over specific actions.

10.5.3 Simulation Policy

In our experiments (see Chapter 6), and in other successful applications of simulation-based search (see Chapter 3), performance can be significantly improved by incorporating domain knowledge into the default simulation policy. However, in many applications domain knowledge is unavailable, or is problematic to acquire and encode.

Reinforcement learning provides a natural approach for automatically learning a default policy. However, at least in Go, naively learning a strong default policy does not necessarily lead to a stronger overall search (see Chapter 9). But does this observation apply beyond Go? In stochastic games such as backgammon (Tesauro and Galperin, 1996) and Scrabble (Sheppard, 2002), a stronger simulation policy has directly led to a stronger overall search. In these games, the randomness inherent to the environment automatically provides diversity, and simulation balancing does not appear to be required. Furthermore, the oscillations in value that we observed in Figure 9.3 are a property of two-player games, and should not occur in single-agent MDPs. For these reasons, it may well be the case that a good default policy can be learnt directly by reinforcement learning, for example using policy gradient algorithms (see Chapter 9).

Unlike Monte-Carlo tree search, temporal-difference search does not require a separate default policy (see Chapter 6). In stochastic, single-agent MDPs, the single simulation policy used by temporal-difference search may perhaps be more effective than a distinct default policy.

10.5.4 Extending the Envelope

We began this thesis by suggesting that computer Go is the best case for AI (see Chapter 1). It is deterministic, it has a discrete state space, a discrete action space, and it is fully observable. We briefly consider how each of these restrictions might be addressed in future work.

Although Go is deterministic, reinforcement learning and simulation-based search are ideally suited to stochastic environments. Indeed, stochastic environments may actually help simulation-based search methods, by providing a rich diversity of simulations. Although stochastic environments may increase the total branching factor of a search tree, the effective branching factor may still be small. For example, if the transition probabilities are concentrated, then a simulation-based search will visit a small number of states much more frequently, regardless of the number of states in the tail distribution.

In continuous state spaces, table lookup methods such as Monte-Carlo tree search cannot be directly applied. However, the state space can be discretised so that table lookup can be applied.

Alternatively, the state space can be abstracted by an appropriate set of features, and function approximation can be applied, for example using temporal-difference search. In high dimensional problems, the curse of dimensionality may be problematic, so that a discretisation or other state abstraction may require very large numbers of features. However, we note that the difficulty of simulation-based search is not necessarily determined by the size of the state space. At each time-step t the agent faces a subproblem starting from time t. If the transitions from s_t are concentrated along narrow regions of the state space, then only a small fraction of the state space need be considered, and the curse of dimensionality is circumvented (Rust, 1997).

Continuous action spaces could in principle be addressed by using policy gradient methods (see Chapter 2) instead of value-based reinforcement learning algorithms. The temporal-difference search algorithm could be extended to use an actor-critic algorithm, using an appropriately parameterised policy, and using temporal-difference learning to evaluate the policy.

It may also be possible to apply simulation-based search to partially observable environments. For example, a simple recurrent network could be used to approximate the value function. The network would receive observations at each time-step as inputs, and output the value. The weights of the network could be updated from real experience by temporal-difference learning. Alternatively, given a generative model of the environment, the weights of the network could be trained from simulated experience, starting from the current state. Finally, as in the Dyna-2 architecture, two sets of weights could be combined together.

10.6 Conclusions

10.6.1 The Future of Computer Go

For the last 30 years, computer Go programs have evaluated positions by using handcrafted heuristics that are based on human expert knowledge of shapes, patterns and rules. However, professional Go players often play moves according to intuitive feelings that are hard to express or quantify. Precisely encoding their knowledge into machine-understandable rules has proven to be a dead-end: a classic example of the knowledge acquisition bottleneck. Furthermore, traditional search algorithms, which are based on these handcrafted heuristics, cannot cope with the enormous search space and branching factor in the game of Go, and are unable to make effective use of additional computation time. This approach has led to Go programs that are at best comparable to weak amateur-level humans.

In contrast, simulation-based search requires no human knowledge in order to understand a position. Instead, positions are evaluated from the outcome of thousands of simulated games of self-play from that position. These simulated games are progressively refined to prioritise the selection of positions with promising evaluations. Over the course of many simulations, attention is focused selectively on narrow regions of the search space that are correlated with successful outcomes. Unlike traditional search algorithms, this approach scales well with additional computation time.

On the Computer Go Server, using 9×9, 13×13 and 19×19 board sizes, traditional search programs are rated at around 1800 Elo, whereas Monte-Carlo programs, enhanced by RAVE and heuristic knowledge, are rated at around 2500 Elo using standard hardware[3] (see Table 4.1). On the Kiseido Go Server, on full-size boards against human opposition, traditional search programs have reached 5-6 Kyu, whereas the best Monte-Carlo programs are rated at 1-*dan* using standard hardware (see Table 4.2). The top programs are now competitive with top human professionals at 9×9 Go, and are winning handicap games against top human professionals at 19×19 Go.

In the Go program *Mogo*, every doubling in computation power led to an increase in playing strength of approximately 100 Elo points in 13×13 Go (see Figure 8.4), and perhaps even more in 19×19 Go. If this trend continues then Moore's law alone may be enough to achieve a computer world champion. However, computer Go research is more active than ever. Simulation-based search is in its infancy, and we can expect exciting new developments over the coming years, so that the inevitable supremacy of computers in Go may arrive sooner than predicted.

10.6.2 The Future of Sequential Decision-Making

In this thesis we have demonstrated that an agent can both learn and plan effectively using reinforcement learning algorithms. We have developed the temporal-difference learning algorithm into a high performance search algorithm (see Chapter 6). We have combined both long and short-term memories together, so as to represent both general knowledge about the whole environment, and specialised knowledge about the current situation (see Chapter 7. We have applied these methods to Monte-Carlo tree search, so as to incorporate prior knowledge, and to provide a rapid generalisation between subtrees (see Chapter 8).

The heuristic MC-RAVE algorithm has proven particular successful in computer Go. While this particular algorithm exploits Go specific properties, such as the *all-moves-as-first* heuristic, our general framework for reinforcement learning and simulation-based search is applicable to a much wider range of applications. The key contributions of this thesis are to combine simulation-based search with state abstraction, with bootstrapping, and with long-term learning. Each of these ideas is very general: given an appropriate model and state representation, they could be applied to any MDP. The Dyna-2 algorithm brings all of these ideas together, providing a general-purpose framework for learning and search in large environments.

In real-world planning and decision-making problems, most actions have long-term consequences, leading to enormous search-spaces that are intractable to traditional search algorithms. Furthermore, also just like Go, in many of these problems, expert knowledge is hard to encode, or even unavailable. Simulation-based search offers a hope for new progress in these formidable problems. Three years ago, it was widely believed that *dan*-strength Go programs were far off in the future; now they

[3] A difference of 700 Elo corresponds to a 99% winning rate.

are a reality. But perhaps the revolution is just beginning: a revolution in how computers learn, plan and act in challenging environments.

Bibliography

Abbeel, P., Coates, A., Quigley, M., and Ng, A. Y. (2007). An application of reinforcement learning to aerobatic helicopter flight. In *Advances in Neural Information Processing Systems 19*, pages 1–8.

Asmussen, S. and Glynn, P. (2007). *Stochastic Simulation: Algorithms and Analysis*. Springer.

Auer, P. (2002). Using confidence bounds for exploitation-exploration trade-offs. *Journal of Machine Learning Research*, 3:397–422.

Auer, P., Cesa-Bianchi, N., and Fischer, P. (2002). Finite-time analysis of the multi-armed bandit problem. *Machine Learning*, 47(2–3):235–256.

Balla, R. and Fern, A. (2009). UCT for tactical assault planning in real-time strategy games. In *21st International Joint Conference on Artificial Intelligence*.

Barto, A. G., Bradtke, S. J., and Singh, S. P. (1995). Learning to act using real-time dynamic programming. *Artificial Intelligence*, 72(1-2):81–138.

Baxter, J., Tridgell, A., and Weaver, L. (2000). Learning to play chess using temporal differences. *Machine Learning*, 40(3):243–263.

Bellman, R. (1957). *Dynamic Programming*. Princeton University Press.

Bertsekas, D. (2007). *Dynamic Programming and Optimal Control (Volumes I and II)*. Athena Scientific.

Billings, D., Castillo, L. P., Schaeffer, J., and Szafron, D. (1999). Using probabilistic knowledge and simulation to play poker. In *16th National Conference on Artificial Intelligence*, pages 697–703.

Bouzy, B. (2004). Associating shallow and selective global tree search with Monte Carlo for 9x9 Go. In *4th International Conference on Computers and Games*, pages 67–80.

Bouzy, B. (2005a). Associating domain-dependent knowledge and Monte Carlo approaches within a Go program. *Information Sciences, Heuristic Search and Computer Game Playing IV*, 175(4):247–257.

Bouzy, B. (2005b). Move pruning techniques for Monte-Carlo Go. In *11th Advances in Computer Games Conference*, pages 104–119.

Bouzy, B. (2006). History and territory heuristics for Monte-Carlo Go. *New Mathematics and Natural Computation*, 2(2):1–8.

Bouzy, B. and Helmstetter, B. (2003). Monte-Carlo Go developments. In *10th Advances in Computer Games Conference*, pages 159–174.

Bradtke, S. and Barto, A. (1996). Linear least-squares algorithms for temporal difference learning. *Machine Learning*, 22(1–3):33–57.

Bruegmann, B. (1993). Monte-Carlo Go. *http://www.cgl.ucsf.edu/go/Programs/Gobble.html*.

Buro, M. (1999). From simple features to sophisticated evaluation functions. In *1st International Conference on Computers and Games*, pages 126–145.

Campbell, M., Hoane, A., and Hsu, F. (2002). Deep Blue. *Artificial Intelligence*, 134(1–2):57–83.

Cazenave, T. (2009). Nested Monte-Carlo search. In *21st International Joint Conference on Artificial Intelligence*.

Chang, H., Fu, M., Hu, J., and Marcus, S. (2005). An adaptive sampling algorithm for solving Markov decision processes. *Operations Research*, 53(1):126–139.

Chaslot, G., Chatriot, L., Fiter, C., Gelly, S., Hoock, J., Perez, J., Rimmel, A., and Teytaud, O. (2008a). Combining expert, online, transient and online knowledge in Monte-Carlo exploration. In *8th European Workshop on Reinforcement Learning*.

Chaslot, G., Winands, M., Szita, I., and van den Herik, H. (2008b). Parameter tuning by the cross-entropy method. In *8th European Workshop on Reinforcement Learning*.

Chaslot, G., Winands, M., and van den Herik, J. (2008c). Parallel Monte-Carlo tree search. In *6th International Conference on Computer and Games*, pages 60–71.

Choi, J., Laibson, D., Madrian, B., and Metrick, A. (2007). Reinforcement learning and savings behavior. Technical Report ICF Working Paper 09-01, Yale.

Coulom, R. (2006). Efficient selectivity and backup operators in Monte-Carlo tree search. In *5th International Conference on Computer and Games*, pages 72–83.

Coulom, R. (2007). Computing Elo ratings of move patterns in the game of Go. In *Computer Games Workshop*.

Coulom, R. (2008). Whole-history rating: A bayesian rating system for players of time-varying strength. In *Computers and Games*, pages 113–124.

Dahl, F. (1999). Honte, a Go-playing program using neural nets. In *Machines that learn to play games*, pages 205–223. Nova Science.

Dailey, D. (2008). 9x9 scalability study. *http://cgos.boardspace.net/study/index.html*.

Davies, S., Ng, A., and Moore, A. (1998). Applying online-search to reinforcement learning. In *15th European Conference on Artificial Intelligence*, pages 753–760.

Dayan, P. (1994). TD(λ) converges with probability 1. *Machine Learning*, 14(1):295–301.

Enderton, H. (1991). The Golem Go program. Technical report, School of Computer Science, Carnegie-Mellon University.

Enzenberger, M. (1996). The integration of a priori knowledge into a Go playing neural network. *http://www.cs.ualberta.ca/ emarkus/neurogo/neurogo1996.html*.

Enzenberger, M. (2003). Evaluation in Go by a neural network using soft segmentation. In *10th Advances in Computer Games Conference*, pages 97–108.

Ernst, D., Glavic, M., Geurts, P., and Wehenkel, L. (2005). Approximate value iteration in the reinforcement learning context. application to electrical power system control. *International Journal of Emerging Electric Power Systems*, 3(1).

Finnsson, H. and Björnsson, Y. (2008). Simulation-based approach to general game playing. In *23rd Conference on Artificial Intelligence*, pages 259–264.

Fürnkranz, J. (2001). Machine learning in games: A survey. In *Machines That Learn to Play Games*, pages 11–59. Nova Science Publishers.

Gelly, S. (2007). *A Contribution to Reinforcement Learning; Application to Computer Go*. PhD thesis, University of South Paris.

Gelly, S., Hoock, J., Rimmel, A., Teytaud, O., and Kalemkarian, Y. (2008). The parallelization of Monte-Carlo planning. In *6th International Conference in Control, Automation and Robotics*, pages 244–249.

Gelly, S. and Silver, D. (2007). Combining online and offline learning in UCT. In *17th International Conference on Machine Learning*, pages 273–280.

Gelly, S. and Silver, D. (2008). Achieving master level play in 9 x 9 computer Go. In *23rd Conference on Artificial Intelligence*, pages 1537–1540.

Gelly, S., Wang, Y., Munos, R., and Teytaud, O. (2006). Modification of UCT with patterns in Monte-Carlo Go. Technical Report 6062, INRIA.

George, A. and Powell, W. (2006). Adaptive stepsizes for recursive estimation with applications in approximate dynamic programming. *Machine Learning*, 65(1):67–198.

Gordon, G. (1996). Chattering in SARSA(lambda) - a CMU learning lab internal report. Technical report, Carnegie Mellon University.

Graepel, T., Kruger, M., and Herbrich, R. (2001). Learning on graphs in the game of Go. In *International Conference on Artificial Neural Networks*, pages 347–352. Springer.

Harmon, A. (2003). Queen, captured by mouse; more chess players use computers for edge. *New York Times, February 6th*.

Hart, P., Nilsson, N., and Raphael, B. (1968). A formal basis for the heuristic determination of minimum cost paths. *IEEE Transactions on Systems Science and Cybernetics*, 4:100–107.

Haykin, S. (1996). *Adaptive Filter Theory*. Prentice Hall.

Hochreiter, S. and Schmidhuber, J. (1997). Long short-term memory. *Neural Computation*, 9(8):1735–1780.

Hunter, R. (2004). MM algorithms for generalized Bradley–Terry models. *The Annals of Statistics*, 32(1):384–406.

Jordan, M. (1995). Why the logistic function? A tutorial discussion on probabilities and neural networks. Technical Report Computational Cognitive Science Report 9503, Massachusetts Institute of Technology.

Kalman, R. (1960). A new approach to linear filtering and prediction problems. *Journal of Basic Engineering*, pages 35–45.

Kearns, M., Mansour, Y., and Ng, A. (2002). A sparse sampling algorithm for near-optimal planning in large Markovian decision processes. *Machine Learning*, 49(2-3):193–208.

Knuth, D. E. and Moore, R. W. (1975). An analysis of alpha-beta pruning. *Artificial Intelligence*, 6:293–326.

Kocsis, L. and Szepesvari, C. (2006). Bandit based Monte-Carlo planning. In *15th European Conference on Machine Learning*, pages 282–293.

Koop, A. (2007). Investigating experience: Temporal coherence and empirical knowledge representation. Master's thesis, University of Alberta.

Korf, R. E. (1990). Real-time heuristic search. *Artificial Intelligence*, 42(2-3):189–211.

Lorentz, R. (2008). Amazons discover monte-carlo. In *Computers and Games*, pages 13–24.

Matthews, C. (2003). *Shape up*. GoBase.

Mayer, H. (2007). Board representations for neural Go players learning by temporal difference. In *IEEE Symposium on Computational Intelligence and Games*.

McCarthy, J. (1997). AI as sport. *Science*, 276(5318):1518–1519.

McClain, D. (2006). Once again, machine beats human champion at chess. *New York Times, December 5th*.

Mechner, D. (1998). All Systems Go. *The Sciences*, 38(1).

Müller, M. (2001). Global and local game tree search. *Information Sciences*, 3-4(135):187–206.

Müller, M. (2002). Computer Go. *Artificial Intelligence*, 134:145–179.

Müller, M. and Enzenberger, M. (2009). Fuego – an open-source framework for board games and Go engine based on Monte-Carlo tree search. Technical Report TR09-08, University of Alberta, Department of Computing Science.

Nakhost, H. and Müller, M. (2009). Monte-Carlo exploration for deterministic planning. In *21st International Joint Conference on Artificial Intelligence*, pages 1766–1771.

Nevmyvaka, Y., Feng, Y., and Kearns, M. (2006). Reinforcement learning for optimized trade execution. In *23rd International Conference on Machine learning*, pages 673–680.

Ng, A. Y., Coates, A., Diel, M., Ganapathi, V., Schulte, J., Tse, B., Berger, E., and Liang, E. (2004). Autonomous inverted helicopter flight via reinforcement learning. In *9th International Symposium on Experimental Robotics*, pages 363–372.

Péret, L. and Garcia, F. (2004). On-line search for solving Markov decision processes via heuristic sampling. In *16th Eureopean Conference on Artificial Intelligence*, pages 530–534.

Puterman, M. (1994). *Markov Decision Processes*. Wiley.

Rummery, G. and Niranjan, M. (1994). On-line Q-learning using connectionist systems. Technical Report CUED/F-INFENG/TR 166, Cambridge University Engineering Department.

Runarsson, T. and Lucas, S. (2005). Co-evolution versus self-play temporal difference learning for acquiring position evaluation in small-board Go. *IEEE Transactions on Evolutionary Computation*, 9(6):628–640.

Russell, S. and Norvig, P. (1995). *Artificial Intelligence: A Modern Approach*. Prentice Hall.

Rust, J. (1997). Using randomization to break the curse of dimensionality. *Econometrica*, 65(3):487–516.

Schaeffer, J. (1989). The history heuristic and alpha–beta search enhancements in practice. *IEEE Transactions on Pattern Analysis and Machine Intelligence*, PAMI-11(11):1203–1212.

Schaeffer, J. (1997). *One Jump Ahead: Challenging Human Supremacy in Checkers*. Springer Verlag.

Schaeffer, J. (2000). The games computers (and people) play. *Advances in Computers*, 50:189–266.

Schaeffer, J., Culberson, J., Treloar, N., Knight, B., Lu, P., and Szafron, D. (1992). A world championship caliber checkers program. *Artificial Intelligence*, 53:273–289.

Schaeffer, J., Hlynka, M., and Jussila, V. (2001). Temporal difference learning applied to a high-performance game-playing program. In *17th International Joint Conference on Artificial Intelligence*, pages 529–534.

Schäfer, J. (2008). The UCT algorithm applied to games with imperfect information. Diploma Thesis. Otto-von-Guericke-Universität Magdeburg.

Schraudolph, N., Dayan, P., and Sejnowski, T. (1994). Temporal difference learning of position evaluation in the game of Go. In *Advances in Neural Information Processing 6*, pages 817–824.

Schraudolph, N., Dayan, P., and Sejnowski, T. (2000). Learning to evaluate Go positions via temporal difference methods. In *Computational Intelligence in Games*, volume 62, pages 77–96. Springer Verlag.

Schultz, W., Dayan, P., and Montague, P. (1997). A neural substrate of prediction and reward. *Science*, 16:1936–1947.

Sheppard, B. (2002). World-championship-caliber Scrabble. *Artificial Intelligence*, 134(1-2):241–275.

Silver, D., Sutton, R., and Müller, M. (2007). Reinforcement learning of local shape in the game of Go. In *20th International Joint Conference on Artificial Intelligence*, pages 1053–1058.

Silver, D., Sutton, R., and Müller, M. (2008). Sample-based learning and search with permanent and transient memories. In *25th International Conference on Machine Learning*, pages 968–975.

Silver, D. and Tesauro, G. (2009). Monte-Carlo simulation balancing. In *26th International Conference on Machine Learning*, pages 119–126.

Singh, S. and Bertsekas, D. (1997). Reinforcement learning for dynamic channel allocation in cellular telephone systems. In *Advances in Neural Information Processing Systems 9*, pages 974–982.

Singh, S. and Dayan, P. (1998). Analytical mean squared error curves for temporal difference learning. *Machine Learning*, 32(1):5–40.

Singh, S., Jaakkola, T., Littman, M., and Szepesvari, C. (2000). Convergence results for single-step on-policy reinforcement-learning algorithms. *Machine Learning*, 38:287–308.

Singh, S. and Sutton, R. (2004). Reinforcement learning with replacing eligibility traces. *Machine Learning*, 22:123–158.

Stern, D., Herbrich, R., and Graepel, T. (2006). Bayesian pattern ranking for move prediction in the game of Go. In *23rd International Conference of Machine Learning*, pages 873–880.

Stoutamire, D. (1991). *Machine Learning, Game Play, and Go*. PhD thesis, Case Western Reserve University.

Sturtevant, N. (2008). An analysis of UCT in multi-player games. In *6th International Conference on Computers and Games*, pages 37–49.

Sutton, R. (1984). *Temporal credit assignment in reinforcement learning*. PhD thesis, University of Massachusetts.

Sutton, R. (1988). Learning to predict by the method of temporal differences. *Machine Learning*, 3(9):9–44.

Sutton, R. (1990). Integrated architectures for learning, planning, and reacting based on approximating dynamic programming. In *7th International Conference on Machine Learning*, pages 216–224.

Sutton, R. (1992). Adapting bias by gradient descent: An incremental version of delta-bar-delta. In *10th National Conference on Artificial Intelligence*, pages 171–176.

Sutton, R. (1996). Generalization in reinforcement learning: Successful examples using sparse coarse coding. In *Advances in Neural Information Processing Systems 8*, pages 1038–1044.

Sutton, R. and Barto, A. (1990). Time-derivative models of pavlovian reinforcement. *Learning and Computational Neuroscience: Foundations of Adaptive Networks*, pages 497–537.

Sutton, R. and Barto, A. (1998). *Reinforcement Learning: an Introduction*. MIT Press.

Sutton, R., Koop, A., and Silver, D. (2007). On the role of tracking in stationary environments. In *17th International Conference on Machine Learning*, pages 871–878.

Sutton, R., McAllester, D., Singh, S., and Mansour, Y. (2000). Policy gradient methods for reinforcement learning with function approximation. In *In Advances in Neural Information Processing Systems 12*, pages 1057–1063. MIT Press.

Tesauro, G. (1988). Connectionist learning of expert preferences by comparison training. In *Advances in Neural Information Processing 1*, pages 99–106.

Tesauro, G. (1994). TD-gammon, a self-teaching backgammon program, achieves master-level play. *Neural Computation*, 6:215–219.

Tesauro, G. and Galperin, G. (1996). On-line policy improvement using Monte-Carlo search. In *Advances in Neural Information Processing 9*, pages 1068–1074.

Tsitsiklis, J. and Roy, B. V. (1997). An analysis of temporal-difference learning with function approximation. *IEEE Transactions on Automatic Control*, 42(5):674–690.

Tsitsiklis, J. N. (2002). On the convergence of optimistic policy iteration. *Journal of Machine Learning Research*, 3:59–72.

van der Werf, E., Uiterwijk, J., Postma, E., and van den Herik, J. (2002). Local move prediction in Go. In *3rd International Conference on Computers and Games*, pages 393–412.

Veness, J., Silver, D., Blair, A., and Uther, W. (2009). Bootstrapping from game tree search. In *Advances in Neural Information Processing Systems 19*.

Wang, Y. and Gelly, S. (2007). Modifications of UCT and sequence-like simulations for Monte-Carlo Go. In *IEEE Symposium on Computational Intelligence and Games, Honolulu, Hawaii*, pages 175–182.

Widrow, B. and Stearns, S. (1985). *Adaptive Signal Processing*. Prentice-Hall.

Williams, R. J. (1992). Simple statistical gradient-following algorithms for connectionist reinforcement learning. *Machine Learning*, 8:229–256.

Winands, M. and Y. Björnsson, Y. (2009). Evaluation function based Monte-Carlo LOA. In *12th Advances in Computer Games Conference*.

Appendix A

Logistic Temporal Difference Learning

Many tasks are best described by a binary goal of success or failure: winning a game, solving a puzzle or achieving a goal state. These tasks can be described by the classic expected-reward formulation of reinforcement learning. The agent receives a binary reward of $r = 1$ for success, $r = 0$ for failure, and no intermediate rewards. The value function $V^\pi(s)$ is defined to be the expected total reward from board position s when following policy π.

We can also describe the same tasks probabilistically. The agent receives a final *outcome* of $z = 1$ for success, and $z = 0$ for failure. The *success probability*, $P^\pi(s)$, is the probability of receiving a successful outcome of $z = 1$ from board position s when following policy π. These views are equivalent: the success probability is identical to the value function,

$$\begin{aligned} V^\pi(s) &= \mathbb{E}_\pi\left[\sum_{t=1}^{T} r_t | s_t = s\right] \\ &= \mathbb{E}_\pi[r_T | s_t = s] \\ &= Pr(z = 1 | s_t = s, \pi) \\ &= P^\pi(s). \end{aligned} \tag{A.1}$$

where T is the time step at which the task terminates.

We can form an approximation $P_\theta(s)$ to the success probability by taking a linear combination of a feature vector $\phi(s)$ and a corresponding weight vector θ. However, a linear approximation, $P_\theta(s) = \phi(s) \cdot \theta$, is not well suited to modelling probabilities. Instead, we use the logistic function $\sigma(x) = \frac{1}{1+e^{-x}}$ to squash the value to the desired range $[0, 1]$ (Jordan, 1995),

$$P_\theta(s) = \sigma(\phi(s) \cdot \theta). \tag{A.2}$$

A.1 Logistic Monte-Carlo Evaluation

The idea of logistic Monte-Carlo is to find the approximation to the success probability that maximises the likelihood of the observed outcomes. Specifically, we seek the weights θ that maximise the likelihood of the observed outcomes over all T_i time steps of all N episodes,

$$\begin{aligned}\mathcal{L}_{MC}(\theta) &= log \prod_{i=1}^{N} \prod_{t=1}^{T_i} P_\theta(s_t^i)^{z_i} (1 - P_\theta(s_t^i))^{1-z_i} &\text{(A.3)}\\ &= \sum_{i=1}^{N} \sum_{t=1}^{T_i} z_i \log P_\theta(s_t^i) + (1 - z_i) \log(1 - P_\theta(s_t^i)), &\text{(A.4)}\end{aligned}$$

which is the total (negative) cross-entropy between the success probability and the actual outcome. We maximise the log likelihood by gradient ascent, or equivalently minimise the total cross-entropy by gradient descent. We proceed by applying the well-known identity for the derivative of the logistic function, $\nabla_\theta(\sigma(x)) = \sigma(x)(1 - \sigma(x))\nabla_\theta x$,

$$\begin{aligned}\nabla_\theta \mathcal{L}_{MC} &= \sum_{i=1}^{N} \sum_{t=1}^{T_i} z_i \nabla_\theta \log P_\theta(s_t^i) + (1 - z_i)\nabla_\theta \log(1 - P_\theta(s_t^i)) &\text{(A.5)}\\ &= \sum_{i=1}^{N} \sum_{t=1}^{T_i} z_i \frac{P_\theta(s_t^i)(1 - P_\theta(s_t^i))\phi(s_t^i)}{P_\theta(s_t^i)} - (1 - z_i)\frac{P_\theta(s_t^i)(1 - P_\theta(s_t^i))\phi(s_t^i)}{1 - P_\theta(s_t^i)} &\text{(A.6)}\\ &= \sum_{i=1}^{N} \sum_{t=1}^{T_i} z_i(1 - P_\theta(s_t^i))\phi(s_t^i) - (1 - z_i)P_\theta(s_t^i)\phi(s_t^i) &\text{(A.7)}\\ &= \sum_{i=1}^{N} \sum_{t=1}^{T_i} (z_i - P_\theta(s_t^i))\phi(s_t^i). &\text{(A.8)}\end{aligned}$$

If we sample this gradient at every time-step, using stochastic gradient ascent, then we arrive at a logistic regression algorithm, applied to the outcomes of episodes,

$$\Delta\theta = \alpha(z_i - P_\theta(s_t))\phi(s_t), \tag{A.9}$$

where α is a step-size parameter. We view this algorithm as a modification of Monte-Carlo evaluation (see Chapter 2) to estimate probabilities rather than expected values. We call this algorithm *logistic Monte-Carlo evaluation*.

A.2 Logistic Temporal-Difference Learning

The non-linear TD(0) algorithm (Sutton and Barto, 1998) can be applied to a logistic-linear value function,

$$\Delta\phi(s, a) = \alpha\delta_t \nabla_\theta V(s_t) \tag{A.10}$$

$$= \alpha(V(s_{t+1}) - V(s_t))V(s_t)(1 - V(s_t))\phi(s_t) \tag{A.11}$$

However, this algorithm is based on an expected value view of the problem, rather than a probabilistic view. As in the previous section, we seek an alternative algorithm that is well-matched to a probabilistic representations of the problem.

We recall from Chapter 2 that the fundamental idea of temporal difference learning is to replace the return with a bootstrapped estimate of the return. Similarly, in *logistic temporal-difference learning* we replace the outcome z in the update equation A.9 with a bootstrapped estimate of the outcome $P_\theta(s_{t+1})$, in an algorithm that we call *logistic TD(0)*,

$$\Delta\theta = \alpha(P_\theta(s_{t+1}) - P_\theta(s_t))\phi(s_t) \tag{A.12}$$

As with linear temporal-difference learning (see Chapter 2), this algorithm introduces bias and is no longer a true gradient descent algorithm. Nevertheless, logistic TD(0) can be viewed intuitively as reducing the *cross-entropy TD-error* between current and subsequent estimates of the success probability,

$$P_\theta(s_{t+1}) \log P_\theta(s_t) + (1 - P_\theta(s_{t+1})) \log(1 - P_\theta(s_t)) \tag{A.13}$$

Logistic TD(0) differs from non-linear TD(0) solely in the absence of the logistic gradient term, $V(s_t)(1 - V(s_t))$. If non-linear TD(0) is viewed as a steepest gradient algorithm, then the update used by logistic TD(0) differs solely by a positive multiplicative constant, and the two different updates must have a positive dot product. In other words, the logistic TD(0) update provides an alternative descent direction, which selects a different path to the same minimum.

Although both algorithms performed similarly in practice, we prefer the simpler logistic TD(0) update throughout this thesis. However, we note that the justification for logistic TD(0) is somewhat heuristic in nature. In particular, it minimises the cross-entropy between the current state and its *expected* successor. This is a mixed backup that combines expected values with probabilities. Although this may be reasonable in the deterministic world of Go, we do not presume that it would outperform nonlinear TD(0) in other, more general settings.